RICE UNIVERSITY

Strategies for the Mitigation of Oxysterol-Induced Cytotoxicity

by

Jacques M. Mathieu

A THESIS SUBMITTED
IN PARTIAL FULFILLMENT OF THE
REQUIREMENTS FOR THE DEGREE

Doctor of Philosophy

APPROVED, THESIS COMMITTEE

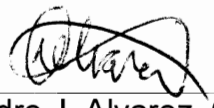

Pedro J. Alvarez, Chair, George R. Brown Professor of Engineering

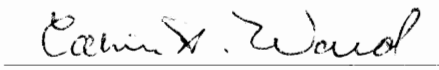

Calvin H. Ward, Professor, Foyt Family Chair of Engineering

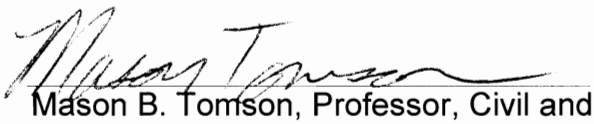

Mason B. Tomson, Professor, Civil and Environmental Engineering

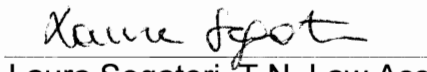

Laura Segatori, T.N. Law Assistant Professor in Chemical and Biomolecular Engineering

Houston, Texas
April 2011

Abstract

Strategies for the Mitigation of Oxysterol-Induced Cytotoxicity

By

Jacques M. Mathieu

Chronic exposure to some oxysterols might contribute to deterioration of human or environmental health. Oxysterols are both biomarkers of oxidative stress as well as mediators of its damage, and play a central role in many independent, but converging, disease processes, such as atherosclerosis, Alzheimer's disease, and age-related macular degeneration. Therefore, the aim of this thesis was to identify enzymes capable of transforming oxysterols to either reduce their toxicity or facilitate their metabolism or excretion. 7-ketocholesterol (7KC), being amongst the most cytotoxic and recalcitrant of these compounds, was the main focus of this work.

We isolated various bacteria capable of utilizing 7KC as a sole carbon and energy source. One of these, *Rhodococcus jostii* RHA1, was subjected to rigorous transcriptomic and mutational analysis to elucidate its 7KC degradation pathway, which was similar, but not identical, to that of cholesterol. Metabolite screening revealed the reduction and subsequent removal of the 7-keto moiety prior to the step catalyzed by HsaC, the enzyme responsible for cleavage of sterol ring A. Furthermore, cloning and expression of a number of reductases from two gene clusters that were highly up-regulated during growth on 7KC

identified three reductases that are active against several closely related structural analogs, though not 7KC itself.

7KC and a number of analogs were assayed for toxicity against human fibroblasts. Several enzymes were overexpressed in these fibroblasts by transient transfection with mammalian expression vectors to screen for their ability to mitigate 7KC-induced cytotoxicity. A LAMP1/cholesterol oxidase chimera was found to be significantly cytoprotective to exposure to up to 50 μM 7KC compared to mock transfection as well as 7KC-transforming enzymes targeted to either the mitochondria or cytosol. Additionally, transfection with LAMP1 alone and treatment with 0.9% hydroxypropyl β-cyclodextrin also reduced toxicity. Therefore, it seems likely that addressing 7KC toxicity within the lysosome is critical for cytoprotection. This work provides preliminary evidence to support this approach, and may have implications for the treatment of oxysterol-associated diseases. However, further research is needed to evaluate the effects and safety of heterologous gene expression within the lysosome, both *in vitro* and *in vivo*.

Acknowledgments

This thesis would not have been possible without the support of many people. First, and foremost, I would like to thank my advisor, Dr. Pedro Alvarez, who provided invaluable guidance throughout the course of my studies, and was integral to my development as a researcher. I would also like to thank my thesis committee, Dr. Herb Ward, Dr. Mason Tomson, and Dr. Laura Segatori for their valuable advice and input during the course of my research.

I gratefully acknowledge Dr. William Mohn, for hosting me at his lab, his gift of *Rhodococcus jostii* RHA1, and his help with the subsequent analysis. I also benefited from my collaboration with Fan Wang, and would like to express thanks for her help with experimental design and mammalian cell studies. I would like to extend my gratitude to Dr. Bill Wilson and Dr. Sean Moran for their much needed help in biochemistry and oxysterol characterization.

I would like to thank my parents for everything they have done for me to help me get to where I am. Also, my most sincere thanks to all of my fellow lab mates, and to the SENS Foundation and Methuselah Foundation for providing the stimulus and financial means to make this research possible. And finally, I would also like to extend my deepest gratitude to my wife, Kelsey, who supported and helped me in innumerable ways. Her dedication, love, and confidence in me have made a tremendous difference, especially in times of stress.

Contents

List of Figures

List of Tables

Chapter 1

Introduction

Recognition of the deleterious effects of some oxysterols has led to increasing concern that chronic exposure might contribute to deterioration of physical or environmental health. Oxysterols are both biomarkers of oxidative stress as well as mediators of its damage, and play a central role in many independent, but converging, disease processes. High oxysterol levels in humans have been associated with seemingly disparate conditions such as atherosclerosis [4, 5], Alzheimer's disease [6, 7], Parkinson's disease [8], diabetes [9], iron and copper toxicity [10-12], age-related macular degeneration [13-15], osteoporosis [16], multiple sclerosis [6], and Niemann-Pick disease [17]. Additionally, oxysterol concentrations are determined by a combination of genetics, age, nutrition and physical environment, and consequently serve as a link between different risk factors. However, while a vast body of literature exists

documenting the effects of various oxysterols, there is an overall deficiency in the knowledge of how to control their levels and mitigate their toxicity.

The aim of this thesis is to identify and characterize enzymes capable of transforming oxysterols in a manner that reduces their toxicity or promotes their metabolism. 7-ketocholesterol (7KC), being amongst the most toxic and recalcitrant of these compounds, is the main focus of this work. Though strong evidence exists for the detrimental effects of 7KC, and other oxysterols, in various biological processes, questions remain regarding the extent of their role in the initiation and progression of pathogenic or endocrine disrupting processes, both in the environment and *in vivo*. Therefore tools capable of the selective transformation of these oxysterols serve two purposes: to verify or reject hypotheses concerning the effects of oxysterols and as potential catalysts to control oxysterol levels and mitigate their impacts in various media.

1.1. General Background

Though eukaryotic cells possess several mechanisms to facilitate the detoxification and elimination of oxysterols, these processes regularly fail in higher organisms, resulting in cell- and tissue-specific accumulations. One reason for this is a lack of sufficient catabolic capacity; many multicellular eukaryotes do not have the enzymes necessary to degrade the steroid nucleus or reverse sterol autoxidation. However, a number of bacteria and fungi are

capable of partial or complete sterol degradation, with some achieving complete mineralization in the absence of other carbon or energy sources [18-20]. Indeed, the microbial transformation of sterols and steroids has been exploited by the pharmaceutical industry since the 1950s for the development of novel compounds and synthesis routes [21]. Research into microbial sterol biodegradation may therefore be beneficial in uncovering enzymes capable of specific oxysterol transformations.

Microbial cholesterol degradation has been continuously and extensively studied for almost a century [18, 22-24]. Partial pathways for testosterone [25], β-sitosterol [26], and cholic acid degradation [27] have also been identified, and share many similarities. However, most research into microbial steroid conversions have focused on hydroxylations and side-chain cleavage [28, 29]; reactions that are used in the pharmaceutical industry for the production of natural or modified steroid analogs [30]. Other bacterial steroid transformations that have been identified include both the hydrogenation of C=C bonds and dehydrogenation of C-C bonds within the steroid nucleus [31, 32], oxidation of alcohols to ketones [33, 34], and the oxidation of ketones to esters or lactones [35]. However, little is known about the enzymes involved, and a complete degradation pathway for any sterol has yet to be elucidated.

1.2. Objectives, Hypotheses and Significance

This thesis investigates both the microbial degradation of the cholesterol derivative 7-ketocholesterol and potential strategies to mitigate its toxicity. Specific objectives include to:

1. Determine whether bacteria capable of metabolizing 7KC exist in the environment and assess their diversity.

We hypothesize that the capacity to transform oxysterols is widely prevalent amongst indigenous microorganisms. Sterols are essential components of animal, plant, and fungal cells, and are therefore common in the environment, where the lack of their accumulation is indicative of their degradation.

2. Determine the genetic basis of 7-ketocholesterol degradation in a microorganism.

We postulate that the diversity of organisms capable of transforming 7KC is broad enough that we will discover a species amenable to laboratory culture for subsequent study. The transcriptomic analysis of an organism grown solely on 7KC (relative to growth on alternative substrates) should discern the catabolic genes and associated enzymes involved in the catabolism of this compound.

3. Characterize candidate enzymes for their ability to transform 7KC, and assess their feasibility for use in controlling oxysterol levels.

Once we have identified candidate enzymes for 7KC transformation, standard molecular biology techniques can be used to clone, express, and assay these enzymes. The feasibility of using any enzyme for therapeutic purposes depends on the toxicity of its product. Accordingly, *we hypothesize that the enzymatic oxidation of 7KC (e.g., by oxidation of the 3β-hydroxyl group or side-chain hydroxylation) or reduction of the 7-keto group (forming 7α-hydroxycholesterol) will reduce the potential toxicity of 7KC metabolites. However, due to the low prevalence of 7KC in comparison to cholesterol, it may be difficult to isolate enzymes that are specific for 7KC. This is important as unintended transformation of cholesterol could have detrimental consequences in regard to membrane integrity, or the accumulation of more toxic intermediates, such as cholest-4-en-3-one.*

The significance of this research relates to the fact that, whereas a large number of studies have extensively detailed the physiological impact of 7KC, none have addressed the microbial degradation of this compound. Addressing this knowledge gap should provide information valuable for the purpose of selectively manipulating oxysterol levels in various matrices while avoiding unintended transformation of other compounds that may play a beneficial role. The ability to accomplish this is particularly relevant due to the high prevalence and cytotoxicity of 7KC, and would have potential implications for a number of fields. Specifically, oxysterols are of concern in environmental toxicology as several environmental contaminants, such as ozone and iron, contribute to their

formation *in vivo*. Additionally, oxysterols may accumulate to high levels outside of pulp mills and other industrial discharge zones where they cause endocrine disruption in susceptible aquatic species. Mitigation of the effects of these pollutants would therefore have implications for human health and safety as well as wildlife. Since oxysterols are rapidly formed during the cooking and processing of food, their concentrations may be unusually high in certain foodstuffs. Controlling dietary levels may therefore be of benefit to the food industry. And in the medical field, the ability to alter oxysterol levels could provide a means to either halt the progression of, or potentially treat, many different diseases.

1.3. Thesis Outline

Chapter 2 provides a summary of the sources, formation, and effects of oxysterols. It also illustrates how the human body metabolizes these compounds, discusses what environmental risk factors exist, and establishes a framework for understanding their relevance in disease processes. Some of the information present in this chapter was published in the form of a review paper [36]:

> Mathieu, J.M., J. Schloendorn, B.E. Rittmann, and P.J. Alvarez, *Medical bioremediation of age-related diseases*. Microb Cell Fact, 2009. **8**: p. 21-39.

Chapter 3 addresses the microbial degradation of 7KC; investigating the phylogenetic diversity of bacteria involved as well as the rate and extent of degradation [37], and was published as:

Mathieu, J.M., J. Schloendorn, B.E. Rittmann, and P.J. Alvarez, *Microbial degradation of 7-ketocholesterol*. Biodegradation, 2008. **19**(6): p. 807-13.

Specific pathways in one model organism, *Rhodococcus jostii* RHA1, are explored in Chapter 4 using mutational analysis, transcriptomics, and metabolite screening as reported in [38]:

Mathieu, J.M, W.W. Mohn, L.D. Eltis, J.C. LeBlanc, G.R. Stewart, C. Dresen, K. Okamoto, and P.J. Alvarez, *7-ketocholesterol catabolism by Rhodococcus jostii RHA1.* Appl Environ Microbiol, 2010. **76**(1): p. 352-5.

Chapter 5 is unpublished work that describes our efforts cloning, expressing, and assaying candidate enzymes from RHA1 as well as several other sources. Chapter 6 is research being submitted for publication that details our investigation into 7KC cytotoxicity and strategies to mitigate its effects *in vivo*. Some of the basis for this chapter was previously published as a collaborative effort [39]:

Schloendorn, J., T. Webb, K. Kemmish, M. Hamalainen, D. Jackemeyer, L. Jiang, J. Mathieu, J. Rebo, J. Sankman, L. Sherman, L. Tontson, A. Qureshi, P. Alvarez, and B. Rittmann, *Medical bioremediation: a concept moving toward reality.* Rejuvenation Res, 2009. **12**(6): p. 411-9.

Chapter 7 concludes with comments on the engineering significance of the final results, recommendations for future work, and addresses the overall impact of the thesis.

Chapter 2

Literature Review

Sterols are hydrophobic lipids present in appreciable quantity in both animal and plant tissue where they serve essential physiological roles as membrane components, hormones or hormone precursors, and modulators of signal transduction. They are characterized by a tetracyclic ring structure (steroid nucleus), a 3β- or 3α-hydroxy group, and a C-17 positioned aliphatic side chain (Figs. 2-1, 2-2). Oxidative modification of the steroid nucleus or side chain may occur through enzymatic or spontaneous mechanisms, forming oxysterols. Although these compounds normally represent a minor fraction of total sterol, 10^{-6} to 10^{-3} in most cases [40], they are uniquely classified due to the alteration in biophysical properties generated by the additional oxygen substituent, which often results in substantial changes in functionality. The effect of these changes is dependent on many factors, though increased concentrations of oxysterols have generally been associated with disruption of cellular homeostasis,

decreased cell viability, and increased cell death [41]. This may lead to dysfunction and injury at the histological level, resulting in the development or exacerbation of several pathological conditions. Indeed, oxysterols have been implicated in atherosclerosis [5, 40, 42], Alzheimer's disease [43, 44], age-related macular degeneration [14, 15, 45], and Parkinson's disease [46]. Recent findings also indicate that some oxidized phytosterols have endocrine disrupting capabilities that result in alterations to the reproductive capacity of certain species [47, 48].

Although considerable research has been performed on the biological effects and fate of a number of oxysterols within mammalian systems (for a thorough review see [49]), to date there is very limited research on the biotransformation of most oxysterols, and a scarcity of peer-reviewed publications regarding their microbial degradation. Knowledge of how these compounds are transformed and degraded by bacteria could prove beneficial for a number of reasons. For example, most oxysterols with C-7 bound oxygen groups have deleterious effects *in vivo*, and the identification and use of microbial enzymes that degrade C-7 oxidized sterols has been proposed as a possible therapeutic approach for the treatment of certain age-related diseases [50]. Furthermore, dietary intake of oxysterols has been reported to result in significant accumulation within human plasma [51], potentially contributing to the elevated oxysterol levels associated with increasing age [52-54]. Thus, information concerning their microbial transformation could also be used to identify enzymes useful in food processing and other biotechnological applications. Finally, the

endocrine disrupting potential of some oxysterols also motivates research on their biodegradation to mitigate their potential ecological and agricultural impact.

2.1. Sources of oxysterols and mechanisms of formation

Cholesterol, β-sitosterol, and ergosterol are the three most abundant sterols, representing the animal, plant, and fungal kingdoms respectively. These three sterols, therefore, serve as parental compounds for the majority of oxysterol species, though cholesterol oxidation products (COP) are by far the most studied of the three (Fig. 2-2). By contrast, very little appears in the literature concerning oxyphytosterols, and even less for oxidized ergosterol derivatives.

The presence of a Δ^5 double bond in cholesterol and β-sitosterol affects the conformation of both rings A and B, and increases the susceptibility of the unsaturation and adjacent allylic positions to a variety of radical as well as non-radical oxidation reactions. Furthermore, as major components of the plasma membrane of cells, these sterols are in a position to encounter reactive oxygen species that cross this barrier. Autoxidation is initiated through hydrogen abstraction creating a carbon-centered radical, predominately at C-7 due to the lower dissociation energy of the carbon-hydrogen bond at this position (Fig. 2-1) [55]. This radical further reacts with oxygen to form a peroxyl radical and, after an additional hydrogen abstraction, yields either 7α- or 7β-hydroperoxide (7α/β-OOHC). These hydroperoxides are further decomposed to 7α/β-alkoxy radicals,

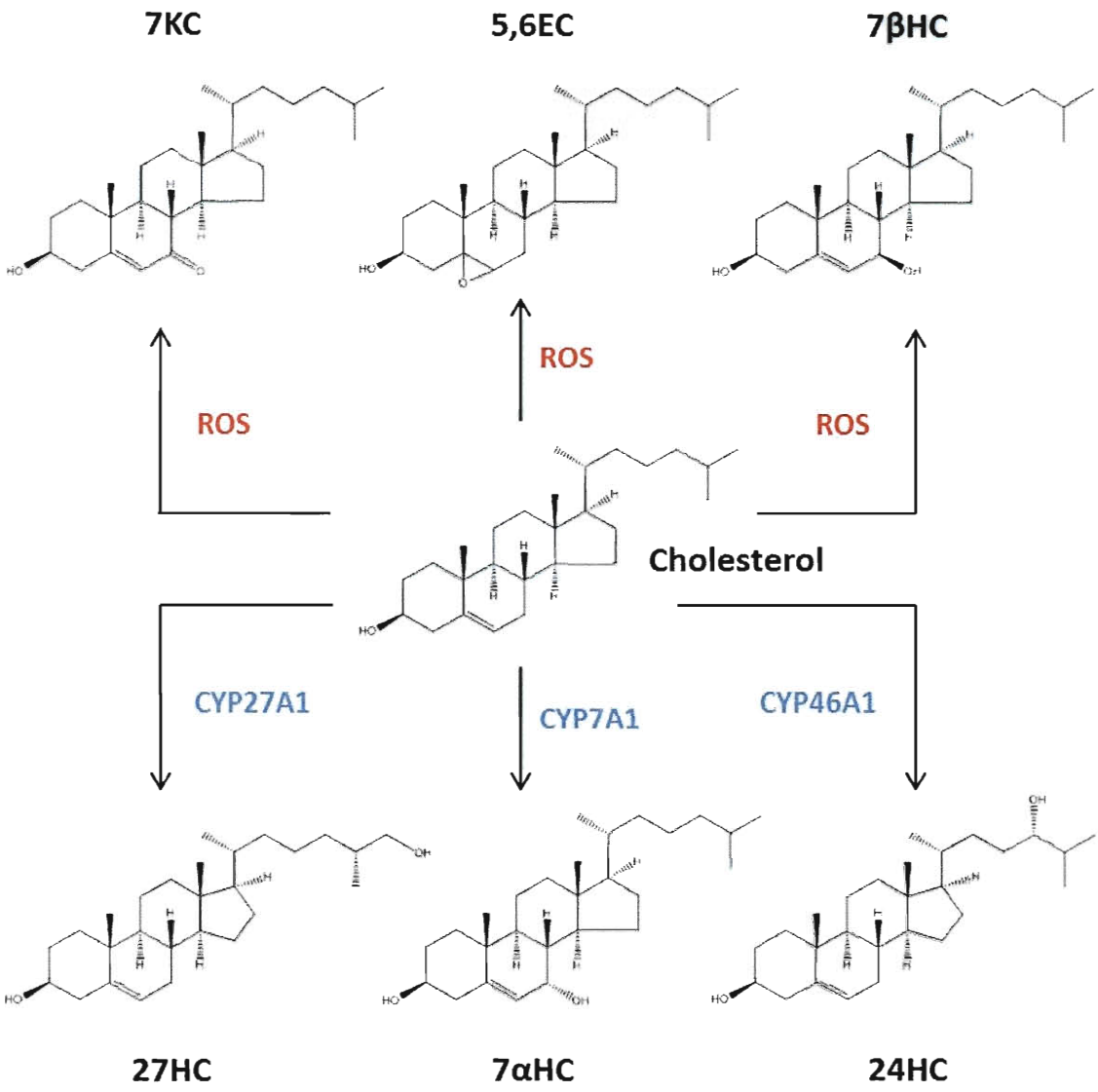

Figure 2-1. Oxysterol formation pathways. 7-ketocholesterol (7KC), 7β-hydroxycholesterol (7βHC), and 5,6-epoxycholesterol (5,6EC) are formed by reaction of reactive oxygen species (ROS) with cholesterol. 7α-hydroxycholesterol (7αHC) is produced primarily in the liver by CYP7A1 during bile acid synthesis, 27-hydroxycholesterol (27HC) is generated in many different tissues through the action of the mitochondrial enzyme CYP27A1, and 24-hydroxycholesterol (24HC) is produced mainly in neural tissue by CYP46A1.

with subsequent reactions generating 7α/β-hydroxysterols and 7-ketosterols [56-58], the major species formed by autoxidation. To a lesser extent, sterol ring oxidation yields the 5α,6α- and 5β,6β-epoxides, which are the result of lipid hydroperoxy radical attack on the Δ^5 double bond with formation of a radical adduct at C-5 or C-6 and subsequent loss of an alkoxyl lipid radical [59]. Though generally a non-enzymatic process, ring oxidation of sterols may also occur through enzymatic processes. The generation of 7α-hydroxycholesterol by CYP7A is the most common example (Fig. 2-1).

In general, side-chain oxidation of cholesterol derivatives occurs through enzymatic modification, with the predominant species being 24-, 25-, and 27-hydroxycholesterol [60]. As an exception to this rule, 25-hydroxycholesterol may also be formed through auto-oxidative processes, but this is less common. 25-hydroxycholesterol is normally a product of cholesterol 25-hydroxylase, a non-heme iron containing protein localized in the endoplasmic reticulum (ER) and Golgi that is expressed in many tissues, albeit at low levels [61]. 24- and 27-hydroxycholesterol are products of the cytochrome P450s cholesterol 24-hydroxylase (CYP46A1) and sterol 27-hydroxylase (CYP27A1), respectively (Fig. 2-1). CYP46A1 is highly expressed in neural cells and localizes to the ER while CYP27A1 is expressed primarily in the liver and macrophages and found in the mitochondria [62, 63].

β-sitosterol and ergosterol, in comparison to cholesterol, seem more susceptible to side chain autoxidation. The additional ethyl group at C-24 allows for

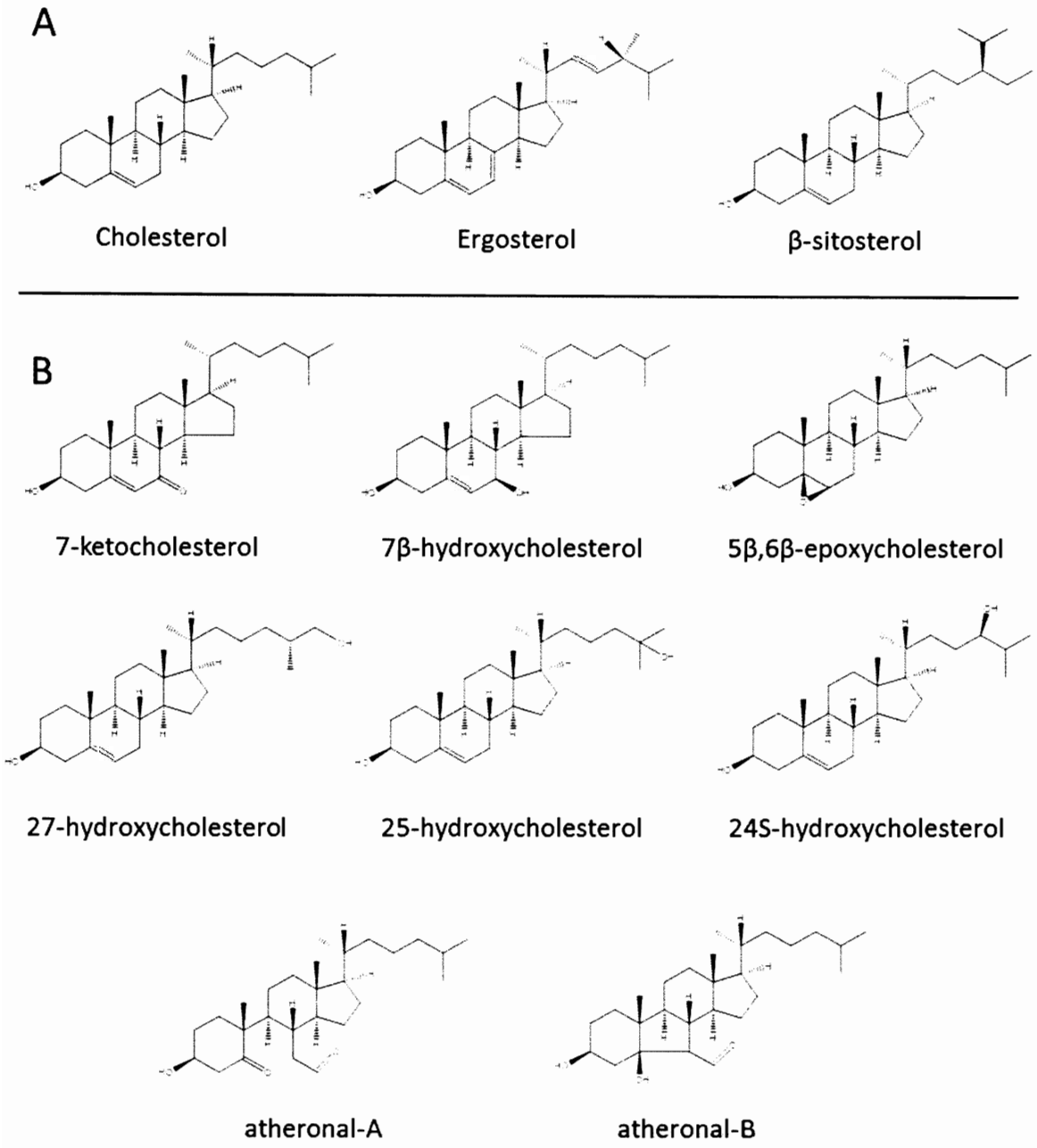

Figure 2-2. Structures of common sterols and oxysterols. Panel **A**, the three most abundant animal, plant, and fungal sterols. Panel **B**, cholesterol oxidation products found in the highest concentrations *in vivo*. Atheronal-A and -B are cholesterol 5,6-secosterols formed by the oxidative cleavage of the steroid nucleus.

a broader range of oxidation products from β-sitosterol, which forms 24-, and 25-hydroxysitosterol [64]. Ergosterol contains not only an additional methyl group, but a double bond in the side chain that increases vulnerability to auto-oxidative forces (Fig. 2-2) [65]. Ergosterol also contains a conjugated diene in ring B that is known to react with singlet oxygen to form ergosterol epidioxide (EEP) and 7-hydroperoxide (EHP). EEP then undergoes immediate enzymatic isomerization to yield 5α,6α-epoxy-(22E)-ergosta-8,22-dien-3β,7α-diol (8-DED), the most predominant ergosterol oxidation product. 9(11)-dehydroergosterol (DHE) is also generated to a lesser extent by decomposition of EHP [66].

2.1. Occurrence of oxysterols

Analytical measurements of oxysterols are experimentally demanding and commonly show great variability between labs. Accurate quantitation may suffer from losses during processing, the presence of interfering materials, artifact formation, the lability of particular species, and insufficient sensitivity of detection [58, 67, 68]. Additionally, losses may occur during separation or hydrolysis steps. Isotope dilution has been found to effectively overcome problems with artifact formation through the use of deuterium-labeled internal standards [69-71]. Solid phase extraction to separate sterols from oxysterols also benefits quantitation as does the use of electrospray ionization mass spectrometry [72, 73].

2.1.1. Environmental oxysterol concentrations

The environmental accumulation of oxysterols may occur in aquatic environments where waste discharge from pulp mills or fat processing facilities takes place. In the pulp and paper industry, lipophilic extractives containing high levels of sterol result in so-called “pitch deposits”. Pitch deposition causes several problems including reduced production, higher equipment and operating costs, and the release of toxic compounds [74]. For 22 US pulp and paper mills tested, total sterol discharge rates ranged from 0.2 g/T to 25 g/T [75]. Approximately 70% of the sterols remaining in bleached pulp were determined to be oxidation products of β-sitosterol [76].

β-sitosterol was also detected in sewage plant effluent in concentrations up to 402 ng/L, and in German rivers and tap water from 60 ng/L [77]. Additionally, it has been found that some natural sterols are not removed from treated wastewater at all [78]. Continuous exposure to these low levels of sterols and oxysterols is enough to elicit endocrine disrupting activity as demonstrated by both field data and experiments with zebrafish [79-81], though no studies have provided definitive evidence as to the identity of the responsible compound(s) [82]. Interestingly, it was found that microbial conversion of phytosterols results in enhanced bioactivity of the transformed fraction [80, 83, 84]. Considering sterol degradation in bacteria is predominantly an oxidative process, it is possible that phytosterol oxidation products may play a role in this phenomenon.

Sterols, and their oxidized derivatives, also accumulate in soil. In three agricultural soils tested, β-sitosterol levels were the highest, with a range from 0.9 to 30 mg kg^{-1}. Ergosterol levels were similar at 0.3 to 24.2 mg kg^{-1}, though cholesterol levels were lower, ranging from 0.2 to 2.4 mg kg^{-1} [85]. The relevance of excessive sterol or oxysterols levels in soil has not been considered, however extreme acidity, lack of aeration, and excessive water content have all been determined as factors that may inhibit the decomposition of sterols, resulting in elevated concentrations [86].

2.1.2. Food oxysterol concentrations

Oxysterols have been found in a variety of foods of both plant and animal origin, including dairy products, liquid eggs and dried egg products, meat and meat products, fried foods, flour, potato products, and vegetable oils [51, 87-90]. In most food, levels are typically low, but their concentrations may be significantly increased due to processing and storage. In particular, heating and exposure to either air or radiation may increase oxysterol concentrations [91, 92]. Studies have shown that both temperature and heating time affect sterol oxidation. Other determining factors are sterol structure and lipid matrix composition. Interactions between different lipid matrices and temperatures have strong effects on oxysterol formation and the reaction pathways of oxidation. Specifically it was found that at low temperatures (< 140^0C) sterols were less stable in an unsaturated matrix than in a saturated matrix, while at high temperatures (> 140^0C) the reverse is true [93]. It has been shown that the oxysterol percent of cholesterol in meat increases between 0.3 to 0.8% during normal cooking, and

that oxysterol content doubled after storage for three months at -20^{0}C [94]. In fact, several studies have indicated oxysterol levels in excess of 1% total cholesterol [91] from food of animal origin. This has been found true of oxidized phytosterols as well, with concentrations routinely found in excess of 1% total sterol [90]. Ghee, a clarified butter product used in Indian cooking, contains over 12% oxysterols as a percent of total sterol [95]. The most common oxysterols in food are the major products of autoxidation, namely the 7-oxygenated derivatives.

2.1.3. Dietary Intake of Oxysterols

Oxysterol concentrations *in vivo* are a combination of endogenous sources and dietary supply. Mean intake for a cholesterol-low diet has been estimated at 3.0 mg/day and 0.7 mg/day for cholesterol and phytosterol oxidation products respectively [87, 89, 96]. However, the use of phytosterol-enriched foods may increase intake dramatically, with certain consumers ingesting an average of 3 to 6 g/day of phytosterol [97]. This would result in approximately 30 to 60 mg/day of phytosterol oxidation products.

After ingestion, sterols, along with any oxysterols, are absorbed by enterocytes and incorporated into chylomicrons which are secreted into the lymph and circulation via the thoracic duct. Ingestion of cholesterol-rich food has been found to cause a maximal increase in free plasma COP concentrations after 3 h and total plasma COP after 8 h, though no change in the total COP:total cholesterol ratio was observed. Analysis of COP in the chylomicron fractions

revealed an identical composition but with differing proportions as compared to diet, indicating different absorption rates for each oxysterol. In particular, 7-ketocholesterol (7KC), cholestanetriol, and cholesterol-α-epoxide were underrepresented in the chylomicron as compared to 7α- and 7β-hydroxycholesterol, which were present in greater proportion [51]. Though the literature contains little data for COP absorption in humans, studies in rats have shown 7KC rates to be only 12% over 24 h, while those of 7α- and 7β-hydroxycholesterol were 30% and 42% respectively [98]. Phytosterol absorption rates are generally lower than those of their cholesterol analogs (< 10%), but it has been found that a diet containing oxidized phytosterols increases the concentration of absorption of cholesterol oxidation products [99].

In the plasma, free COP may serve as a substrate for lecithin:cholesterol acyltransferase (LCAT). Esterification by LCAT promotes the incorporation of COP into lipoproteins, and movement of esters between different lipoproteins is facilitated by cholesteryl ester transfer protein [100, 101]. The extent of esterification varies substantially for each cholesterol derivative, though approximately 90% of total COP in the plasma is in the form of acyl esters [51, 70]. Esterification of oxysterols decreases their solubility in the plasma and immobilizes them in the lipoprotein fraction. This has significant implications regarding the plasma clearance of these oxysterols and their associated lipoproteins. Normal metabolism of chylomicrons involves their extra-hepatic conversion to chylomicron remnants by endothelial lipoprotein lipase. During this transformation, lipids and fat-soluble antioxidants are retained and subsequently

transported to the liver for incorporation into VLDL [102]. However, it has been found that inclusion of oxysterols into chylomicrons reduces their metabolism and uptake by extra-hepatic tissue through alterations to chylomicron structure and composition. This results in increased delivery to, and retention of these particles by, the arterial wall [103, 104], and it has been found that their increased antioxidant content may further enhance uptake in macrophages [105, 106]. This implies that oxysterols may be selectively concentrated in certain cells and tissues relative to levels throughout the rest of the body.

2.1.4. De novo synthesis and intracellular transport of cholesterol and oxysterols

In higher eukaryotes, all nucleated cells are able to synthesize cholesterol through the melavonate pathway. The initial step in cholesterol biosynthesis is the formation of acetoacetyl-CoA from two acetyl-CoA molecules. Condensation of a third acetyl-CoA results in production of 3-hydroxy-3methylglutaryl coenzyme A (HMG-CoA). The reduction of HMG-CoA yields melavonate, which undergoes a series of phosphorylations and a decarboxylation to produce isopentenyl pyrophosphate (IPP). IPP polymerizes to form geranyl pyrophosphate (GPP) and farnesyl pyrophosphate (FPP). Since FPP is utilized in several biosynthetic pathways, the first dedicated step of sterol synthesis is condensation of two molecules of FPP to yield squalene. Further cyclization and demethylation yields cholesterol [107].

De novo synthesis is estimated to account for 70% of total body cholesterol [108], with a production rate of approximately 9 mg/day/kg body weight [109]. While most cells are capable of endogenous cholesterol synthesis, the liver is the primary site of production and turnover, producing as much as the rest of the body does collectively. Excess hepatic cholesterol may be excreted as bile, used for steroid hormone synthesis, or secreted in the plasma through incorporation into VLDL. VLDL is processed into IDL, and subsequently LDL, by endothelial lipoprotein lipase. The smaller size of LDL particles allows them to penetrate the endothelium, where they may be assimilated by cells expressing LDL receptor (LDLR) or through pinocytosis.

LDLR-mediated uptake is estimated to account for 65-80% of the clearance of LDL in humans [109]. LDLR is present on the plasma membrane of most cells, where it binds particles containing apolipoproteins B or E. Bound particles are endocytosed by clathrin-coated vesicles and transported to endocytic compartments for hydrolysis. Acid lipase hydrolyzes cholesteryl esters transported by the LDL, allowing the free sterol to exit the compartment.

Besides being a carrier of cholesterol, LDL may incorporate oxysterols in the liver or undergo oxidative modification in the sub-endothelial region [110]. Extracellular oxidized LDL (oxLDL) undergoes receptor-mediated uptake by macrophage type I or type II class A scavenger receptors (MSR-A) [111], CD36 [112] and lectin-like oxLDL receptor-1 (LOX-1) [113, 114]. Unlike the normal route of LDL uptake, these receptor-mediated pathways are not regulated by cellular cholesterol content and may lead to high intracellular levels of oxLDL and

its associated oxysterols. LDL is also susceptible to oxidative modification within the lysosome, resulting in the production of free or esterified 7KC and 7β-hydroxycholesterol [115, 116].

2.1.5. Environmental risk factors

Environmental exposure to certain toxins or pollutants may also increase oxysterol concentrations *in vivo*. Ozone exposure has been found to increase the levels of 5β,6β-epoxycholesterol and secosterol in lung epithelium through reactions with cholesterol [117, 118]. Secosterols are unique cholesterol oxidation products in that they are formed via the oxidative cleavage of the steroid nucleus, whereas all other oxysterols are products of peripheral oxidation. Atheronal-A and -B (Fig. 2-2) are two such secosterols that have been detected in human lung surfactant, plasma, and atherosclerotic plaques. Plasma levels of atheronal-B vary from 20 to 500 nM, though ranges between 3 and 25 μM are thought to exist within atherosclerotic plaques, with effects similar to 7KC at these concentrations [119].

Exposure to high levels of either iron or copper is strongly correlated with increased levels of oxysterols. While iron and copper are both essential to life, they are also transition elements that catalyze the formation of reactive oxygen species through Fenton chemistry:

$$(1) \quad Fe^{2+} + H_2O_2 \rightarrow Fe^{3+} + OH\cdot + OH^-$$

$$(2) \quad Fe^{3+} + H_2O_2 \rightarrow Fe^{2+} + OOH\cdot + H^+$$

In vivo, excess metals are normally stored and transported bound to other molecules; by ferritin and transferrin in the case of iron, and metallothioneins and ceruloplasmin for copper. However, saturation of these metal-binding proteins may occur, increasing the labile iron and copper pools, and consequently ROS levels as well. ROS subsequently react with sterols to produce oxysterols. Interestingly, it has also recently been discovered that iron nanoparticles, while displaying limited toxicity of their own, significantly enhance the cytotoxic and pro-inflammatory action of 7KC towards cardiac cells [10].

Smoking has also been found to increase the levels of circulating oxysterols [9]. The same study reported similar increases in patients suffering from diabetes mellitus. It is likely that any process which results in increased ROS generation will consequently raise oxysterol levels.

2.2. Effects of oxysterols

The proper proportion of sterol in the plasma and organellar membranes is essential for many cellular functions. Therefore, understanding intracellular sterol dynamics is critical to understanding how excessive levels of oxysterols can disrupt cellular homeostasis. Compared to other lipids, the atypical structure of sterols provides them with unique transport properties that allow them to quickly reach a state of chemical equilibrium within the cell. This

characteristic provides sterols, and their oxidation products, with an influential role in determining membrane properties [120].

2.2.1. Intracellular sterol dynamics

In a typical mammalian cell, there exist approximately 6 x 10^8 sterol molecules, 35% of which are located in the endocytic compartment, and 50% contained in the plasma membrane. Sterol equilibration between the plasma membrane and the endocytic compartment occurs within 2-3 minutes, at a rate of 10^6 sterol molecules per second. This process is thought to be facilitated by soluble lipid transfer proteins (LTP), which may interact with membrane proteins in the targeted bilayer. However, it was found that most sterol is still delivered to the endocytic compartment in preference to other organelles even when targeting capability was lacking. This may imply that the cytosolic leaflet of the endocytic compartment is maintained in a state thermodynamically favorable for sterol acceptance [120, 121].

The "umbrella model" has been used to describe the biophysical basis for sterol membrane stabilization. This model suggests that the mismatch between the hydroxyl group of cholesterol and the size of its non-polar region necessitates protection from exposure to water by other membrane lipids (Fig. 2-3). Therefore phospholipids with larger heads, such as phosphatidylcholine or sphingomyelin (~70 $Å^2$), preferentially associate with cholesterol, as compared to those with smaller heads such as phosphatidylethanolamine (~40 $Å^2$). As membrane sterol levels increase, the phospholipid heads are stretched and the acyl chains

become more tightly packed with cholesterol. This increased density is also the reason for the decrease in membrane permeability associated with elevated cholesterol concentrations. However, too large of a cholesterol concentration results in exposure of some molecules to water. These unshielded sterols have a greater chemical activity, or availability for a chemical or physical transition, and as such have a greater propensity to leave the membrane [120, 122, 123]. Acyl chain unsaturation is also important within this framework because of the effects it may have on lipid geometry in the bilayer. A larger degree of unsaturation results in a greater cross-section of the acyl chain, providing less space for cholesterol. Based on this, it is apparent that the phospholipid composition of a membrane helps determine its sterol concentration. Some evidence of this can be seen by comparing the acyl chain saturation of the plasma membrane to the endoplasmic reticulum (ER). Only 25% of phosphatidylserine acyl chains are saturated in the ER, while almost 90% are saturated in the plasma membrane. Accordingly, the ER retains only 5% of total cell cholesterol while the plasma membrane holds 35% [120].

The chemical activity coefficient is useful in explaining the asymmetric distribution of sterols in different subcellular locations:

$$\alpha = \gamma c \qquad [1]$$

where α is chemical activity, γ is the chemical activity coefficient, and c is the sterol concentration [120]. From Eq. 1 it is easy to see how the chemical activities of different membranes can be in equilibrium while maintaining different

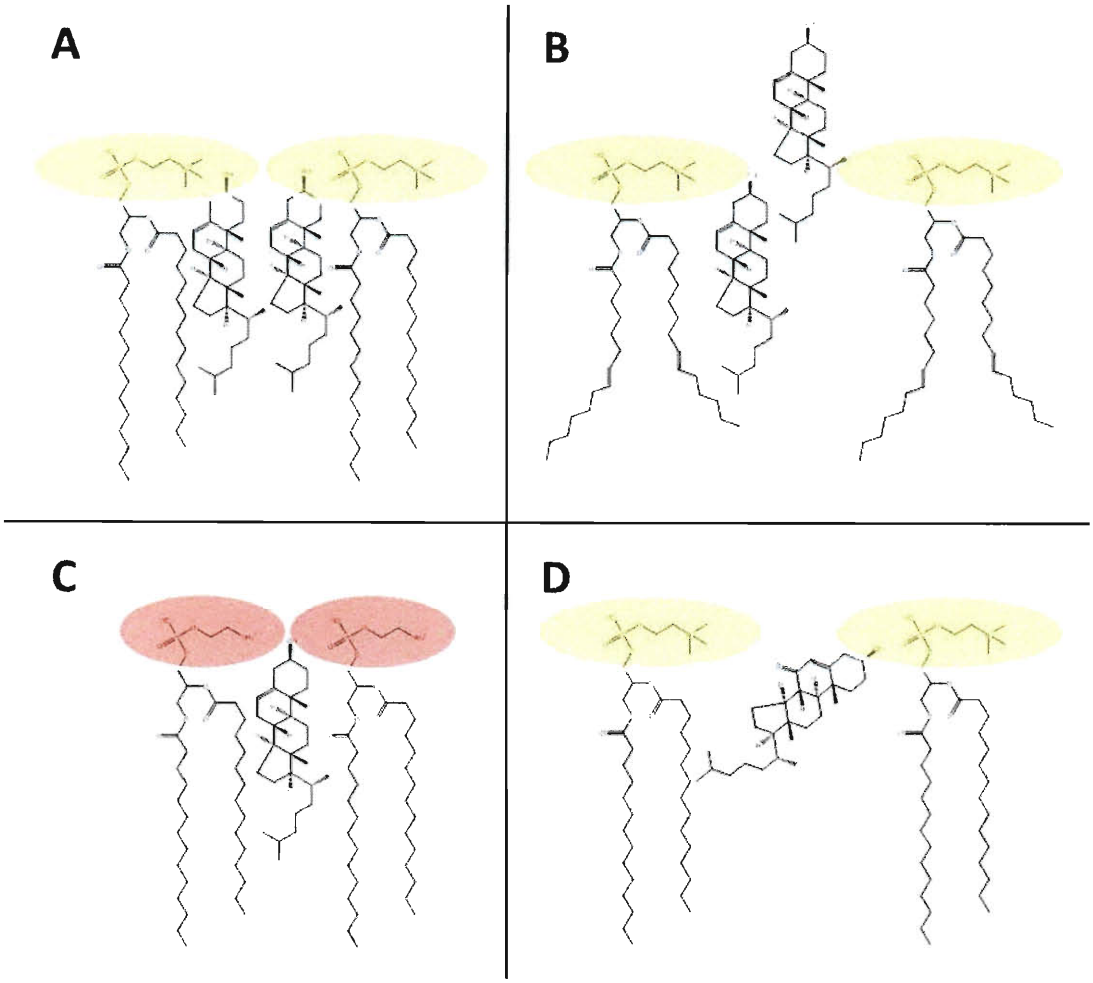

Figure 2-3. Sterol membrane interactions. Various sterol/phospholipid configurations are shown to illustrate the effect of oxysterols on membrane properties. **A**. Cholesterol preferentially associates with phosphatidylcholine (PC) due to its larger head size, which shields the hydrophobic body of cholesterol. **B**. The spacing between phospholipids is partially determined by the degree of acyl chain saturation. Greater saturation results in less room for cholesterol, and therefore increases its chemical activity and propensity to leave the membrane. **C**. Smaller phospholipid heads, such as that of phosphatidylethanolamine, can shield fewer cholesterol molecules, also increasing chemical activity. **D**. 7KC, due to its additional oxygen moiety, inserts in the membrane at a tilt with respect to cholesterol, increasing the distance between phospholipids with resultant depletion of cholesterol and increased membrane permeability.

concentrations of sterols (due to differing phospholipid composition). The coefficient may be lowered by favorable interactions, resulting in an increased membrane capacity of sterol.

One of the principal roles of cholesterol is organization of membrane structure, which it accomplishes through increasing bilayer thickness, decreasing interfacial hydration, decreasing membrane permeability, restricting acyl chain movement, and formation of liquid-ordered (L_o) domains [124-128]. L_o domains, or lipid rafts, are regions of laterally organized lipid that exist within the bilayer. Proteins are hypothesized to target these regions due to interactions with cholesterol and sphingolipid, which encase the protein in a lipid shell [129, 130]. Several important roles are attributed to L_o domains, including endocytosis and signal transduction events [131].

2.2.2. The impact of oxysterol enrichment on cellular membranes

Oxysterols that are incorporated into cellular membranes effectively displace cholesterol and may alter the biophysical properties of the membrane [128, 132]. Additionally, they are capable of passing between membranes orders of magnitude faster than cholesterol and may inhibit cholesterol-mediated processes [133]. The exact effect a given oxysterol has is dependent on the location and extent of oxidation, though side-chain oxidized sterols favor a horizontal orientation to the membrane surface, while nucleus oxidized sterols adopt a tilted orientation [128, 134, 135]. These differences in orientation, as compared to cholesterol, would tend to increase the chemical activity of

membrane sterol, resulting in depletion of cholesterol with corresponding changes in membrane organization. Results have indicated that 7-oxygenated sterols do not insert as far into the lipid bilayer as cholesterol, and are less efficient at forming L_o domains [128]. Enrichment of L_o domains with 7KC, for example, results in reduced cholesterol efflux [136], increased apoptosis due to Ca^{2+} influx [137], and increased intercellular communication which may disrupt differentiation and proliferation [138, 139]. Although it has been suggested that normal oxysterol levels are too low to cause significant effects, recent evidence has indicated that in high-cholesterol membranes the difference in cholesterol between L_o and L_d domains is small [140, 141]. Additionally, some oxysterols preferentially partition to L_o domains, increasing their concentration beyond what would normally be expected [136, 137]. The effect of oxysterol displacement, therefore, could be substantial. Differences in interactions between phospholipids and oxysterols may also have effects on membrane curvature, with implications for transmembrane proteins [132, 142]. Furthermore, due to their increased hydrophilicity, many oxysterols have reduced membrane condensing activity with consequent increases in permeability [143], and have also been found to partition to organellar membranes that are typically low in cholesterol.

Some oxysterols, notably 7KC, are potent inducers of phospholipidosis, a lysosomal storage disorder characterized by the presence of cytosolic lamellar bodies containing phospholipids as well as lipoprotein and other lipids [144, 145]. Currently, however, it is uncertain whether this is a defense response, or part of the cell death pathway. Incubation of U937 cells with 7KC caused lysosomal and

mitochondrial membrane permeabilization in a sequential manner, ultimately inducing either apoptosis or necrosis [146]. Eukaryotic cells contain at least two separate calcium-dependent apoptotic pathways: one modulated by calpain and the other calpain-independent [147]. Calpain has also been implicated in neuronal death following ischemic insult by initiating lysosomal rupture and subsequent cathepsin B release [148, 149]. The ability of 7KC to disrupt cellular Ca^{2+} homeostasis is likely integral to its toxicity [137, 150, 151]. Evidence for this is also supported by the prevention of 7KC-induced mitochondrial damage through the addition of calmodulin inhibitors [152]. How 7KC induces Ca^{2+} influx is still a matter of research, though it was found that it and several other oxysterols could increase ion conductivity in membranes lacking proteins [143].

2.2.3. The role of oxysterols in disease

Due to the ability of oxysterols to dysregulate normal physiological function, they are also potential contributors to the initiation and development of disease. The most commonly encountered oxysterols are those with either a keto or hydroxyl group at the C-7 position of the steroid nucleus, and these also tend to be the species most detrimental to cell viability. C-7 modified sterols commonly have pro-apoptotic, pro-oxidative, and pro-inflammatory activities [40, 41, 146, 153]. Amongst these compounds, 7KC is one of the most predominant and widely studied, principally due to its suspected involvement in various human pathological conditions such as atherosclerosis [5, 40, 154] and Alzheimer's disease [6, 7, 44, 72]. Oxysterols are also suspected to play a role in the progression of age-related macular degeneration [15, 45] and cataract formation

[155]. Levels of oxysterols in the lens and retinal pigment epithelial cells are known to accumulate to quantifiable levels with advancing age and may trigger cytotoxic effects. Furthermore, structural analogues of 7KC, such as 7-ketositosterol and 7β-hydroxysitosterol which are derived from β-sitosterol, have been found to be cytotoxic to a number of cell lines [156] and accumulate intracellularly [99].

While many of the diseases affected by oxysterols are independent of each other, they share convergent processes. Many only manifest at an advanced age, presumably due to the associated increase in oxidative stress or inflammation. This leads to increased *in vivo* oxysterol production which accelerates cell death, and consequently may initiate or accelerate the development of disease. Moreover, oxysterols have been found to increase ROS production [146], thereby creating a positive feedback loop for their own production. Several diseases in which oxysterols play a prominent role are explored in the following sections.

2.2.3.1. Atherosclerosis

Atherosclerosis is a progressive disease of the arterial blood vessels and the principle contributor to the pathogenesis of myocardial and cerebral infarction. As such, it is the leading cause of all mortality in the United States, Europe, and Japan [157]. Though the disease is highly ubiquitous, it has an extremely complex etiology that hinders the development of effective treatments. The earliest symptoms are lesions known as “fatty streaks,” an aggregation of

lipid-rich macrophages and T-lymphocytes within the sub-endothelial matrix that may be a result of arterial injury [158]. Remarkably, these early-stage lesions were found to exist in half of autopsy samples from children aged 10 to 14 [159]. Initiation and progression of "fatty steaks" to fibrous plaques is an inflammatory process that increases cell influx and proliferation at the site of injury, finally leading to the development of the advanced lesions that precede heart attack or stroke.

A major component of atherosclerotic plaques is the foam cell: macrophages or smooth muscle cells containing large amounts of lipid derived from low-density lipoprotein (LDL). LDL is capable of diffusing passively through endothelial cell junctions, and its accumulation is a primary event in atherosclerosis, though its uptake in native form is not rapid enough to generate foam cells [111]. Native LDL, however, is oxidized in the sub-endothelial region [110] or within the lysosome [116] by various processes likely mediated by free radicals or reactive oxygen species (ROS). Extracellular oxidized LDL (oxLDL) undergoes receptor-mediated uptake by macrophage type I or type II class A scavenger receptors (MSR-A) [111], CD36 [112] and lectin-like oxLDL receptor-1 (LOX-1) [113, 114]. Unlike the normal route of LDL uptake, these receptor-mediated pathways are not regulated by cellular cholesterol content and may lead to high intracellular levels of oxLDL. Inhibition of MSR-A and CD36 has been shown to reduce atherosclerotic plaque size [160] and foam-cell formation [161]. Conversely, normal macrophages treated with oxLDL quickly become foam cells, accumulating free cholesterol (FC) and displaying reduced lysosomal

cholesteryl ester (CE) hydrolysis [162]. OxLDL is now widely regarded as a primary factor contributing to the development of atherosclerotic lesions, having been found cytotoxic to a variety of cell types. OxLDL also possesses a number of other atherogenic properties, such as inhibition of cholesterol efflux, increased expression of cellular adhesion molecules, and stimulation of macrophage proliferation [5, 40, 163, 164]. Taken together, these properties may lead to plaque instability, increasing the chance of rupture.

After endocytosis, LDL is delivered to the lysosome, where CE may be hydrolyzed and FC released. Lysosomal FC egress is mediated by Niemann Pick C proteins Type 1 and 2 (NPC) [165], which are believed to transfer FC to acceptor vesicles or directly to the plasma membrane before proceeding to the endoplasmic reticulum [166]. Typically macrophages are protected from excess FC accumulation through acyl-coenzyme A:cholesterol acyltransferase (ACAT) re-esterification in the cytosol and cholesterol efflux. In atherosclerosis, however, intralysosomal FC accumulation occurs, followed by CE accumulation [167]. This series of events has been observed not only in macrophages treated with oxLDL, but in aggregated LDL (aggLDL) and CE dispersion particles (DISP) [168]. Acetylated-LDL (acLDL), however, is not able to achieve FC accumulation, instead forming cytosolic CE inclusions [169]. This is curious, because acLDL is endocytosed by MSR-A, as is oxLDL. AcLDL is not endocytosed by LOX-1, however [113], and was not found to induce apoptosis at the concentration of oxLDL. Similarly, native LDL and cholesterol could not initiate apoptosis at as low of a level as oxLDL [170].

Recent research shows that intra-lysosomal FC accumulation inactivates the vacuolar-ATPases that maintain lysosomal pH, likely by partitioning to the lysosomal membrane and exerting a direct effect on the proteins [162]. This drop in pH subsequently inactivates acid lipase and other hydrolases, leading to CE accumulation. And while it may seem obvious that the unregulated uptake of modified LDL through scavenger receptors could provide the excess FC, the question arises as to why acLDL does not cause the same accumulations, especially considering aggLDL and DISP are unoxidized as well. Answers to this may lie in the resistance of oxLDL to lysosomal degradation [171] and to the observation that acLDL is degraded even more rapidly than native LDL [172]. OxLDL is also more resistant to degradation than either aggLDL or DISP [168], and it is also possible that aggLDL and DISP are oxidized within the lysosome [116].

Many of the effects of oxLDL, including cytotoxicity, can be attributed to one of its primary components, 7KC [5]. The average LDL particle contains approximately 600 molecules of cholesterol and 1600 molecules of cholesteryl ester (CE), all of which are susceptible to oxidation prior to and during uptake [173]. Non-enzymatic oxidation of cholesterol predominately occurs at the 7-carbon of the steroid nucleus, a region associated with the greatest cytotoxicity [5, 40, 41, 146, 153]. Similar to cholesterol, 7KC partitions intracellularly to the plasma and organellar membranes [174], though its slightly higher polarity alters their biophysical properties [128, 175]. Several studies have found 7KC to increase disorder in membrane structure, altering curvature and the properties of

nearby membrane-bound proteins [132, 142]. In smooth muscle cells, 7KC was discovered to increase ROS production through up-regulation of NAD(P)H oxidase [176]. 7KC is also known to induce several pro-inflammatory cytokines, including interleukin-1β [177], interleukin-6 (IL6) [178], and interleukin-8 (IL8) [53, 179].

Due to its high concentration in atherosclerotic plaques [180-182], cytotoxicity, and other pro-atherogenic properties, 7KC is a prominent target for attenuation of atherosclerosis. Contributing to the rationale for its elimination is that 7KC has also been associated with Alzheimer's disease by several studies [7, 43, 183]. These two diseases share many similar risk factors, notably many involving cholesterol homeostasis. While FC alone has the ability to destabilize lysosomes and hinder CE hydrolysis, the etiology of atherosclerosis is clearly a complex process, and 7KC certainly contributes. Reducing levels of 7KC may subsequently reduce the rate of LDL uptake and apoptosis, slowing atherosclerotic progression.

2.2.3.2. Alzheimer's Disease

Alzheimer's disease (AD) is a progressive neurodegenerative disorder that increasingly affects millions worldwide and is the greatest cause of dementia in Western society. It is estimated that US annual incidence rates will surpass 950,000 by 2050, affecting 62% of those 85 and older [184]. It has also been estimated that delaying the onset of AD by just two years would decrease the number of cases in the US in 50 years by approximately two million [185].

AD is characterized by two neuropathological hallmarks: senile plaques composed primarily of extracellular amyloid beta (Aβ) deposits [186, 187] and neurofibrillary tangles (NFT) generated from intraneuronal accumulations of abnormal tau protein. Aβ is a peptide of 39-43 amino acids formed by successive cleavage of amyloid precursor protein (APP) by β- and γ-secretases. While Aβ40 is the most common isoform, Aβ42 is most typically associated with progression of AD, accumulating first intracellularly, where it alters the normal metabolism of APP and promotes lysosomal APP accumulation [188]. Tau proteins are microtubule-associated proteins with six isoforms that exist in brain tissue. Hyperphosphorylation of tau causes self-assembly into paired helical filaments that are present in AD and several other tautopathies [189].

It should be noted that many factors involved in AD have also been found determinate of other pathologies. For example, over 100 genes have been found to be associated with AD, and many of these are also highly correlated with atherosclerosis [7, 183]. In fact, APP and Aβ can oxidize cholesterol to 7β-hydroxycholesterol, which can be subsequently oxidized to 7KC [44]. Another association between atherosclerosis and AD are the parallels found between Niemann-Pick disease and both aforementioned diseases [190]. Lysosomal dysfunction likely has a primary role in all of these processes [191]. Relationships between frontotemporal dementias, Parkinson's disease, and AD have also been discovered [192]. These may be a result of inflammatory processes, increased tissue transglutaminase [193], or some other factor, but usually the causes of pathogenesis are attributed to just a few compounds. In

AD, this is most often Aβ or tau proteins, both of which may be useful targets for therapy, however 7KC may play a vital role as well, and reducing its levels could help stall AD progression. Apolipoprotein D, a neuroprotective protein that attenuates 7KC formation by binding cholesterol, is highly expressed in AD, as well as Parkinson's, Niemann-Pick, and other types of brain injury [194]. This may be indicative of the need to protect from 7KC formation. While total membrane cholesterol turnover is typically only 0.7% per day, this rate is much lower in the central nervous system, averaging approximately 0.03% per day [195]. The implication of this is that oxysterols may persist longer in the brain. Granted, oxidation should increase the efflux of these compounds, but this may not be enough to overcome an overall accumulation of oxysterols to concentrations that are cytotoxic. The ability to control oxysterol levels in the CNS may therefore be beneficial in the case of many neurodegenerative disorders where oxidative stress is a hallmark.

2.2.3.3. Age-related macular degeneration

Age-related macular degeneration (AMD) is a complex group of diseases that are the leading cause of blindness in people over 50 years of age in the developed world [196]. It currently affects approximately 8 million adults in the US, with an expected increase of over 50% by the year 2020 [197]. The first signs of AMD are typically deposits of protein and lipid, called drusen, which form between the retinal pigment epithelium (RPE) and Bruch's membrane. Damage to the RPE, as well as a chronic inflammatory response, lead to retinal atrophy, and subsequent choroidal neovascularization. These newly formed blood vessels

are often malformed and fragile, allowing blood to contact photoreceptors and other retinal cells, resulting in massive damage to the surrounding tissue [198].

7KC is present in appreciable quantity in the retina, where it is believed to be formed through iron-catalyzed free radical oxidation [199-201]. The retina contains high levels of iron that is normally bound to either ferritin or cytochrome c. However, light is known to liberate iron from ferritin [202], and hydrogen peroxide may cause iron release from cytochrome c [203], leaving the iron free to participate in Fenton chemistry. Additionally, drusen may accumulate significant levels of 7KC, which promotes macrophage migration, and consequent secretion of vascular endothelial growth factor and metalloproteinases. The former may lead to neovascularization while the latter can initiate membrane disruption [14]. Therefore, reduction of 7KC levels in the retina may help slow the progression of AMD, or help reduce the chance of its onset.

2.2.4. Other diseases

While atherosclerosis, Alzheimer's, and AMD are the most commonly cited diseases with regard to oxysterols, recent research is revealing a broader pathological role for these molecules. We have already mentioned the ability of oxysterols to perturb normal membrane structure and increase ROS formation. ROS, in turn, are capable of damaging many cell components, including DNA, lipids, and proteins. Accumulating damage can cause changes in gene expression with further consequences. Additionally, several studies have labeled particular oxysterols (commonly including 7KC) as mutagenic, as their levels are

correlated to both nuclear and mitochondrial DNA damage [204, 205]. Subsequently, these same oxysterols were determined to play a role in carcinogenesis [206]. And, as shown by Smith *et al.*, normally non-mutagenic cholesterol that is heated in air becomes mutagenic to *Salmonella typhimurium*. This indicates a direct role for oxysterols, instead of an indirect role, regarding DNA damage. Oxysterols have also been found to cause an increase in protein ubiquitination and elicit changes in proteosomal degradation [207]. Clearly the etiology of oxysterol-induced toxicity is complex and may affect almost every area of cell function.

2.3. Elimination and detoxification of oxysterols

Many enzymes that transform cholesterol are also able to utilize oxysterols as substrates (Fig. 2-4). Both ACAT and LCAT esterify oxysterols, which helps mitigate their cytotoxicity [100, 208]. In fact, the majority of both circulatory and intracellular oxysterols are esterified [70, 174, 209]. Esterification of intracellular free cholesterol is necessary for proper regulation of membrane cholesterol levels, and the additional use of oxysterols as substrates allows for their incorporation into the same metabolically inert cytoplasmic pool.

Side chain hydroxylation is effective in facilitating reverse cholesterol transport, and the same process may also help control intracellular oxysterol levels. Sterol 27-hydroxylase (CYP27A1) is known to act on some ring-oxidized

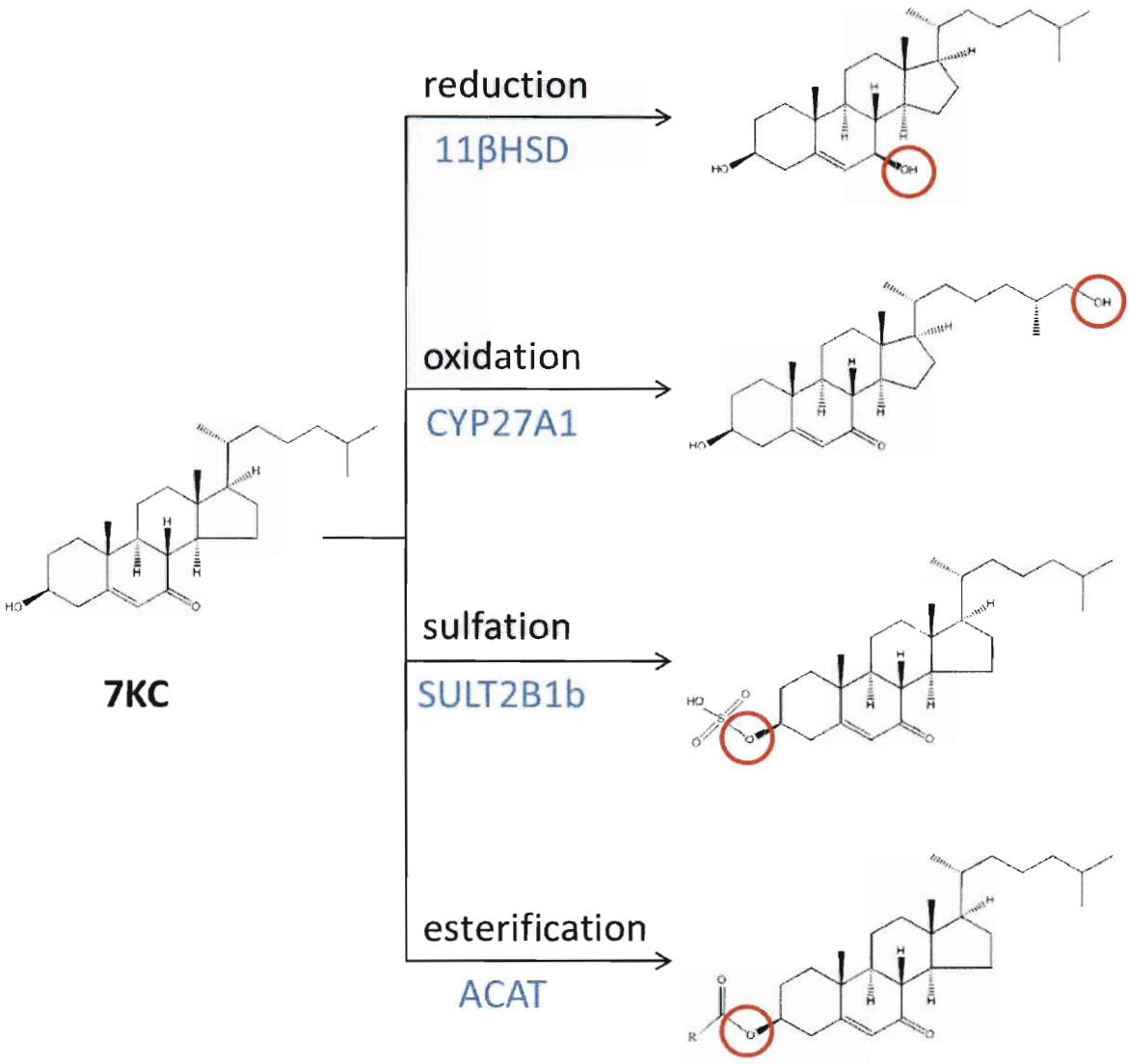

Figure 2-4. Mammalian pathways of 7KC detoxification. 7KC undergoes several transformations in mammalian cells, including reduction to 7βHC by 11β-hydroxysteroid dehydrogenase; side chain hydroxylation by CYP27A1; sulfation of the 3β-OH moiety by SULT2B1b; and esterification by ACAT.

sterols, resulting in reduced cellular toxicity [210]. Elimination of oxysterols also proceeds via sulfation, catalyzed by cholesterol sulfotransferase enzyme (SULT2B1b). Expression of SULT2B1b has been found to attenuate the toxicity of some ring-oxidized sterols as well as suppress cholesterol biosynthesis [211, 212].

Oxysterol export may occur via lipophilic acceptors such as HDL, a process mediated by membrane lipid transporters. ATP-binding cassette, subfamily A, member 1 (ABCA1) has been found to export 7KC to apolipoprotein A1 (apoA1), though at a much lower rate than cholesterol [136, 213]. ABCG1 is also thought to promote export of both 7KC and 7β-hydroxycholesterol to HDL, and there is evidence that it can protect against apoptosis and impaired endothelial cell function [214, 215]. However, mass transfer of 7KC is also seen from HDL to cells if the oxysterol content of HDL is sufficiently elevated. This mechanism of traffic is more consistent with scavenger receptor BI-mediated transport. In fact, cholesterol and oxysterol transport may occur in opposite directions simultaneously depending on the state of sterol loading [216, 217].

So how would it be possible to mitigate the effects of 7KC in vivo? A number of transformations may reduce its toxicity, with the most obvious example being side-chain hydroxylation. The addition of an oxygen-containing group to the 24- or 27-carbon of the cholesterol side chain increases its ability to traverse cell membranes and allows migration through the blood-brain barrier for easier excretion [218, 219]. Sterol 27-hydroxylase catalyzes the formation of 27-hydroxycholesterol, the most abundant oxysterol found in atherosclerotic

plaques, and is present in macrophages as well as the liver and several other organs [220-222]. It was also found to utilize 7KC as a substrate, facilitating its secretion [223]. Unfortunately, high levels of 27OH-7KC still accumulate in lesions and foam cells. This may indicate that expression of sterol 27-hydroxylase alone is not sufficient to overcome atherosclerotic progression or that the enzyme is not expressed highly enough to compensate for the increased cholesterol and oxysterol burden. Further testing of this enzyme is warranted.

Another potential route of remediation would be removal of the 7-keto moiety, which generates cholesterol, reducing toxicity to corresponding levels. A mechanism was recently discovered through which 7KC is reduced to 7β-hydroxycholesterol (7β-OH-Ch) by 11β-hydroxysteroid dehydrogenase type 1 [224]. 7β-OH-Ch, however, is more cytotoxic than 7KC; thus, hydrolysis of the hydroxyl group would be necessary. Conversion of 7KC to 7α-OH-Ch is preferable, as the latter has a much reduced toxicity and is normally formed as an intermediate in the production of bile acid in the liver by cholesterol 7α-hydroxylase [225]. Because an enzyme catalyzing the removal of the 7-OH group is not endogenous to humans, this function would have to be supplied exogenously. Our lab recently found evidence of a hydrolase in *Rhodococcus jostii* RHA1 capable of removing a 7-OH group from 7-hydroxycholesterol and a number of its metabolites. Research is being performed to see if this enzyme will be an effective catalyst in human foam cells.

Many microorganisms that catabolize cholesterol are able to cleave the steroid nucleus [20, 31, 226]. Steroid ring fission may facilitate endogenous

enzymatic attack in humans, though this is a purely speculative idea and it is unclear what effect the byproducts would have. Another possibility is manipulation of esterification. It has been theorized that oxLDL could accentuate accumulation of CE through inactivation of lysosomal acid lipase (LAL). In fact, exogenous supplementation with lysosomal acid lipase was previously shown to reduce the size of atherosclerotic plaques in mice [227]. Therefore, controlling the esterification of oxysterols may help reduce toxicity or facilitate efflux.

2.4. Summary

Oxysterols are a large class of compounds that were previously regarded as minor sterol metabolites with little physiological impact. Research over the past two decades has exposed their role as important, biologically active compounds that affect a wide variety of intracellular processes despite their low concentrations. The delay in understanding the effects of oxysterols is likely due to the difficulties encountered during their analysis, however new analytical techniques and research into the effect of different oxysterols on membrane properties has yielded promising results and accelerated the pace of research.

Nevertheless, critical gaps in our knowledge still exist regarding oxysterols. For example, most cytotoxicity studies have used exogenously added oxysterols, often simply solubilized in ethanol, assuming that this method replicates conditions found *in vivo*. However, many oxysterols are formed intracellularly, and those of dietary origin usually enter the cell as oxLDL.

Additionally, many studies assay oxysterols individually while, in fact, they have been shown to work synergistically.

Perhaps one of the most limiting factors in oxysterol research is an inability to selectively control their levels, whether *in vitro* or *in vivo*. Few studies have examined the subcellular distribution of these compounds, though where and how they accumulate is of paramount importance. For example, lysosomal accumulations of 7KC can lead to apoptosis, while accumulation in the ER initiates the unfolded protein response. Developing methods to reduce oxysterol levels in specific subcellular compartments would be invaluable in helping elucidate their effects, especially their association with age-related disease. In this thesis we investigate both novel methods of transforming 7KC and strategies for reducing its concentration intracellularly, particularly the lysosome. The broad diversity of organisms displaying the ability to degrade oxysterols provides a wide range of enzymatic mechanisms that can not only effect the transformation of 7KC, but also cholesterol or other sterols that may contribute to pathogenesis. It is our hope that in mining the catabolic capacity of these organisms we are able to discover enzymes capable of transforming oxysterols, and that we can successfully apply this knowledge to controlling intracellular levels of 7KC.

Chapter 3

Microbial Degradation of 7-Ketocholesterol

3.1. Introduction

Oxysterols are oxidized derivatives of cholesterol that are widely distributed in nature and often exert potent and diverse biological effects. Although these compounds normally make up only a minute fraction of total sterol present when found naturally, usually 10^{-6} to 10^{-3} in most cases [228], oxysterols display high biological activity with synergistic effects observed even at low concentrations [229].

Many of the most commonly encountered oxysterols are those with either a keto or hydroxyl group at the C-7 position of the steroid nucleus. Amongst these compounds, 7-ketocholesterol (7KC) is one of the most predominant and widely studied, principally due to its suspected involvement in various human

pathological conditions such as atherosclerosis [5] and Alzheimer's disease [44]. There is considerable evidence suggesting that 7KC promotes these conditions through various cytotoxic modes of action, including induction of apoptosis [170]. In addition, 7KC has been found to increase Na+/K+ ATP-ase activity in fibroblasts [154], decrease Ca^{2+} uptake in human erythrocytes [230], stimulate monocyte differentiation [231], inhibit proliferation and stimulate differentiation in lens epithelial cells [155], and promote oxidative stress through reactive oxygen intermediate generation in murine macrophages [232]. Many oxysterols, including 7KC, have also been shown to inhibit HMG CoA-reductase [233], the first enzyme in the mevalonate pathway which controls a multitude of cellular processes such as cholesterol and sterol biosynthesis, proliferation, apoptosis, and possibly inflammation.

In addition to human pathogenicity, some plant-derived sterols (phytosterols) are endocrine disruptors that can adversely affect environmental health. For example, β-sitosterol (a phytosterol commonly present in pine pulp and paper mill effluents [234]) has been linked to the masculinization of resident fish populations [79], possibly through its microbial conversion to androstenedione [83]. Furthermore, structural analogues of 7KC, such as 7-ketositosterol and 7β-hydroxysitosterol which are derived from β-sitosterol, have been found to be cytotoxic to a number of cell lines [156] and accumulate in the bodies of animals [99].

While microbial degradation of cholesterol has been extensively studied [18, 23, 24], and considerable research has been performed on the biological effects and fate of a number of oxysterols within mammalian systems, to date there is very limited research on the biotransformation of most oxysterols, and no peer-reviewed publications regarding the microbial degradation of 7KC. Knowledge of how these compounds are transformed and degraded by bacteria could prove beneficial for a number of reasons. For example, most oxysterols with C-7 bound oxygen groups have deleterious effects, and the identification and use of microbial enzymes that degrade 7KC has been proposed as a possible therapeutic approach for the treatment of certain age-related diseases [50]. Furthermore, dietary intake of oxysterols, the largest percent of which was 7KC, has been reported to cause significant accumulation within the plasma of humans [51]. Thus, information concerning the microbial degradation of 7KC and other oxysterols could also be used to help remove some of these substances from food. Finally, the endocrine disrupting potential of some oxysterols also motivates research on their biodegradation to mitigate their potential ecological and agricultural impact.

In this paper, we report the isolation of diverse bacteria capable of using 7KC as a sole carbon and energy source. Thus, this study serves as a stepping stone to understand the microbial degradation of oxysterols for potential applications in wastewater treatment, food technology, and medical bioremediation.

3.2. Materials and Methods

3.2.1. Media and substrate.

7KC was obtained from Sigma (St. Louis, MO) (97.1% pure as determined by gas chromatography). A modified Hunter's Mineral Base medium (MSB) consisting of a dilution of three stock solutions was used in all experiments. The medium consists of 40 ml of solution A (141.2 g Na_2HPO_4 and 136 g KH_2PO_4 per liter, pH 7.25), 20 mL of solution B (10 g nitrilotriacetic acid, 14.45 g $MgSO_4$, 3.33 g $CaCl_2 \cdot 2H_2O$, 9.25 mg $(NH_4)_6Mo_7O_{24} \cdot 4H_2O$, 99 mg $FeSO_4 \cdot 7H_2O$, and 50 ml Metals 44 per liter) and 5 ml of solution C (200g $(NH_4)_2SO_4$ per liter). Metals 44 is composed of 2.50 g EDTA, 10.95 g $ZnSO_4 \cdot 7H_2O$, 1.54 g $MnSO_4 \cdot 7H_2O$, 5.00 g $FeSO_4 \cdot 7H_2O$, 392 mg $CuSO_4 \cdot 5H_2O$, 248 mg $Co(NO_3)_2 \cdot 6H_2O$, and 177 mg $Na_2B_4O_7 \cdot 10H_2O$ per liter (final pH 7).

3.2.2. Enrichment and isolation of bacteria.

Activated sludge samples were acquired from the 69th Street Wastewater Treatment Plant and the Shell Westhollow Technology Center, both in Houston, TX. Soil samples were collected from numerous sites within Houston. Both the activated sludge and soil were exposed to 7KC within two hours of sampling. Enrichment cultures (100 ml) were created by transferring 1 ml of activated sludge (10^{-3} dilution with sterile water) or 1 ml of soil seed (suspended 10 g 100

ml^{-1} into 100 ml of MSB amended with 7KC (1 g l^{-1} or 0.0025 M) as the sole carbon source. Because 7KC is relatively insoluble (Table 1), the medium was sonicated prior to inoculation for 30 minutes in a bath sonicator to homogenize the solution and decrease 7KC particle size. 7KC initially floats on top of the medium until saturated and subsequently settles to the bottom of the flask. Sonication notably increases the turbidity of the solution and breaks up larger aggregates. Each culture was incubated at 30°C and 150 rpm in a gyratory shaking incubator until growth could be determined through visual inspection, and positive cultures were aliquoted (100 µl) onto MSB agar plates with 5.0 mg of 7KC in methanol evaporated to dryness on the surface. Plates were then incubated for 72 hours at 30°C and all colonies were picked and grown in batch cultures as above. One-ml samples of that the pure cultures that grew on 7KC were then added to 1 ml of sterile 40% glycerol and stored at -70°C until needed.

3.2.3. Carbon dioxide measurements.

Heterotrophic activity was measured per CO_2 accumulation and respiration rates using a MicroOxymax respirometer (Columbus Instruments, Columbus, OH). Batches were prepared as above, though the volume used was 50 ml and the temperature was 25°C. Each batch was inoculated with 5 µl of cells that had been grown overnight in LB media, centrifuged at 10,000g for 10 minutes and washed in MSB minimal media a total of three times. Cells were resuspended to an OD_{600} of 1.0 prior to inoculation.

3.2.4. HPLC analysis.

High performance liquid chromatography (HPLC) was used to verify 7KC degradation by the strains isolated. 25 ml batches were prepared as above and incubated at 30°C and 150 rpm. Five 100 µl samples were taken from each batch using large bore pipette tips. The samples were pooled and each processed in triplicate. 7KC was then extracted from the pooled samples twice, using 3 ml of 3:2 hexane/isopropanol, and 1.0 ml of the organic layer was filtered through a 0.22 µl Whatman syringe filter and capped inside an analytical vial. This filtrate was analyzed by reverse phase HPLC (0.72 ml min^{-1}, 85:10:5 methanol/water/acetonitrile) using a Waters 2695 Separation Module with a Waters 996 photodiode array (235 nm) and a Waters NovaPak C_{18} column (3.9 by 150 mm). Chromatographic data was analyzed with the Empower 2 software suite (Waters, Milford, MA).

3.2.5. Growth on 7KC in the presence of a surfactant.

To overcome grow-rate limitation by the rate of dissolution of 7KC, growth experiments were also conducted in the presence of Tween 80, a surfactant that is widely used to enhance the solubility of hydrophobic compounds. *Pseudomonas aeruginosa* was grown in 100 ml batches containing 2mM 7KC in MSB (30°C, 150 rpm). The 7KC was first dissolved in 7 ml of methanol, filter sterilized, and the methanol was evaporated off, allowing a fine crystalline layer to form along the bottom of the flasks to which 0.5-ml Tween 80 and 99.5-ml MSB were added. Controls were prepared in the same manner without the

addition of 7KC. Optical density (600 nm) was measured at one hour time intervals until log phase was reached. Thereafter measurements were taken at 30 minute intervals. Samples with OD measurements over 0.4 were diluted and re-measured until readings were under 0.4. The final OD in these cases was determined by multiplying by the dilution factor.

3.2.6. DNA extraction and amplification.

DNA extractions were performed using an UltraClean Microbial DNA Isolation Kit (Mo Bio, Solana Beach, CA) according to the manufacturer's protocol. Amplification of 16S rDNA was performed by polymerase chain reaction (PCR) using extracted DNA with a Taq PCR Master Mix Kit (Qiagen, Valencia, CA) and DGGE primers (DGGE-F: 5' -ATGGCTGTCGTCAGCT- '3 and DGGE-R: 5'-CGCCCGCCGCGCC CCGCGCCCGGCCCGCCGCCCCCGCCCCACGGG CGG TGTGTAC -3') on a Biometra T-Gradient thermocycler (Goettingen, Germany). Amplification mixtures had a final volume of 100 µl and contained 0.5 µM of each primer, 200 µM dNTPs, 1X PCR buffer, and 2.5 units of Taq polymerase. The temperature cycle for the PCR was 1 minute of denaturation at 94°C, 1 minute of annealing, and 3 minutes of primer extension at 72°C. The annealing temperature was initially set at 53°C and reduced 1°C each cycle until it reached 43°C. This was followed by 20 additional cycles at 43°C and a final primer extension for 10 minutes.

3.2.7. Phylogenetic analysis

Denaturing gradient gel electrophoresis (DGGE) analysis of the 16S rDNA gene sequence was used to ensure strain purity and identify bacteria for which DNA had been extracted. Analysis was performed on a Bio-Rad DCode™ system (Richmond, CA) (35 volts, 14 hours) and the gel (using denaturing gradients from 30% to 80%) stained in ethidium bromide before visualization under UV. Samples which displayed one or a small number of bands had those excised, the DNA reamplified, and were sequenced (LoneStar Labs, Houston, TX). The sequences were matched against the NCBI GenBank Database (http://ncbi.nlm.nih.gov/Blast) and the Sequence Match facility of the Ribosomal Database Project (http://www.cme.msu.edu/RDP) for phylogenetic identification of the bacteria.

3.3. Results and Discussion

3.3.1. Isolation and identification of 7KC-degraders.

Numerous bacterial species were isolated from soil and activated sludge by virtue of their ability to grow on 7KC as sole carbon and energy source. Two of five soil sample enrichment cultures, and all of the activated sludge samples tested utilized 7KC. After incubating aliquots of the cultures on MSB agar plates with 7KC as the sole carbon source, numerous colony-forming units (CFUs)

could be observed with distinct morphology and color. Each of these CFUs was then transferred into batch culture as described above, and those that retained the ability to grow were analyzed for strain purity using DGGE. Typically, visual evaluation of growth occurred between five and ten days for any culture surviving transfer from the plates to enrichment culture. 16S rDNA gene analysis based on percent similarity from NCBI BLAST search revealed γ-*Proteobacterium* Y-134 (99%), *Sphingomonas* sp. JEM-1 (98%), *Nocardia nova* (99%), and *Pseduomonas aeruginosa* (97%). Another mixed culture which we have been unsuccessful at plating on 7KC and MSB agar, but which grows well in enrichment culture, could not be reliably identified and were most closely associated with *Xanthomonas* sp. (85%) and uncultured *α-Proteobacterium* sp. (79%). This mixed culture was isolated from an activated sludge sample as were the γ-Proteobacterium Y-134 and *Pseudomonas aeruginosa*. *Sphingomonas* sp. JEM-1 and *Nocardia nova* were both isolated from soil samples. In addition to those isolated, *Rhodococcus* sp. RHA1 (provided by William Mohn, University of British Columbia) was also tested for growth on 7KC. All of these isolates are either from the Proteobacteria or Actinobacteria phyla.

3.3.2. Evidence of degradation

The results of the HPLC analysis for 7KC degradation are presented in Figure 3-1. The most rapid degradation was observed with *Nocardia nova*, a known producer of biosurfactants [235], which removed the 7KC below detection levels within 20 days. It is likely that the degradation rate was dissolution limited,

as is the case with many hydrophobic compounds that experience faster degradation in the presence of biosurfactants [236, 237]. All other cultures still contained measurable amounts of 7KC at 25 days. UV detection from 190 nm to 400 nm revealed no measurable accumulation of metabolites within that range. The absorption maximum for 7KC is 233 nm, allowing accurate determination of 7KC concentration. However, other oxysterols are generally not as strong UV absorbers, so the extracellular presence of degradation intermediates cannot be ruled out.

CO_2 accumulation and respiration rates were determined through respirometry as illustrated in Figure 3-2 and Figure 3-3 respectively. For the γ-*Proteobacterium* Y-134., *Nocardia nova*, and the *Sphingomonas* sp JEM-1, noticeable respiration did not begin to occur until approximately 100 hours after inoculation, and peaked at just past 200 hours for all three. *Rhodococcus* sp RHA1, however, did not begin noticeable respiration until 150 hours' time, and peaked at approximately 250 hours. The percent mineralization over a 300 hour period was 43% for γ-*Proteobacterium* sp., 24% for *Sphingomonas* sp., 21 % for *Nocardia nova,* and 14% for *Rhodococcus* sp. RHA1. The purity of the 7KC was 97.1%, allowing a maximum of approximately 100 µmoles of CO_2 generated from other potential co-substrates. *Rhodococcus* sp. RHA1 gave the lowest amount of accumulated CO_2, which was 460 µmoles. γ-Proteobacterium sp. released the highest amount of CO_2 at 1442 µmoles.

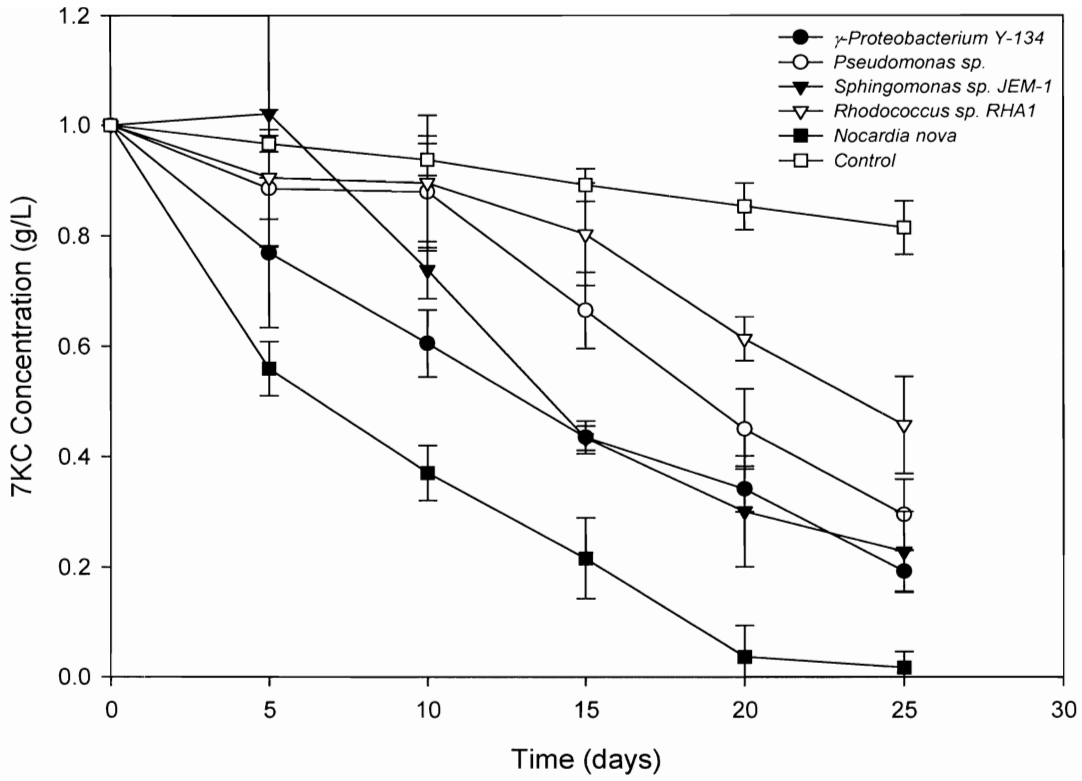

Figure 3-1. HPLC analysis of 7KC degradation. 7KC degradation by *γ-Proteobacterium* Y-134, *Sphingomonas sp.* JEM-1, *Nocardia nova*, and *Rhodococcus sp.* RHA1. This experiment was conducted at 30 °C, pH 7.

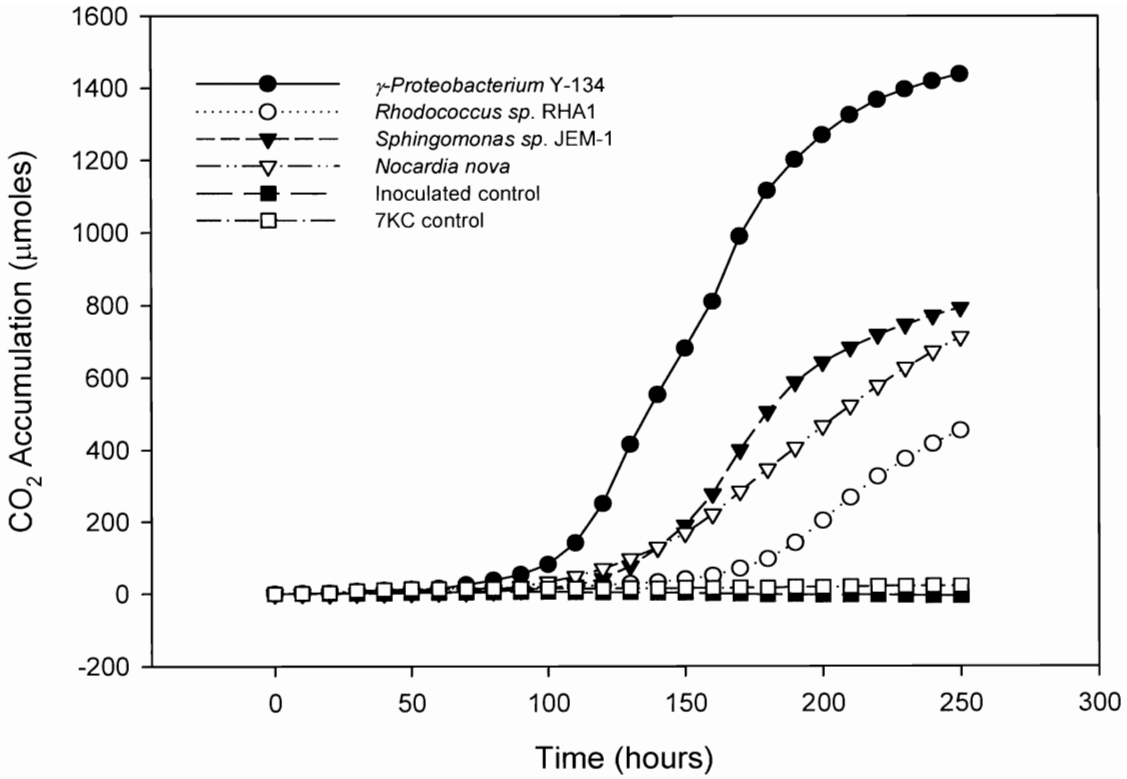

Figure 3-2. Evidence for 7KC mineralization. CO_2 accumulation (µmoles) in batch reactors by *γ-Proteobacterium* Y-134, *Rhodococcus sp.* RHA1, *Sphingomonas sp.* JEM-1, and *Nocardia nova* in mineral salts media with 0.1% 7KC as the sole carbon source. Controls contained no 7KC. This experiment was conducted at 25°C, pH 7.

3.1. Growth on 7KC in the presence of a surfactant

Due to the hydrophobicity of 7KC, which results in polydispersed colloidal particles with a tendency to precipitate, it is difficult to measure optical density unless the solution is properly suspended and diluted. In order to achieve a fine suspension, 7KC was first dissolved in methanol and filter-sterilized and evaporated to form a crystalline layer before the addition of Tween 80 (0.5 %) and MSB. This surfactant enhanced bacterial growth on 7KC. As shown in Figure 3-4, exponential growth was achieved within hours when 7KC was present while no growth occurred without 7KC. This proves that 7KC rather than the surfactant or residual methanol served as sole carbon and energy source to support growth. In contrast, the HPLC (Fig. 3-1) and respirometry data (Fig. 3-2) suggest that, in the absence of surfactant, overcoming the lag phase took much longer, normally at least five days. .These results support the notion that 7KC biodegradation might be dissolution limited, and that compounds that enhance its effective solubility and bioavailability are likely to enhance degradation kinetics.

3.1. Conclusion

A diversity of bacteria from the Proteobacteria and Actinobacteria phyla were isolated from soil and activated sludge from wastewater treatment plants, based on their ability to exploit the biodegradation of 7KC as a metabolic niche.

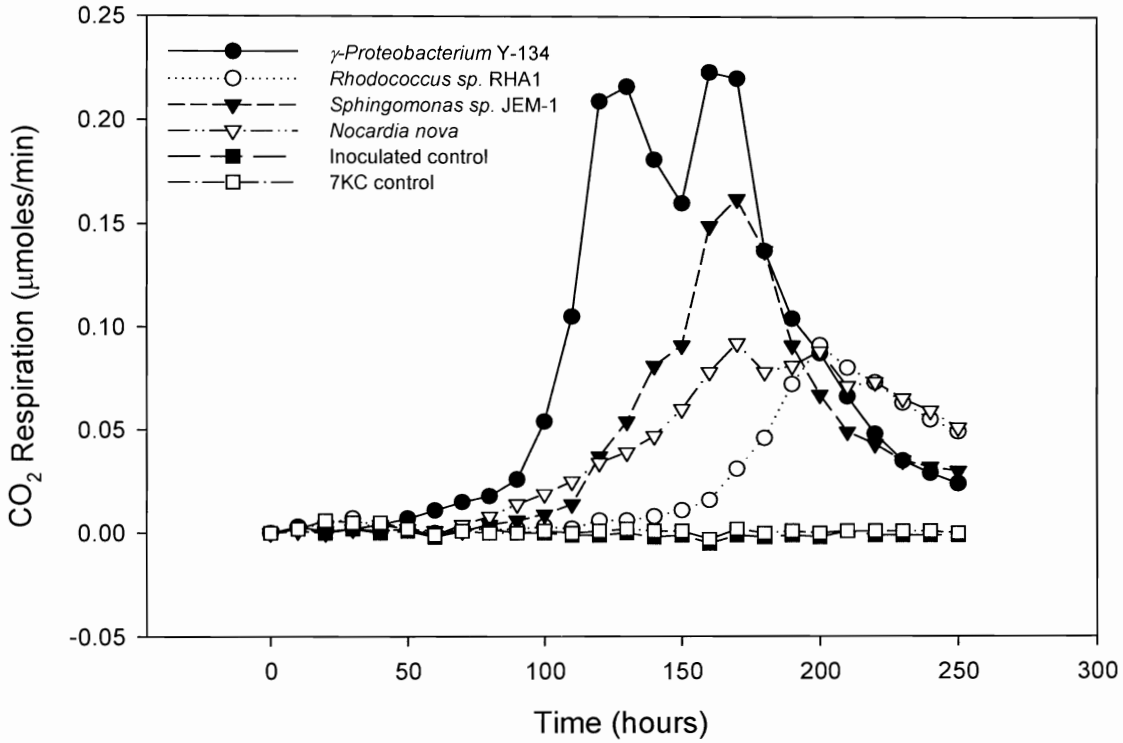

Figure 3-3. CO_2 evolution rates during 7KC catabolism. Rates of CO_2 evolution (µmoles/min) in batch reactors inoculated with *γ-Proteobacterium* Y-134, *Rhodococcus sp.* RHA1, *Sphingomonas sp.* JEM-1, or *Nocardia nova* in mineral salts media with 0.1% 7KC as the sole carbon source. Controls contained no 7KC. This experiment was conducted at 25 °C, pH 7.

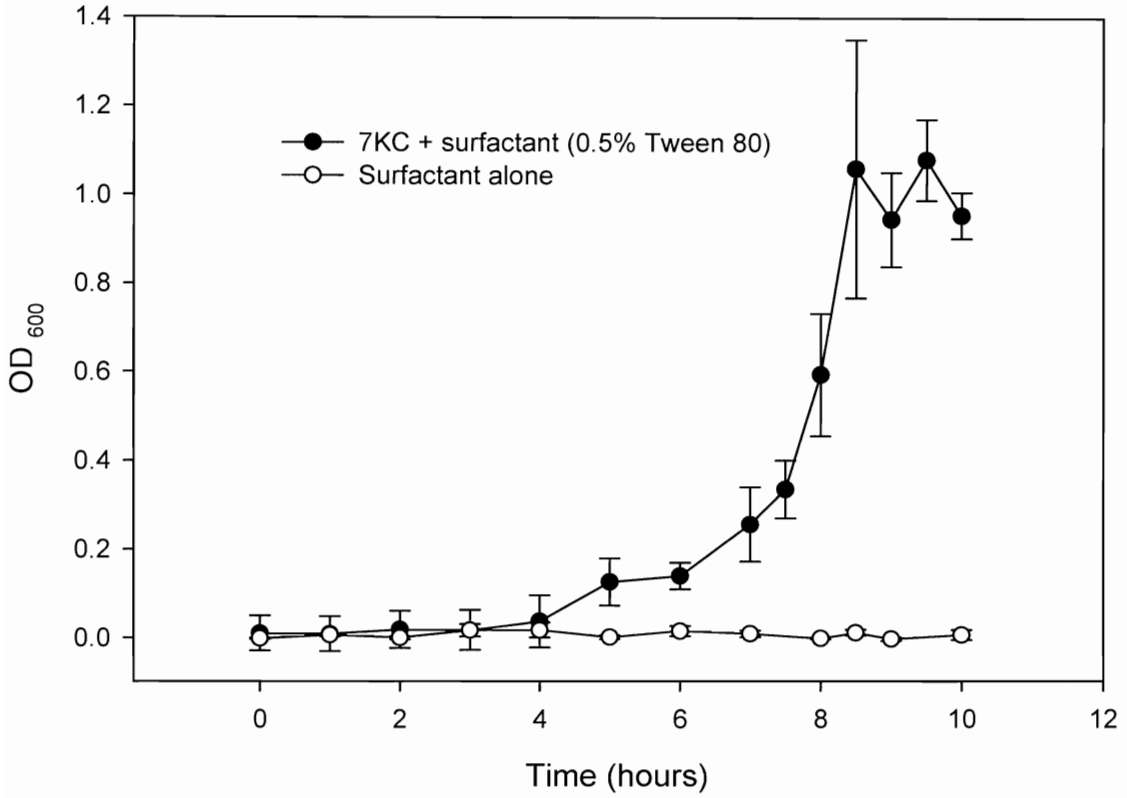

Figure 3-4. Effect of surfactants on 7KC catabolism. Growth of *Pseudomonas sp.* in MSB media and 0.5% Tween 80 with and without 7KC (ca. 1 g l^{-1}). Optical density was determined at 600 nm. This experiment was conducted at 30 °C, pH 7.

Carbon dioxide evolution in incubations with 7KC (but not in unamended controls) indicated extensive mineralization. Growth on 7KC as sole carbon source was also demonstrated, and noted to proceed faster in the presence of a surfactant; this suggests that 7KC dissolution might be a rate-limiting step. Overall, these results support the notion that oxysterol levels might be controlled in different matrices by biodegradation processes, and motivate further investigation into the specific pathways involved in microbial 7KC degradation, with the goal of identifying novel enzymes capable of transforming oxysterols for potential environmental, industrial, pharmaceutical, and medical applications.

Chapter 4

7-Ketocholesterol Catabolism by *Rhodococcus jostii* RHA1

4.1. Introduction

Oxysterols are oxygenated sterol derivatives with potent and diverse activities in a wide range of organisms. In organisms and environments where sterols occur, oxysterols occur as abiotic degradation products, comprising a small fraction of total sterols, typically much less than 0.1%. Nevertheless, oxysterols may exert significant effects at low concentrations and act synergistically. The predominant oxysterol species form through free radical reactions involving oxidation of the C-7 position due to the unsaturated ring structure of many sterols [238]. 7-Ketocholesterol (7KC), one of the most abundant and most biologically active oxysterols, has been the focus of a large body of research. 7KC is cytotoxic in mammalian cells [5, 41, 152], induces

apoptosis [146, 170, 239], and is associated with the pathogenesis of atherosclerosis [5, 40], Parkinson's disease [46], age-related macular degeneration [15, 45] and Alzheimer's disease [43, 44]. 7KC and other oxysterols can also modify the biophysical properties of cellular membranes, decreasing their fluidity and increasing their permeability. In certain cases this increases the calcium influx, decreases cholesterol efflux, and disrupts eukaryotic lipid rafts [128, 175]. Oxysterols derived from phytosterols have similar cytotoxic properties as 7KC, increasing early apoptosis and decreasing cell viability in several cell lines [99, 156, 240]. Although oxysterols may be generated in vivo in humans and animals [116], a significant amount can also be absorbed through the intestinal tract when cholesterol-rich food is ingested [51].

Mammalian cells are typically not capable of degrading the steroid nucleus, and 7KC or other oxysterols may accumulate intracellularly to pathogenic levels [41, 174]. This has prompted interest in medical bioremediation, the targeted use of exogenous enzymes (or the genes that encode them) to supply missing, or augment insufficient, catabolic functions in human cells [36, 50]. The aim is to enhance the degradation of recalcitrant pathogenic substances such as 7KC to prevent or ameliorate associated diseases. Thus, enzymes that could safely and effectively transform 7KC to a metabolizable form may have significant therapeutic value. In addition, research into oxysterol degradation pathways could be useful in mitigating the potential ecological and agricultural impact of oxysterols. While oxysterols are presumably degraded by microorganisms during decomposition, mechanisms for this

degradation have not been previously reported. We recently identified a variety of bacteria that were able to mineralize 7KC [241]. Among these, *Rhodococcus jostii* RHA1 was selected for further investigation of 7KC degradation due to the availability of the annotated RHA1 genome sequence (http://www.rhodococcus.ca) as well as knowledge of its cholesterol degradation pathway [1].

RHA1 belongs to the Actinobacteria, a diverse and ubiquitous group of gram-positive bacteria that are abundant in soil and other environments. The 9.7-Mb genome of RHA1 encodes the degradation of a broad range of organic compounds, including various steroids [242, 243]. Based on previous identification of genes encoding bacterial steroid catabolism [244-247], RHA1 appears to have several large gene clusters that encode steroid catabolism (Fig. 4-1). These clusters encode a number of enzymes that may be isofunctional or catalyze analogous reactions with metabolites of different steroids. Transcriptional analysis indicated that many of the genes in Cluster 1 were up-regulated during growth of RHA1 on cholesterol [1]. Further bioinformatic studies and analysis of gene deletion mutants permitted elucidation of several steps of cholesterol catabolism by RHA1 (Fig. 4-3). However, it is not yet known whether enzymes encoded in Cluster 1 degrade other steroids. Furthermore, the possible roles of enzymes encoded in the other clusters in steroid degradation remains to be explored.

This study compared cholesterol and 7KC catabolism by RHA1, with the aim of identifying enzymes particular to 7KC metabolism. We utilized microarray

transcriptomic analysis to compare gene expression in RHA1 cells grown separately on pyruvate, cholesterol, or 7KC as the sole organic substrate. Reverse-transcriptase quantitative PCR (RT-qPCR) was used to verify selected microarray results. To assess the roles of selected enzymes, gene deletion strains were tested for growth and metabolite accumulation.

4.2. Materials and Methods

4.2.1. Bacterial Growth

RHA1 was cultivated at 30^0C on a shaker (200 rpm) in a modified mineral salts medium (pH 7.2) consisting of $NaNH_4HPO_4 \cdot 4H_2O$ 1.74 g/l, $NaH_2PO_4 \cdot H_2O$ 0.54 g/l, $MgSO_4 \cdot 7H_2O$ 0.2 g/l, KCl 0.04 g/l, $FeSO_4 \cdot 7H_2O$ 5.0 mg/l, and trace mineral solution 1 mL/l [248]. The composition of the trace mineral solution was H_3BO_3 2.86 g/l, $MnCl_2 \cdot 4H_2O$ 1.81 g/l, $ZnSO_4 \cdot 7H_2O$ 0.22 g/l, $CuSO_4 \cdot 5H_2O$ 0.08 g/l, $CoCl_2 \cdot 6H_2O$ 0.06 g/l, and $Na_2MoO_4 \cdot 2H_2O$ 25.0 mg/l. All media were supplemented with 20 mM pyruvate, 2 mM cholesterol, or 2 mM 7KC. Bath sonication was used to reduce particle size and facilitate suspension of both 7KC and cholesterol in the media. Continuous shaking was sufficient to prevent aggregate formation.

Triplicate cultures were used for all experiments, including measurement of specific growth rate, growth of mutants, RT-qPCR, and microarray analysis. Growth rates were measured by protein assay for 7KC and cholesterol, and

optical density (OD_{600}) for pyruvate. Total protein content was measured in cells disrupted by alkaline lysis using the microBCA (bicinchoninic acid) protein assay (Thermo Scientific, Rockford, IL).

For both microarray and RT-qPCR analysis, cells were harvested from cultures in mid-log phase, corresponding to total protein values of 60, 80 and 40 µg/ml for cultures grown on pyruvate, cholesterol and 7KC, respectively. Prior to harvesting cells, a 1/10 volume of "stop solution", consisting of 10% phenol in ethanol, was added to the cultures to preserve RNA. Cells were then centrifuged at 7,000 × g for 10 min at 4^0C and resuspended in 1 mL of supernatant. 2 mL of RNAProtect (Qiagen) was added to the suspension, which was incubated for 5 min at room temperature. The mixture then underwent additional centrifugation at 14,000 x g for 2 min, after which the supernatant was removed and the cells frozen at -80°C.

4.2.2. RNA Extraction and Microarray Analysis.

Total RNA was isolated from RHA1 as previously described [249]. Briefly, this consisted of vortexing cells with glass beads (3 mm), phenol and sodium dodecyl sulfate (SDS), after which debris was removed with phenol and chloroform. Nucleic acids were precipitated using isopropanol and treated with DNase I (15 U/225 µl RNA sample)(Invitrogen). Samples used for RT-qPCR were subjected to an additional treatment of TURBO DNase (2 U per 225-µl RNA sample; Ambion, Austin, TX). The RNA was purified by phenol-chloroform

extraction, isopropanol precipitation, and an RNeasy kit using the manufacturer's protocol (Qiagen, Valencia, CA).

Transcriptomic analysis was done using indirectly labeled cDNA and an 8,313-gene microarray with 70-mer probes. The current array (GEO platform reference GPL7627) is an expansion of a previously described version [250]. cDNA synthesis, labeling and microarray hybridizations were performed as described [249], and data analyzed by GeneSpring (Agilent Technologies, Palo Alto, CA) using Locally Weighted Linear Regression (Lowess).

4.2.3. RT-qPCR

In order to validate the microarray data, the expression ratios of ten genes (Table 4-1) were determined relative to the expression of a housekeeping gene, DNA polymerase IV (Gene ID *ro01702*). DNA polymerase IV is steadily expressed under a variety of growth conditions and therefore serves as a suitable endogenous control [249]. RNA prepared for RT-qPCR, was reverse transcribed using a First Strand cDNA Synthesis Kit (Fermentas, Hanover, MD) and random hexamers according to the manufacturer's instructions.

Amplification of RT-qPCR products was carried out using SYBR Green as a detection system. Primers were designed using PrimerQuest (http://www.idtdna.com/Scitools/ Applications/Primerquest/Default.aspx) with real-time PCR as the parameter set. Each reaction mixture contained 25 µl Power SYBR Green PCR Master Mix (2X), 0.5 µM forward and reverse primers,

50 ng template cDNA, and RNase-free water to bring the final volume to 50 µl. The conditions for RT-qPCR were 2 min at 50^0C, 10 min at 95^0C, 40 cycles of 15 sec at 95^0C and 1 min at 60^0C, followed by a final step of 1 min at 60^0C. The C_t values were normalized (ΔC_t) by subtracting those of the endogenous control, and confidence levels were tested using a two-sample t-test. Relative expression results were compared using the $2^{-\Delta\Delta Ct}$ method [1]. Purity of the amplified products was determined by the presence of a single band of the correct size in a 2% agarose gel stained with ethidium bromide.

4.2.4. Gene deletion and replacement

Two RHA1 strains with unmarked deletions of the *supAB* and *mce4ABCDEF* genes as well as one strain in which the *hsaC* gene was replaced by an apramycin resistance gene were previously described (Table 4-2). Unmarked deletions of *hsaA* and *cyp125* were performed using the *sacB* counter selection system [246]. GeneRunner software was used to design oligonucleotides with appropriate restriction sites that amplified flanking regions of each gene. Vector plasmids were transformed into *E. coli* DH5α by electroporation, verified, and then transformed into S17 *E. coli* competent donor cells maintained with 25 µg ml^{-1} kanamycin. Conjugative plasmid transfer was achieved by co-culturing the donor and *R. jostii* RHA1 on selective LBP plates amended with 30 µg ml^{-1} nalidixic acid plus 50 µg ml^{-1} kanamycin followed by *sacB* counter selection. Confirmation of the removal of the target gene in

Table 4-1. Genes and primers used for SYBR Green quantitative PCR assays.

Gene ID	Protein Function	Primer
ro01702	DNA polymerase IV	Forward Primer: 5'GACAACAAGTTACGAGCCAAGATC3'
		Reverse Primer: 5'CCTCCGTCAGCCGGTAGAT3'
ro02489	hydroxylase	Forward Primer: 5'AACCGATCACTGCGACTGGATCTT3'
		Reverse Primer: 5'TTCCGGACGATGATGTCCTTGGAA3'
ro04538	ketosteroid-9-α-hydroxylase	Forward Primer: 5'ACCTGGAACTCCATGCTGATCGAA3'
		Reverse Primer: 5'TTGAAGTACGTCGGGAACGCGTAA3'
ro04539	3-HSA hydroxylase	Forward Primer: 5'ACGTCGTATTCCCGACGATTCCAT3'
		Reverse Primer: 5'TGCCAGTTGTGGACACCGATGAT3'
ro04541	3,4-DHSA dioxygenase	Forward Primer: 5'GCTCCGCAAGAAGGTCAAGATGT3'
		Reverse Primer: 5'GGGTCTTCATGTAGAACGACAGCA3'
ro04679	cytochrome P450 CYP125	Forward Primer: 5'AGAAGTTCGACATCATGCGGGAGA3'
		Reverse Primer: 5'CAGGTGATCCGCAATCGCATTGAA3'
ro04698	MCE family protein	Forward Primer: 5'ACATGATGTCGCTGATTCCCTCCA3'
		Reverse Primer: 5'AGACCGTGTTGAACTCGACGGTAA3'
ro05068	hydroxylase	Forward Primer: 5'TTGTTCAACATGCCGTACTCCTGC3'
		Reverse Primer: 5'TTCTCCTATCGCACTGAGCACGTA3'
ro05802	hydroxylase	Forward Primer: 5'AAGGATGCGTTCATTCCTCAGCAC3'
		Reverse Primer: 5'AGATGCACGAGAACGGGAAGTTGT3'
ro05812	probable hydroxylase	Forward Primer: 5'ACCGGATCAAGAGGAACTACGAGA3'
		Reverse Primer: 5'TCGTTCCCGCATGAACGTCAAGTA3'
ro05833	ketosteroid-9-α-hydroxylase	Forward Primer: 5'CCTGGACGAAGACCTGATCCTGTT3'
		Reverse Primer: 5'GTTCGCGTACACCAGAACGACTTT3'

kanamycin-sensitive, sucrose-resistant colonies was verified by colony PCR using two sets of primers: the “external” pair matched sequences flanking the target gene and “internal” pair matched sequences within the target gene.

Screening of the *hsaA* mutant yielded the expected 0.72 kb fragment using the external pair and no band using the internal pair. By contrast, wild-type RHA1 yielded fragments of 1.54 and 1.00 kb, respectively. Similarly, screening of the *cyp125* mutant yielded the expected 1.99 kb fragment using the external pair and no band using the internal pair. By contrast, wild-type RHA1 yielded fragments of 3.22 and 1.26 kb, respectively.

4.2.5. Bioinformatic analysis

Promoter, gene, terminator, and operon prediction was performed for the entire RHA1 genome using both the fgenesB and PromScan algorithms, and through submission to RAST (Rapid Annotation using Subsystem Technology) [251]. Annotations were compared to those found at the *Rhodococcus* Genome Project (http://www.rhodococcus.ca). Genes that were both up-regulated on 7KC and were differently annotated by RAST versus the previous report were further examined using ClustalW multiple sequence alignments with reference sequences in order to determine the most probable function for the encoded proteins. Comparison was also made using FIGfam data and cluster analysis from RAST. Protein localization was performed using a combination of the PSortB, SignalP 3.0, and Subloc 1.0 algorithms [252-254].

Table 4-2. Strains and plasmid used in this study.

Strain or plasmid	Characteristic(s)	Source
Strains		
R. jostii RHA1		
RHA1	Wild type	M. Fukuda
RHA010	RHA1 with *hsaC* replacement	[1]
RHA017	RHA1 with *hsaA* deletion	This study
RHA018	RHA1 with *cyp125* deletion	This study
RHA020	RHA1 with *mceABCDEF* deletion	[1]
RHA021	RHA1 with *supAB* deletion	[1]
E. coli		
DH5α	Host used to clone and maintain conjugative plasmid	Bethesda Research
S17-1	Donor strain for conjugation	[255]
Plasmids		
pK18mobsacB	mobilizable suicide vector used for triple ligation; *sacB alphII*	[246]
pHsaADL	pK18mobsacB containing 1.9 kb fusion PCR fragment flanking *hsaA* to make strain RHA0XX	This study
pCYP125DL	pK18mobsacB containing 2.0 kb fusion PCR fragment flanking *cyp125* to make strain RHA0XX	This study

4.2.6. Metabolite Analysis

RHA1 and the *ΔhsaC* mutant were grown on 20 mM pyruvate plus 1 mM 7KC. Apramycin (50 mg/l) was also included for the *ΔhsaC* mutant. Exponentially growing cells were harvested, washed and suspended in fresh medium with 1 mM 7KC at a cell density corresponding to 0.33 mg of protein per ml. Cell suspensions were incubated for 48 h at 30^0C, and samples were periodically removed. Samples were centrifuged to remove cells, and the supernatant was acidified and extracted with ethyl acetate. The extracts were dried under nitrogen and re-dissolved in pyridine. For gas chromatography-mass spectrometry (GC-MS), the extracts were derivatized using bis(trimethylsilyl)trifluoroacetamide/trimethylchlorosilane (99:1) (Sigma-Aldrich Canada, Oakville, Ont.) at room temperature and analyzed with an Agilent 6890N chromatograph equipped with an HP-5ms capillary column (50 m by 0.25 mm) and a mass-selective detector.

To identify catecholic metabolites, a 10-mL sample was extracted as described above and suspended in 3 mL sodium phosphate, pH 7.5. Purified HsaC from *Mycobacterium tuberculosis* H37Rv [1] was added to a final concentration of 0.1 mg/mL and incubated for 1 min at room temperature. The course of the reaction was monitored spectrophotometrically at 397 nm, the absorption maximum of the enolate form of the ring-cleaved product of 3,4-DHSA. The reaction mixture was analyzed by GC-MS as described above.

For nuclear magnetic resonance (NMR) analysis, a 100-mL cell suspension was prepared, incubated and extracted as described above. The dried extract was re-dissolved in 2 mL phosphoric acid/methanol (6:4) for high-performance liquid chromatography with a Waters 2695 system equipped with a Hewlett Packard ODS Hypersil C18 column (5 µm, 125 x 4 mm). The peak corresponding to the metabolite of interest was collected, extracted with ethyl acetate, dried under nitrogen and dissolved in D-acetone for proton, (H,H)-correlation spectroscopy (COSY), Heteronuclear Single Quantum Coherence (HSQC) and Heteronuclear Multiple Bond Correlation (HMBC) nuclear magnetic resonance (NMR) analyses.

4.3. Results

4.3.1. Growth of RHA1 on 7KC

Under our experimental conditions, RHA1 grew at a specific growth rates (± standard deviation) of 0.23 ± 0.02, 0.023 ± 0.002 and 0.018 ± 0.006 h^{-1} on pyruvate, cholesterol and 7KC, respectively. Both steroids formed precipitate in the initial medium, and their low solubility may have been a factor in the slow growth on the steroids. The similar growth rates on 7KC versus cholesterol suggest that 7KC has no substantial toxicity to RHA1.

4.3.2. Overall transcriptomic analysis

When growing on 7KC, RHA1 differentially expressed a large suite of genes that were mainly distinct from those differentially expressed during growth on cholesterol. Microarray analysis of RHA1 revealed 1,240 genes differentially expressed during growth on 7KC versus pyruvate. Of these, 911 were distinct from those differentially expressed during growth on cholesterol versus pyruvate (Fig. 4-1, Fig.4-2, Appendix A). Moreover, higher expression ratios were observed between 7KC versus pyruvate (range, 148 to 0.12) than between cholesterol versus pyruvate (range, 12 to 0.07). However, when expression of genes on 7KC versus cholesterol was directly compared, only 363 genes were differentially expressed, and the expression ratios were again generally small (range, 12 to 0.05). Predictably, a large proportion of genes more highly expressed on 7KC versus cholesterol were also among those more highly expressed on 7KC versus pyruvate. However, few of the genes more highly expressed on cholesterol versus 7KC were among those more highly expressed on cholesterol versus pyruvate. The overall analysis indicates that much of the difference between the 7KC and cholesterol transcriptomes is due to relatively small expression ratios, except for a small subset of differentially expressed genes that were substantially more highly expressed on 7KC than on cholesterol.

4.3.3. Steroid catabolism gene clusters

Conspicuously, most of the highly up-regulated genes in cells grown on 7KC are located in three large gene clusters that contain putative steroid

catabolism genes. RHA1 contains four such clusters which are largely defined by genes predicted to encode catabolism of steroid rings A and B (Fig. 4-1, Appendix B). These genes include *kstD, kshA, hsaABCDEFG* and their homologs. This core set of nine genes is present in each of Clusters 1, 3 and 4, while Cluster 2 lacks *hsaDEFG*. Cluster 3 has two homologs each of *kstD* and *hsaA*. Cluster 1 additionally contains the *mce4* operon and *cyp125*, neither of which have homologs in the other clusters. The *mce4* operon encodes an uptake system for cholesterol and certain other steroids [243]. The *cyp125* gene encodes a cytochrome P450 that initiates the oxidative degradation of the cholesterol side chain [2]. Each of the four clusters contains a large number of additional genes that are predicted to encode steroid catabolic functions, but their specific roles remain undefined.

During growth on 7KC, genes in Clusters 3, 2 and 1 were up-regulated (Fig. 4-1, Table 4-3, Appendix B), with average 7KC:pyruvate expression ratios in each cluster of 28.7, 8.6 and 3.2, respectively. By contrast, during growth on cholesterol, only Cluster 1 genes were up-regulated; the genes of Clusters 3, 2 and 1 had average cholesterol:pyruvate expression ratios of 1.2, 1.2 and 4.2, respectively. The direct microarray comparison of cells grown on 7KC versus cholesterol confirmed that most genes in Clusters 2 and 3 were more highly expressed on 7KC than on cholesterol (expression ratios > 2.0), while most genes in Cluster 1 had similar

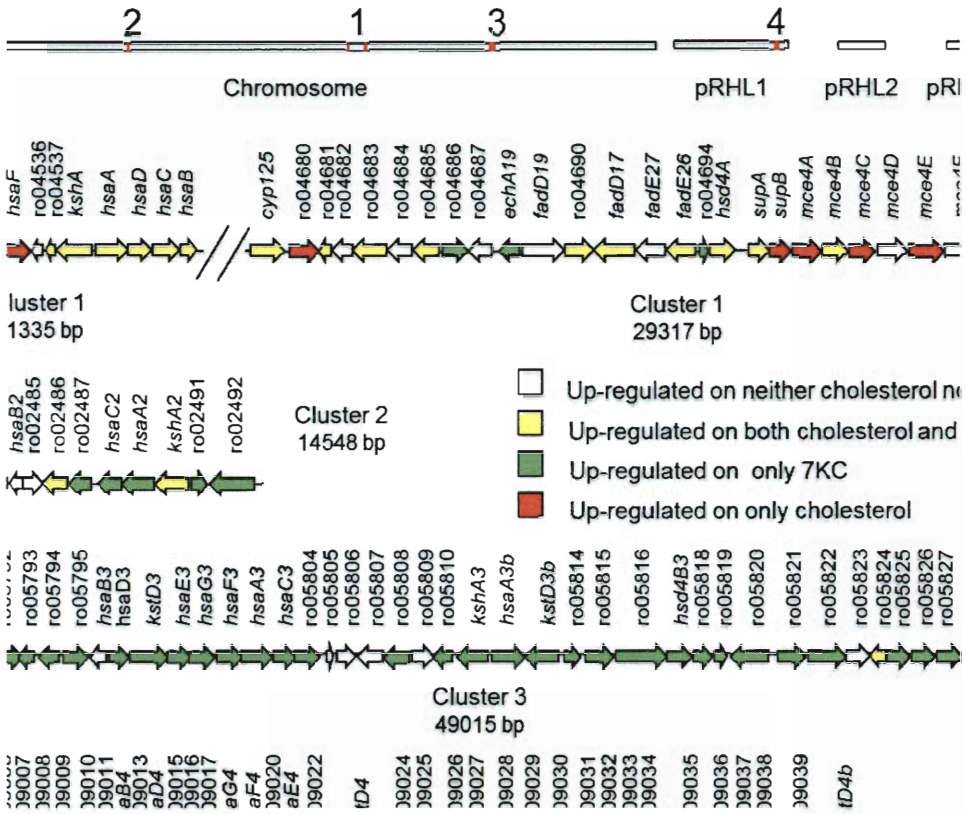

Figure 4-1. Gene clusters encoding enzymes involved in steroid catabolism in RHA1. A. Locations of clusters (red) in the genome. B. Genes with expression ratios greater than 2.0 on 7KC or cholesterol versus pyruvate.

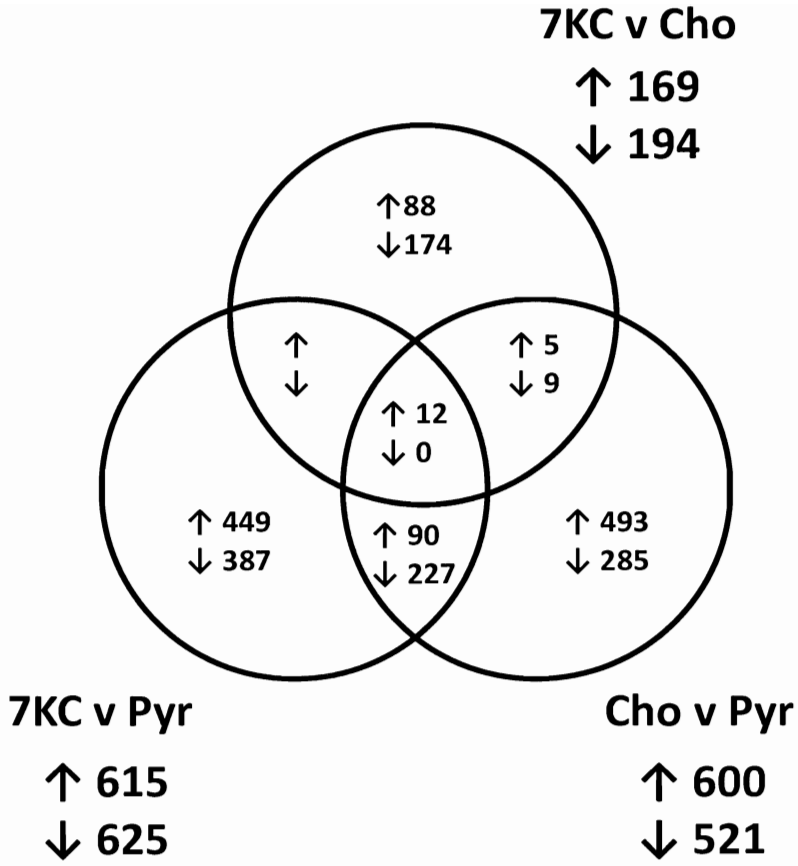

Figure 4-2. Numbers of genes differentially expressed in microarray analyses of RHA1 grown on different substrates. Key: Cho, cholesterol; Pyr, pyruvate; ↑, expression ratio > 2.0; ↓, expression ratio < 0.5.

levels of expression on both steroid substrates (expression ratios between 0.5 and 2.0).

While each of the three up-regulated clusters appears to include multiple operons, our bioinformatic analysis was only able to predict a small number of

transcriptional promoters and transcriptional terminators. Specifically, one promoter was putatively identified in Cluster 2, located upstream of the putative transcript containing *ro02486-ro02487*. Terminator sequences were found following *ro02484* and *ro02488-ro02490* in this cluster as well. Promoters were predicted in Cluster 3 upstream of *ro05815-ro05818* and *ro05795*. And in Cluster 3, terminator sequences were found following *ro05793-ro05794* as well as *ro05814*. In Cluster 2, *hsaA2* and *hsaC2* are contiguous, but based on their different expression patterns (Table 4-3, Appendix B), it is not clear that they are co-transcribed. In Cluster 3, all but one of the *hsa* genes is in a putative operon, *hsaD3-kstD3-hsaE3G3F3A3C3-ro05804*, with all eight of these genes up-regulated to a similar extent. The *hsaB3* gene is divergently transcribed from this operon and was not up-regulated on 7KC. Similarly, *hsaB2* was not up-regulated on 7KC. The *hsaB* and *hsaB2* genes encode reductases that putatively function with oxygenases encoded by *hsaA* and *hsaA2,* respectively. It is not unusual for such reductases to be present in lower amounts than their cognate oxygenases (unpublished data).

4.3.4. Other differentially expressed genes

Of the most highly up-regulated genes during growth on 7KC (versus pyruvate), which are not in the above clusters, many are in putative operons or larger clusters that were coordinately up-regulated on 7KC (Appendix A). Moreover, the majority fall into a few functional groups: 13 involved in signaling and transcriptional regulation; 24 in catabolism; 18, arranged in 2 clusters,

possibly involved in gas vesicle synthesis; 2 in transport; and 16 in cell wall biosynthesis, arranged in a single cluster. The regulatory genes include a cluster (*ro02115-8*) encoding a sigma factor, anti-sigma factor and anti-sigma factor antagonist, which were all up-regulated about 10-fold. Unlike the genes in Clusters 2 and 3, most of these up-regulated genes were not differentially expressed on 7KC versus cholesterol, with expression ratios nearly always between 0.5 and 2.0 in the direct microarray comparison. The only exceptions were some of the catabolic genes, which were more highly expressed on 7KC versus cholesterol, encoding a possible hydroxy-steroid dehydrogenase and a short-chain dehydrogenase (*ro01882-3*), a steroid delta-isomerase (*ro03609*), a probable 3-oxyacyl-(acyl-carrier-protein) reductase (*ro03841*), an acyl-CoA dehydrogenase (*ro04283*) and a possible bile acid 7-alpha dehydratase (*ro06638*).

The genes that were most extensively down-regulated during growth on 7KC (versus pyruvate) are largely involved in energy metabolism and growth (Appendix A). Most of these genes were down-regulated three- to five-fold, and

Table 4-3 Comparison of RTq-PCR and microarray expression ratios for RHA1 grown on either cholesterol or 7KC relative to pyruvate.

	RT-qPCR Expression		Microarray Expression	
Gene Name	**Cholesterol**	**7KC**	**Cholesterol**	**7KC**
hsaA2	47.0 (15.5-142.7)	302.3 (42.7-2142.1)	0.8	10.6
kshA	54.2 (31.7-92.7)	23.3 (8.6-63.0)	4.6	4
hsaA	124.9 (90.7-172.0)	64.8 (30.3-138.9)	20.3	12
hsaC	79.8 (54.1-117.6)	56.9 (23.5-137.6)	2.1	2.2
cyp125	53.9 (22.6-128.3)	40.8 (13.9-119.8)	11	5.7
mce4A	6.0 (4.2-8.6)	10.3 (4.1-25.9)	2.3	1.6
hsaAb	10.0 (4.8-20.9)	4.6 (1.9-11.1)	2	2.8
hsaA3	12.6 (2.9-55.4)	244.4 (75.8-788.0)	1	5.8
hsaA3b	59.4 (9.5-371.8)	603.1 (181.8-2000.0)	1.8	5.4
kshB	8.3 (2.3-29.4)	77.1 (18.5-321.0)	1.5	1

many are in putative operons that were coordinately down-regulated. The functional groups represented by these genes include electron transport (17 genes in 4 clusters), a H^+-driven ATPase (8 genes in 1 cluster), the tricarboxylic-acid cycle and glycolysis (20 genes, including clusters of 5 and 10 genes), translation (49 genes, including clusters of 11 and 33 genes) and cell wall synthesis (16 genes, including a cluster of 11 genes). Additional genes down-regulated on 7KC encode transporters (6 genes, including a cluster of 4 genes encoding an ABC transporter) and chaperone proteins (5 genes). Interestingly, one gene possibly involved in steroid metabolism, encoding a probable C-5 sterol desaturase (*ro04159*), was down-regulated more than five-fold. With few exceptions, the genes down-regulated on 7KC versus pyruvate were not differentially expressed on 7KC versus cholesterol.

4.3.5. RT-qPCR confirmation of gene expression

The expression of nine of the above mentioned genes known or suspected to be involved in steroid degradation or uptake were quantified using RT-qPCR. In all cases, the RT-qPCR analysis confirmed up-regulation of genes detected by the microarray, and the two methods generally agreed with respect to whether 7KC or cholesterol caused greater up-regulation of the particular genes (Table 4-3). Four genes, *hsaA2*, *hsaA3*, *hsaA3b*, and *kshB*, exhibited much higher RT-qPCR expression ratios during growth on 7KC versus on cholesterol. The expression ratios tended to be higher with RT-qPCR than with the microarray, up to 100-fold higher, which is typical [249, 250]. The RT-qPCR

assay is probably more quantitatively accurate than the microarray analysis, so it appears that the magnitude of up-regulation of steroid catabolism genes ranged from approximately 10- to 600-fold.

4.3.6. Gene deletion analysis

Unmarked, in-frame gene deletions, and in one case, a gene replacement (Table 4-2) were used to determine the roles of several genes in the growth of RHA1 on 7KC. These genes are in Cluster 1 and were previously implicated in cholesterol catabolism. Two mutants have deletions of a total of eight genes, *supAB* and *mce4ABCDEF*, respectively, encoding the Mce4 steroid uptake system [243]. Both of these mutants were able to grow on pyruvate, but lost the ability to grow on 7KC, indicating that the Mce4 system is essential for uptake of 7KC. Growth on 7KC was also completely abolished by the replacement of *hsaC* and deletion of *cyp125,* individually. This strongly implicates the ring-cleavage dioxygenase, HsaC, and the cytochrome P450, Cyp125, in the pathway for degradation of 7KC. By contrast, deletion of *hsaA,* encoding the oxygenase of a two-component hydroxylase, partially impaired, but did not prevent growth on 7KC, suggesting that HsaA contributes to 7KC catabolism but is not essential.

4.3.7. Metabolite Analysis

When incubated with 7KC, the hsaC mutant cells accumulated several potential metabolites, seven of which were not produced by wild-type RHA1. The 7KC used for this experiment had no detectable cholesterol impurity, so the

metabolites detected are clearly from 7KC. All of these metabolites accumulated during the first 20 hours of incubation, and there were no major changes in the compounds detectable after that time. Purified HsaC from H37Rv was used to transform the mixture of metabolites in order to identify catecholic compounds that are transformed by HsaC, and so, likely true intermediates of 7KC catabolism. Four metabolites were completely removed from the mixture by HsaC. These four metabolites (Fig. 4-4) were identified on the basis of the mass spectra of their derivatives. The ability of HsaC_H37Rv to transform these compounds strongly suggests that they are structurally similar to one another and supports the interpretation of the mass spectra.

The results of the GC-MS are as follows: 3,4-DHSA, TMS derivatized: Rt = 15.91 min EI-MS (70 eV, EI); m/z: 460 ([M+], 74%), 294 (45%), 281 (36%), 267 (8%), 251 (70%), 207 (100%), 193 (49%), 73 (97%). 3,4,7-THSA, TMS derivatized: Rt = 16.25 min EI-MS (70 eV, EI); m/z: 548 ([M+], 25%), 458 (7%), 382 (12%), 367 (8%), 281 (24%), 267 (100%), 207 (65%), 73 (73%). 3,4-DHSAP, TMS derivatized: Rt = 20.60 min EI-MS (70 eV, EI); m/z: 590 ([M+], 70%), 557 (10%), 381 (54%), 294 (94%), 281 (22%), 267 (5%), 207 (48%), 193 (28%), 73 (100%). 3,4,7-THSAP, TMS derivatized: Rt = 20.46 min EI-MS (70 eV, EI); m/z: 678 ([M+], 4%), 588 (5%), 397 (60%), 367 (6%), 281 (22%), 253 (6%), 233 (10%), 207 (45%), 161 (11%), 133 (12%), 73 (100%).

NMR analysis of 3,4,7-THSA yielded the following data: ^{1}H NMR (500 MHz, $CDCl_3$): δ = 6.58 (d, J = 8.7 Hz, 1H, 1), 6.53 (d, J = 8.7 Hz, 1H, 2),

4.27 (ddd, *J* = 9.8, 3.7, 2.5 Hz, 1H, 7), 3.01 (dd, *J* = 13.5, 9.8 Hz, 1H, 6*x*), 2.83 (dd, *J* = 13.5, 2.5 Hz, 1H, 6*y*), 2.82 (dd, *J* = 14.7, 3.7 Hz, 1H, 8), 2.50 (dd, *J* = 18.4, 8.6 Hz, 1H, 16*x*), 2.61 (dd, *J* = 15.9, 7.6 Hz, 1H, 11*x*), 2.48-2.42 (m, 1H, 14), 2.37 (dd, *J* = 15.9, 2.6 Hz, 1H, 11*y*), 2.32-2.20 (m, 1H, 15*x*), 2.24 (m, 1H, 16*y*), 2.22 (s, 3H, 19), 1.90 (m, 1H, 15*y*), 1.90-1.63 (m, 2H, 12), 1.12 (s, 3H, 18). ^{13}C NMR (125.8 MHz, $CDCl_3$): δ = 217.9 (17), 211.9 (9), 144.6 (4), 144.3 (3), 128.8 (10), 126.1 (5), 122.4 (1), 112.8 (2), 72.0 (7), 55.7 (8), 48.1 (13), 46.1 (14), 38.1 (11), 36.4 (16), 32.1 (6), 30.1 (12), 23.8 (15), 19.5 (19), 14.0 (18).

4.4. Discussion

The current studies demonstrated that three of the four identified steroid catabolic gene clusters in RHA1 were up-regulated during growth on 7KC. Of these three, the cholesterol catabolic cluster was much less up-regulated than the other two. This was established by both the microarray and RT-qPCR results, with the latter demonstrating that genes of Clusters 2 and 3 were up-regulated up to 600-fold while genes of Cluster 1, encoding cholesterol catabolism, were only up-regulated up to 10-fold (Table 4-3). Nevertheless, studies using the gene deletion mutants clearly indicated that proteins encoded in Cluster 1 are essential for catabolism of 7KC by RHA1, including the Mce4 transporter, the sidechain-degrading Cyp125, and the ring-cleaving extradiol dioxygenase, HsaC (Fig. 4-3). The results do not exclude the possibility that one

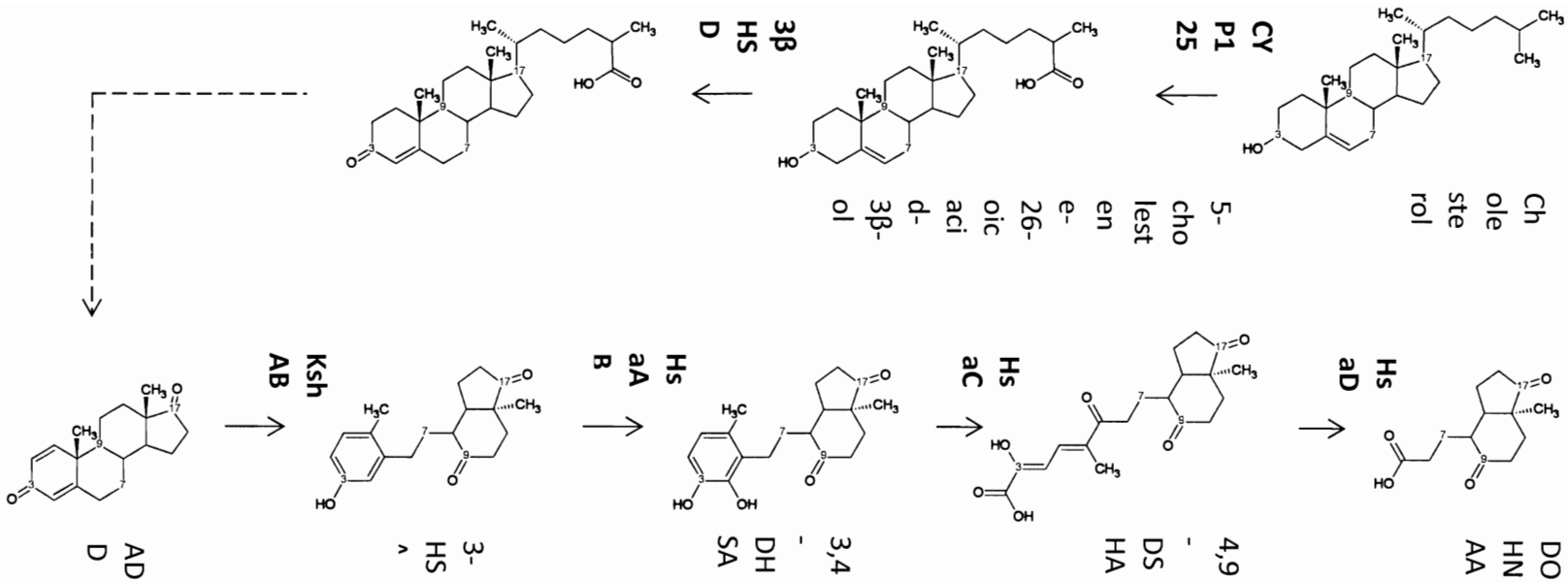

Figure 4-3. Proposed cholesterol degradation pathway [1-3]. Enzymes: CYP125, sterol 26-monooxygenase; 3βHSD, 3β-hydroxysteroid dehydrogenase; KshAB, ketosteroid-9-α-hydroxylase; HsaAB, 3-HSA hydroxylase; HsaC, 3,4-DHSA dioxygenase; HsaD, 4,9-DHSA hydrolase. Intermediates: ADD, 3-HSA, 3,4-DHSA, 4,9-DSHA, DOHNAA. R represents an oxidized side chain of undetermined length.

or more of the 62 genes in Clusters 2 and 3 are essential for growth on 7KC, but it is clear that neither cluster encodes a complete pathway for 7KC catabolism. It thus appears that 7KC gratuitously induces some, perhaps a large number of steroid catabolism genes, neither involved in, nor essential for 7KC metabolism.

The simultaneous up-regulation of three clusters during growth on 7KC is in marked contrast to the previously reported transcriptional response to growth on cholesterol [1], in which only Cluster 1 was up-regulated (Fig. 4-1). Despite the structural similarity of these two growth substrates, the presence of the 7-keto substituent on the substrate had a major impact on expression of steroid catabolism genes, either directly by affecting the function of the molecule as a regulatory effector or indirectly by affecting the occurrence of metabolites influencing gene regulation. Because of its low abundance, 7KC is unlikely to be a major substrate to which RHA1 is adapted. However, 7KC may resemble one or more other steroids that are important substrates. In particular, bile acids are abundant steroids with a C-7 substitution, and genes induced by 7KC may play a role in their metabolism.

The requirement of Mce4 transport system for uptake of 7KC by RHA1 is consistent with what is known about the specificity of this ABC transporter [1, 243]. This system is essential for uptake of cholesterol and other steroids supporting growth of RHA1, including β-sitosterol, 5-α-cholestanol and 5-α-cholestanone [243]. 7KC shares structural similarity with the known Mce4 substrates, particularly a long, hydrophobic side chain. The 7-keto substituent of 7KC does not appear to impede uptake by Mce4. While the 11-gene operon

(*ro04696-ro04706*) encoding the Mce4 system was not highly up-regulated on 7KC or cholesterol, according to the microarray analysis, the RT-qPCR assay of *mce4A* indicates that the operon was up-regulated approximately 10-fold on 7KC. In a previous study [243], the constitutive level of expression of the Mce4 system on pyruvate was sufficient for measureable cholesterol uptake, so extensive up-regulation of the Mce4 system does not appear necessary to support growth on steroids. The current results further indicate that an MFS transporter encoded by *ro05792* in Cluster 3 is not able to transport 7KC. While RHA1 has three additional partial or complete *mce* operons, the *mce4* operon is the only one proximal to steroid catabolism genes.

The current results are consistent with the hypothesis that in RHA1, cholesterol and 7KC are initially transformed by Cyp125 and that the 3β-hydroxy substituent is oxidized to a ketone by a cytoplasmic 3β-hydroxysteroid dehydrogenase (3β-HSD). Recent work suggests that Cyp125 hydroxylates the side chain as an essential early step in catabolism of cholesterol by RHA1 [2]. The inability of the RHA1 Δcyp125 mutant to grow on 7KC suggests that Cyp125 has the same function in 7KC and cholesterol metabolism (Fig. 4-3). Of the four clusters of steroid catabolism genes, Cluster 1 is the only that contains a P450 gene. Cyp125 is a cytoplasmic enzyme that transforms 3-hydroxy, but not 3-keto-steroids [2]. These characteristics are inconsistent with an alternate hypothesis that 3β-hydroxy substituent of cholesterol is oxidized to a ketone by a secreted cholesterol oxidase, as reported for some bacteria [256, 257]. While RHA1 has three genes encoding proteins annotated as secreted cholesterol oxidases

(ro03863, ro04305 and ro06201), none was up-regulated on either 7KC or cholesterol, and none is proximal to steroid catabolism genes. By contrast, a gene encoding a 3β-HSD (ro04707) is part of Cluster 1 and was up-regulated on both 7KC and cholesterol (Appendix B). Moreover, Ro04707 is the best reciprocal hit for a 3β-HSD from *M. tuberculosis,* which was demonstrated to transform cholesterol to cholest-4-ene-3-one [258]. Other RHA1 genes encoding possible 3β-HSDs, *ro04260, ro04612* and *ro05893*, were not up-regulated on either steroid substrate.

Both HsaA and HsaC play critical roles in cleavage of ring A of 7KC (Fig. 4-3). Despite the up-regulation of genes in Clusters 2 and 3 encoding isozymes of HsaA and HsaC (Fig. 4-1 Appendix B), deletion mutants of *hsaA* and *hsaC* were partially and completely impaired, respectively, in growth on 7KC. Similarly, the growth rate of the *ΔhsaC* mutant on cholesterol was previously found to be 60% lower than that of the wild-type [1]. The simplest explanation for these observations is that the isozymes of HsaA and HsaC have limited or no ability to transform intermediates of 7KC degradation. The slow growth of the *ΔhsaA* mutant on 7KC could be due to complementation by any one of several isozymes including Ro02489, Ro05068, Ro05802, and Ro05812; however investigation of enzyme specificity is necessary to distinguish the relative catalytic abilities of isozymes encoded in the steroid catabolism gene clusters.

The 7KC metabolites accumulated by the *ΔhsaC* mutant indicate that the RHA1 pathways for 7KC and cholesterol metabolism preceding the step

catalyzed by HsaC are analogous (Fig. 4-3). Both 3,4-DHSA and 3,4-DHSAP were previously found as cholesterol metabolites of the *ΔhsaC* mutant [1]. The production of these metabolites plus 3,4,7-THSA and 3,4,7-THSAP by the *ΔhsaC* mutant incubated with 7KC indicates that the 7-keto substituent is reduced to a hydroxyl group prior to the HsaC ring-cleavage step (Fig. 4-4). Nevertheless, it is clear that removal of the 7-hydroxy substituent and complete side chain degradation are not required for cleavage of ring A to occur. Further, this study demonstrated that either or both the 7-keto and 7-hydroxyl substituents as well as the C-17 propionic acid side chain can be transformed by the enzymes preceding the HsaC step and by HsaC of *M. tuberculosis*.

No enzymes were identified that are unique to 7KC metabolism and that could facilitate the selective degradation of 7KC over cholesterol. The only part of the 7KC pathway that is clearly unique is the removal of the 7-keto substituent, putatively via the sequential activities of a reductase and dehydratase. RHA1 has three genes, *ro02479*, *ro06638*, and *ro05687*, encoding proteins similar to bile acid 7α-dehydratases, which might catalyze removal of the 7-hydroxy substituent during 7KC metabolism. Of these, *ro05687* was up-regulated on 7KC but not cholesterol (Appendix B). Another, *ro02479*, was not significantly up-regulated in the microarray experiment. However, this may be a false-negative result, as it is part of Cluster 2 and appears to be part of a co-transcript that was up-regulated on 7KC. That co-transcript also includes *ro02478*, encoding a reductase. Nevertheless, the most promising candidates for the reductase and 7α-dehydratase appear to be *ro06637* and *ro06638*, respectively, as both were

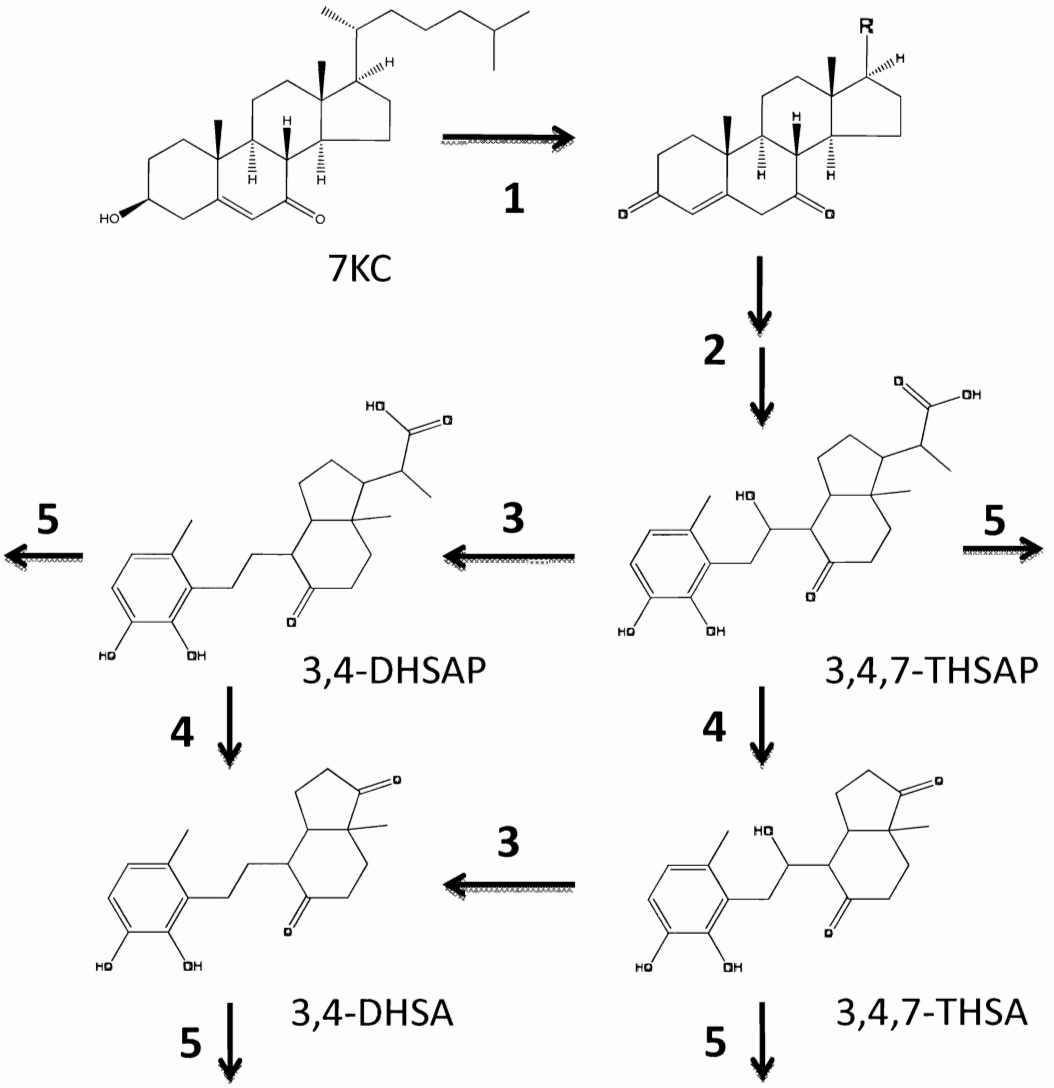

Figure 4-4. Proposed scheme for 7KC metabolism based on metabolites accumulated by the RHA1 Δ*hsaC* mutant. 1. Degradation of the C-17 side chain and 3β-OH dehydrogenation appear to occur concurrently, followed by **2**. degradation of rings A and B and 7-keto reduction. **3**. Removal of 7-OH by putative dehydratase. **4**. Side chain degradation. **5**. Reaction catalyzed by HsaC. Key: R, side chain intact or in various stages of degradation; 3,4,7-THSAP, 3,4,7-trihydroxy-9,10-seconandrost-1,3,5(10)-triene-9,17-dione proprionic acid; 3,4-DHSAP, 3,4-dihydroxy-9,10-seconandrost-1,3,5(10)-triene-9,17-dione proprionic acid; 3,4,7-THSA, 3,4,7-trihydroxy-9,10-seconandrost-1,3,5(10)-triene-9,17-dione.

significantly up-regulated on 7KC. These genes and their corresponding protein products clearly warrant further investigation for possible selective transformation of 7KC.

Expression patterns of RHA1 genes outside of the above three steroid catabolism gene clusters suggest that general physiological conditions were similar in cells growing on the two steroid substrates and distinct from conditions in cells growing on pyruvate. Most genes outside of the clusters did not have very high or low expression ratios in the 7KC versus cholesterol comparison, and the few exceptions to this trend are genes possibly involved in steroid catabolism (Appendix A). The lower expression levels, during growth on steroids, of genes involved in electron transport, ATP synthesis, central metabolism and translation is consistent with the lower growth rates of cells on steroids relative to cells on pyruvate. The reason for the reduced expression of chaperone proteins on steroids is less obvious but may also be related to growth rates. The observation that some cell wall synthesis genes were down-regulated on steroids, while others were up-regulated, may reflect remodeling of the cell wall during growth on steroids. Finally, the up-regulation of a sigma factor system during growth on steroids suggests that a major regulatory network is modulated in order for RHA1 to adapt to growth on steroids.

Chapter 5

Isolation and Expression of Selected Genes from *Rhodococcus jostii* RHA1

5.1. Introduction

As discussed in Chapter 4, genomic and transcriptomic analyses of the actinomycete *Rhodococcus jostii* RHA1 during growth on 7KC revealed the presence of four gene clusters encoding putative steroid-degrading enzymes [1]. One of these clusters (Cluster 1) was also up-regulated during catabolism of cholesterol, while growth on 7KC induced many genes in this cluster as well as in Clusters 2 and 3 [38]. No other substrates (i.e., cholic acid, androsterone, or cholesterol) significantly up-regulated Cluster 2, though many genes in Cluster 3 were also highly expressed during growth on cholic acid, which contains a 7α-OH group. Furthermore, metabolic screening using a *ΔhsaC* mutant (*hsaC* deletion) determined that reduction of the 7-keto substituent with concomitant removal of

the 7-OH moiety could occur prior to the incorporation of dioxygen catalyzed by HsaC (Fig. 4-4), an extradiol dioxygenase that is responsible for the *meta*-cleavage of ring A of the steroid nucleus during cholesterol degradation (Fig. 4-3) [3].

Our primary motive for researching the microbial degradation of 7KC is to identify enzymes that can transform this oxysterol in a manner that will reduce its toxicity or promote its further metabolism or excretion, while simultaneously avoiding nonspecific (unintended) transformations. Since cholesterol and most endogenous sterols lack a 7-keto substituent, the most obvious means to accomplish this would be through reduction or removal of this group. Reduction of 7KC can result in the formation of either 7α- or 7β-hydroxycholesterol (7α/β-HC) [259], however 7β-HC displays greater cytotoxicity than 7KC while 7α-HC is innocuous in comparison [260-262].

Cluster 2 contains two significantly up-regulated short chain dehydrogenase /reductases (*ro02478* and *ro02480*) that flank a putative dehydratase (*ro02479*). Since removal of the 7-keto group was previously indicated, and the likely enzymes involved would consist of a reductase/dehydratase pair, these two genes make good candidates for further evaluation. Furthermore, these are the only two potential reductases in this cluster except for *ro02483,* which is a 3-ketosteroid-delta-1-dehydrogenase homolog. Although not associated with one of the steroid-degrading gene clusters, ro06637 and ro06638 were also both significantly up-regulated by 7KC,

and encode a reductase/dehydratase pair as well. Additionally, Cluster 3 contains a large number of reductases, one of which could potentially catalyze reduction of the 7-keto substituent. Based on this information we decided to clone and express several of these enzymes to assay them for their ability to transform 7KC or a downstream metabolite.

5.2. Materials and Methods

5.2.1. Bacterial strains and growth

Rhodococcus jostii RHA1 and *E. coli* strains were cultivated aerobically in Luria-Bertani (LB) broth or agar plates at 30^0C or 37^0C, respectively. Liquid cultures were also subjected to shaking at 200 rpm. For cloning and plasmid propagation, both *E. coli* TOP10 (Invitrogen, Carlsbad, CA) and *E. cloni* 10G (Lucigen, Middleton, WI) chemically competent cells were used. For protein expression, *E. coli* BL21 Star cells were used. When appropriate, media was supplemented with ampicillin (100 µg/ml) or kanamycin (50 µg/ml) for plasmid maintenance. Protein expression was induced using isopropyl β-D-1-thiogalactopyranoside (IPTG) (100 µg/ml). All strains were stored as 20% glycerol stocks at -80^0C.

5.2.2. Cloning of 7KC up-regulated genes

Cells from overnight cultures of RHA1 (2 ml) were pelleted (10,000 × *g*, 30 s) and extracted using an UltraClean® Microbial DNA Isolation Kit (Mo Bio Labs, Inc., Solana Beach, CA) according to the manufacturer's protocol. Briefly, cells were resuspended in buffer and SDS prior to mechanical cell lysis by bead beating. Cell debris was separated from the supernatant by centrifugation (10,000 x *g*, 30 s) and the supernatant was transferred to a new tube where non-DNA contaminants were precipitated and separated by further centrifugation. The supernatant was passed through a silica column, bound DNA washed with ethanol, and eluted with distilled water. All DNA concentrations were determined using a NanoDrop 1000 spectrophotometer at 260 nm. The 260/230 and 260/280 ratios were used to determine DNA purity.

Primers (IDT, Coralville, IA) were designed for whole gene amplification (Table 5-1) without the endogenous stop codon, and the T_m and propensity for dimer formation were analyzed using OligoAnalyzer (IDT, Coralville, IA). Genes were amplified by PCR using a Biometra TGradient thermocycler (Goettingen, Germany). Each 20 µl reaction consisted of 0.2 µl Phusion® High-Fidelity DNA Polymerase (New England Biolabs, Beverly, MA), 4 µl 5x HF buffer, 0.4 µl 10mM dNTPs, 0.5 µM each primer, 10-20 ng DNA template, and sterile deionized water. Some genes with high GC content were difficult to amplify and required the addition of CES, a PCR enhancing solution [263]. Cycling conditions were an initial denaturation of 98°C for 1 minute followed by 30 cycles of 98°C for 35

seconds, T_m - 5°C for 35 seconds, and 72°C for 1 minute, except for plasmid linearizations, which required 2 minutes. A final extension time of 5 minutes was also included. Cycling times were slightly greater than standard due to our use of thick-walled PCR tubes. Product amplification was verified using gel electrophoresis followed by staining with SYBR Safe DNA gel stain (Invitrogen, Carlsbad, CA). Size was estimated by comparison to a standard DNA ladder (Fermentas, Hanover, MD).

All genes were inserted into pET101/D-TOPO (Invitrogen, Carlsbad, CA) (Fig. 5-1), either using the manufacturer's protocol or by circular polymerase extension cloning (CPEC) [264]. Briefly, for CPEC cloning, vectors were linearized by PCR and gel purified using a Gel Extraction Kit (Qiagen, Valencia, CA). Genes were PCR amplified with 15-20 base pair vector-overlapping regions added to their 5' and 3' ends, and gel purified as well. 200 ng of the vector was then added to an equimolar amount of insert in a 20 µl reaction volume containing Phusion® High-Fidelity DNA Polymerase mix. The DNA was denatured at 98°C for 30 seconds, reannealed at 55°C for another 30 seconds, and then allowed to extend for 2 minutes. This was repeated for five cycles. For either cloning method, 3 µl of the reaction was subsequently used for transformation of chemically competent *E. coli* TOP10 or *E. cloni* 10G. Cells were then plated on ampicillin containing LB agar plates and incubated overnight at 37°C. Colony PCR with T7 primers was used to verify the presence of the correct sized insert. The PCR product from positive colonies was verified by sequencing (SeqWright, Houston, TX).

Table 5-1. Primers used in the cloning of *Rhodococcus jostii* RHA1 genes.

Gene ID	Protein Function	Primers
ro02478	short chain dehydrogenase	Forward Primer: 5'GACAACAAGTTACGAGCCAAGATC3' Reverse Primer: 5'CCTCCGTCAGCCGGTAGAT3'
ro02480	short chain dehydrogenase	Forward Primer: 5'AACCGATCACTGCGACTGGATCTT3' Reverse Primer: 5'TTCCGGACGATGATGTCCTTGGAA3'
ro04707	3β-hydroxysteroid dehydrogenase	Forward Primer: 5'ACCTGGAACTCCATGCTGATCGAA3' Reverse Primer: 5'TTGAAGTACGTCGGGAACGCGTAA3'
ro05790	short chain dehydrogenase	Forward Primer: 5'ACGTCGTATTCCCGACGATTCCAT3' Reverse Primer: 5'TGCCAGTTGTGGACACCGATGAT3'
ro05791	short chain dehydrogenase	Forward Primer: 5'GCTCCGCAAGAAGGTCAAGATGT3' Reverse Primer: 5'GGGTCTTCATGTAGAACGACAGCA3'
ro05810	short chain dehydrogenase	Forward Primer: 5'AGAAGTTCGACATCATGCGGGAGA3' Reverse Primer: 5'CAGGTGATCCGCAATCGCATTGAA3'
ro05819	short chain dehydrogenase	Forward Primer: 5'ACATGATGTCGCTGATTCCCTCCA3' Reverse Primer: 5'AGACCGTGTTGAACTCGACGGTAA3'
ro05821	NADPH-dependent flavin reductase	Forward Primer: 5'TTGTTCAACATGCCGTACTCCTGC3' Reverse Primer: 5'TTCTCCTATCGCACTGAGCACGTA3'
ro05832	short chain dehydrogenase	Forward Primer: 5'AAGGATGCGTTCATTCCTCAGCAC3' Reverse Primer: 5'AGATGCACGAGAACGGGAAGTTGT3'
ro06637	short chain dehydrogenase	Forward Primer: 5'ACCGGATCAAGAGGAACTACGAGA3' Reverse Primer: 5'TCGTTCCCGCATGAACGTCAAGTA3'

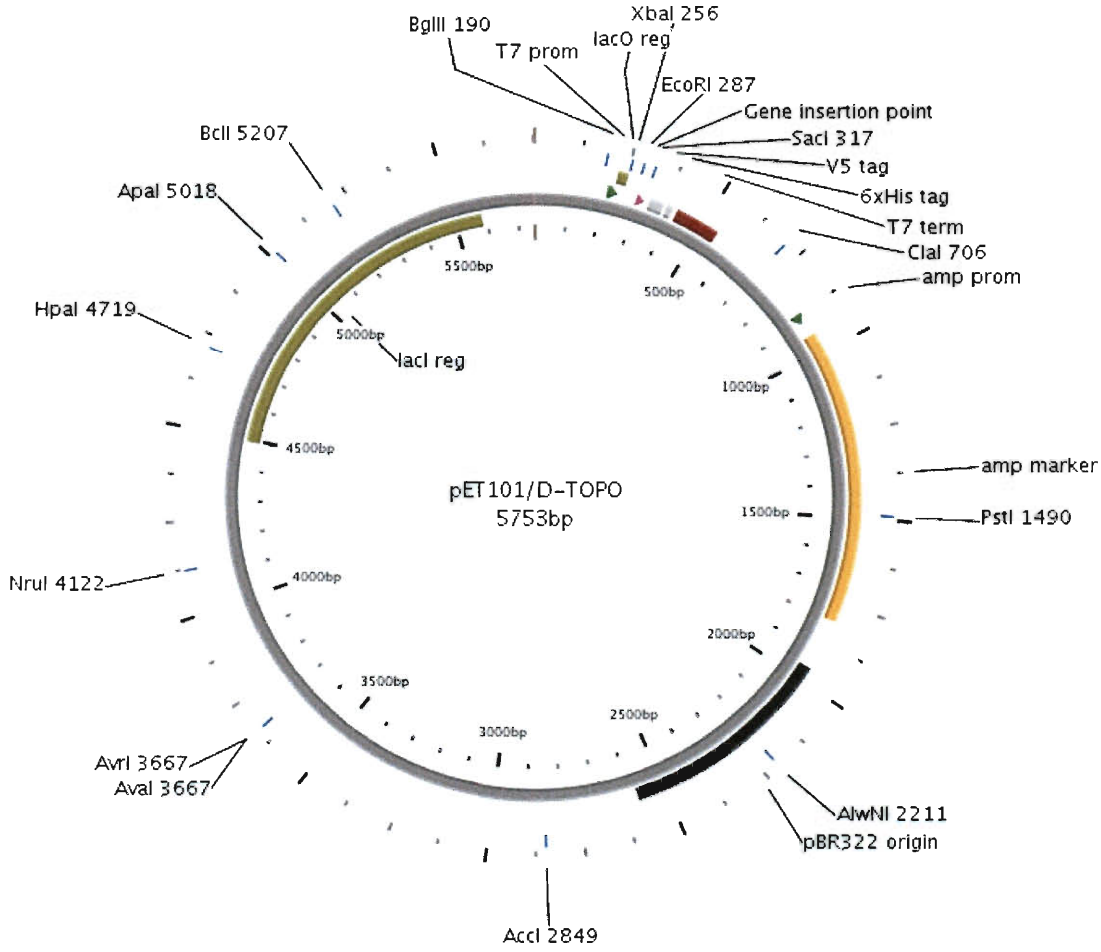

Figure 5-1. pET101/D-TOPO plasmid map. Vector used for all cloning of RHA1 genes. Genes were inserted without stop codons so they would include the 6xHis tag for affinity purification. Insertions were made between base pairs 305 and 306.

5.2.3. Protein expression and purification

Plasmid DNA from positive clones was extracted from overnight cultures using a 6 Minute Mini Plasmid Prep Kit (Mo Bio, Solana Beach, CA) according to the manufacturer's instructions. This DNA was used to transform chemically competent *E. coli* BL21 Star cells. Transformed cells were grown overnight in LB broth with ampicillin, and 2 ml of this was used to inoculate 100 ml of additional media. After 2 hours, cultures were induced with 1mM IPTG and allowed to grow for four more hours, at which time they were split into 50 ml Falcon tubes and harvested by centrifugation (5000 rpm, 10 min). Cell pellets were aspirated and stored at -80°C.

Cells were weighed and subsequently lysed with an appropriate amount of B-PER protein extraction reagent (Thermo Fisher Scientific, Waltham, MA), lysozyme, and DNase I. This was followed by centrifugation (15,000 x *g*, 5 min) and recovery of the supernatant. Crude extracts were split and half subjected to Ni-NTA column purification (HisPur Ni-NTA resin, Pierce Biotechnologies, Rockford, IL) under native conditions. Columns were loaded with 1.5 ml of resin and rinsed once with sterile water and twice with binding buffer (50 mM NaH_2PO_4, 0.5 M NaCl). 8 ml of lysate was then added and allowed to bind under gentle agitation for 1 hour. The resin was then washed four times with wash buffer (binding buffer with 20 mM imidazole) and then eluted with elution buffer (binding buffer with 250 mM imidazole). The eluent was then concentrated and desalted using Pierce 9K MWCO protein concentrators and 0.1M potassium

phosphate buffer. Proteins were stored at 4°C with the addition of Halt Protease Inhibitor (Pierce Biotechnologies, Rockford, IL).

Protein concentrations were determined using a BCA protein assay (Pierce Biotechnologies, Rockford, IL) according to the manufacturer's instructions. SDS-polyacrylamide gel electrophoresis (SDS-PAGE) was used to determine the presence of the correct size protein band as well as protein purity. Aliquots of protein from different stages in the purification process were mixed with equal volumes Laemmli sample buffer (containing 0.5% 2-mercaptoethanol) and boiled for 5 minutes in a water bath. 20 µl was loaded into each well of a 4-20% ReadyGel Tris-HCl precast gel in a Mini-PROTEAN Tetra Cell (Bio-Rad, Richmond, CA). Spectra™ Multicolor Broad Range Protein Ladder (Fermentas) was used to monitor the progress of electrophoresis and determine protein size. Gels were stained with Coomassie brilliant blue G-250 and allowed to destain overnight.

5.2.4. Enzyme activity assays

Dehydrogenase activity was assayed by monitoring NAD^+ or $NADP^+$ reduction at 340 nm using an Ultrospec 2100 Pro UV spectrophotometer (Amersham Biosciences, Piscataway, NJ). The standard assay mixture contained 100 mM potassium phosphate buffer, 0.1% Triton X-100, 200 µM NAD^+ or $NADP^+$, 20-200 µM substrate, and an appropriate amount of enzyme in a 2 ml reaction volume. Reductase activity was also assayed in a similar manner, except that NAD^+ and $NADP^+$ were replaced by NADH and NADPH, and a

decrease in absorbance at 340 nm was used to verify activity. Substrates tested were cholesterol, 5-cholestene-26-oic acid-3β-ol, cholic acid (CA), 7KC, 7-keto dehydroepiandrosterone (7KDHEA), 7-ketodeoxycholic acid (7KDC), and 7-ketolithocholic acid (7KLC)(Steraloids, Newport, RI). *E. coli* is known to harbor an innate reductase activity against bile acids, so an empty vector control was used to determine background activity. Additionally, three bile acid reductases were used as positive controls for 7KLC and 7KDC reduction [265-267] (provided by Dr. James P. Coleman, ECU). These enzymes were also PCR amplified and inserted into pET101/D-TOPO without their stop codons to incorporate the 6xHis tag.

The Michaelis-Menten equation was used to determine enzyme kinetic parameters:

$$v = \frac{V_{max}[S]}{K_m + [S]}$$

where v is the reaction rate, V_{max} is the maximum reaction rate, K_m is the substrate concentration required to reach one-half of V_{max}, and [S] is the substrate concentration. This equation was fit to each data set in Matlab R2008b (MathWorks Inc., Natick, MA) by nonlinear least squares regression, which uses an iterative search algorithm to determine the best-fit values of the hyperbolic parameters K_m and V_{max}.

HPLC-based assays were also performed with 7KC (absorption maxima = 235.8 nm) using the same standard assay mixtures and incubating the reactions

overnight at room temperature with gentle shaking. Lipids were then extracted using the method of Bligh and Dyer [268]. Briefly, 7.5 ml chloroform:methanol (1:2 v/v) was added to each 2 ml reaction and vortexed. This was followed by the addition of 2.5 ml of chloroform with vortexing. 2.5 ml of water was added and, following vortexing, each sample was centrifuged (1000 rpm, 5 mins) to give a two phase separation. 1 ml of the bottom organic layer was removed by Pasteur pipette, filtered through a 0.22 μm ReZist filter (Whatman, Piscataway, NJ), and allowed to evaporate to dryness under a nitrogen stream inside an analytical vial. Each sample was analyzed by reverse phase HPLC (1.0 ml min^{-1}, 100% methanol) using a Waters 2695 Separation Module with a Waters 996 photodiode array (235 nm) and a Waters NovaPak C_{18} column (3.9 by 150 mm). Chromatographic data was analyzed with the Empower 2 software suite (Waters, Milford, MA).

5.2.5. Protein modeling

A crystal structure for an *E. coli* 7α-hydroxysteroid dehydrogenase complexed with NADH and 7-oxo glycochenodeoxycholic acid (PDB code 1FMC) was used to construct a homology model of *Bacteroides fragilis* 7α-hydroxysteroid dehydrogenase. ClustalW (Biology Workbench, UCSD) was used to perform multiple sequence alignments. The protein homology model was created using PRIME (Schrodinger, New York, NY)[269, 270]. Structural figures and graphical rendering were done using PyMOL (Schrodinger, New York, NY). The three-dimensional structures of 7KC and 7KDC were prepared using the

LigPrep module of Maestro v.9.1.207 (Schrodinger, New York, NY). Bond orders were fixed and the structures calculated at pH 7. Ligands were then docked into the homology model using Glide (Schrodinger, New York, NY)[271] in standard precision mode without further minimization.

5.3. Results

5.3.1. Cloning of 7KC up-regulated genes

In total, 10 dehydrogenase/reductases from *Rhodococcus jostii* RHA1 were cloned and expressed in *E. coli* (Table 5-1). While we were able to PCR amplify all the genes from RHA1, cloning them by the standard protocol was problematic. Specifically, many of our cloning reactions contained empty vectors. This occurred using several different cloning techniques, such as topoisomerase-based cloning, CPEC, and restriction-free cloning. All the genes were high GC-content, which may have contributed to the difficulty we had cloning. Due to an additional hydrogen bond (in comparison to AT-bonds), regions of high GC-content tend to fold in upon themselves causing the formation of secondary structures that make certain cloning techniques difficult. To remedy this, and to optimize for expression in *E. coli*, the majority of these genes were synthesized (Genscript, Piscataway, NJ). No amino acids were changed, and all the products from PCR amplification of the synthesized genes were easily cloned into our expression vector.

5.3.2. Activity assays

None of the crude extracts from the recombinant *E. coli* proved to be active against 7KC, though those containing *ro02480*, *ro05819*, and *ro05832* were active against 7KLC (after normalization). This activity remained after affinity purification. One dehydrogenase, ro04707, proved to be active against cholesterol and was purified to homogeneity. This enzyme, a putative 3β-hydroxysteroid dehydrogenase, was determined to have a K_m and V_{max} of 75±6 μM and 6.9±1.2 U/mg respectively when utilizing cholesterol as a substrate (Fig. 5-2). None of the enzymes proved to be active against 7KDHEA, however *ro02480*, *ro05819*, and *ro5832* displayed activity after oxidation of the 3β-OH group using a cholesterol oxidase. Unfortunately, we were not able to completely purify these enzymes using Ni-NTA affinity chromatography, however control reactions were used with an empty vector to establish a baseline for innate reductase activity that may have co-purified.

Three 7α-hydroxysteroid dehydrogenases were also assayed against 7KC as well as the bile acids 7KLC and 7KDC. None of the three were active against 7KC, though they were capable of reducing the two bile acids, as previously reported [265-267]. The *Bacteroides fragilis* dehydrogenase, which was the most active, was successfully purified and assayed against several different 7KC/phospholipid combinations, but no activity was measured. The K_m and V_{max} for this enzyme were measured as 71.7±10.2 μM and 13.3±2.0 U/mg respectively against 7KLC, and 83.8±9.2 μM and 6.2±1.5 U/mg for 7KDC (Fig.

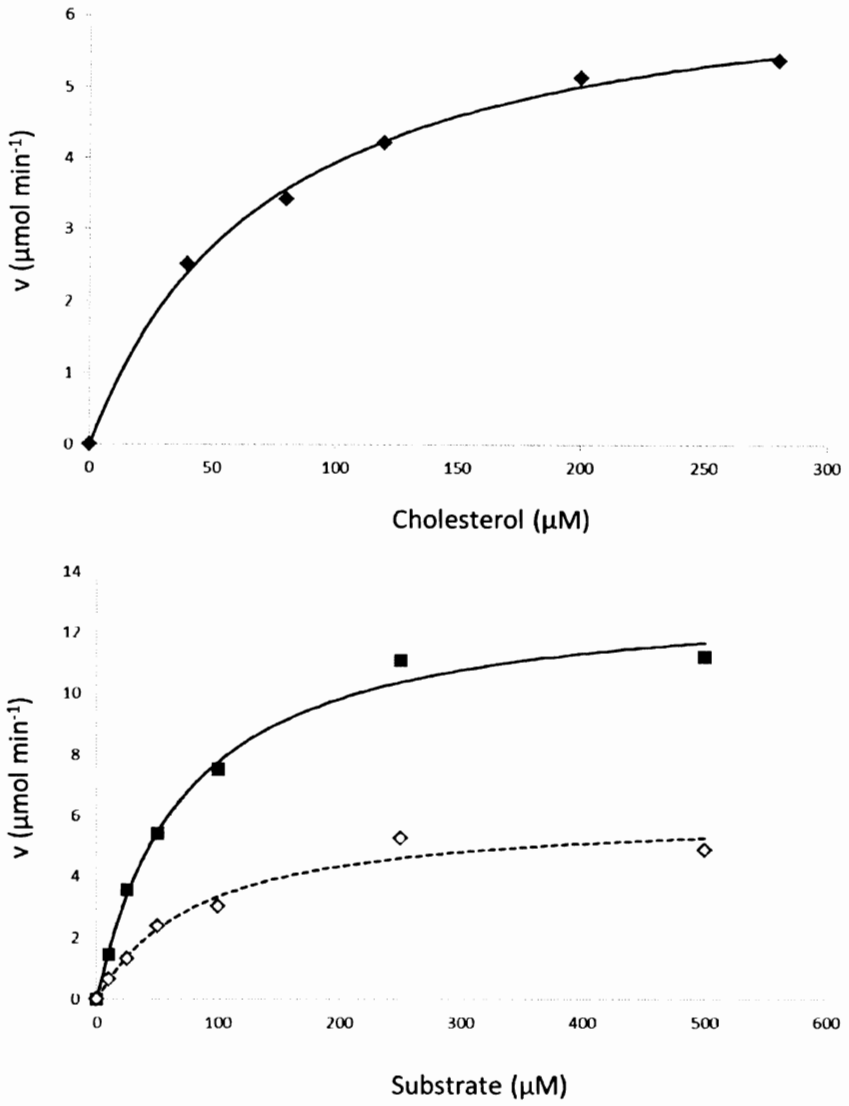

Figure 5-2. Dehydrogenase and reductase reaction rates. Reaction rate data was fit to the Michaelis-Menten equation using nonlinear regression for **A**. *R. jostii* RHA1 3β-hydroxysteroid dehydrogenase (*ro04707*) utilizing cholesterol as a substrate, and **B**. *B. fragilis* 7α-hydroxysteroid dehydrogenase, utilizing 7KLC (solid line) and 7KDC (dotted line) as substrates.

5.2). These numbers differed slightly from previously reported parameters [266], however this could possibly be attributed to the fusion of the 6xHis tag and V5 epitope to the C-terminus of the enzyme.

5.3.3. 7α-hydroxysteroid dehydrogenase protein model

Molecular simulations indicated that 7KDC docked into the 7α-hydroxysteroid dehydrogenase (7α-HSD) active site in proximity to the NADH cofactor, and oriented with its 7-keto substituent able to form a polar contact with Tyr158 (Fig 5-3A). This positioning results in reduction of the 7-keto group to 7α-OH. When 7KC was docked, however, the molecule inserts in a turned and flipped orientation with respect to 7KDC (Fig. 5-3B). The molecule is therefore unable to form a polar contact from its 7-keto group and reduction does not occur. These results are supported by our enzyme activity assays.

5.4. Discussion

The failure to identify an RHA1 enzyme that initiates transformation of 7KC was unfortunate, but not surprising. The RHA1 mutants we tested for growth on 7KC indicated that neither Cluster 2 or 3 encoded a complete set of 7KC-degrading enzymes, as evidenced by the failure of the *ΔhsaC* and *Δcyp125* mutants to grow on 7KC [38]. This argument is also supported by the fact that

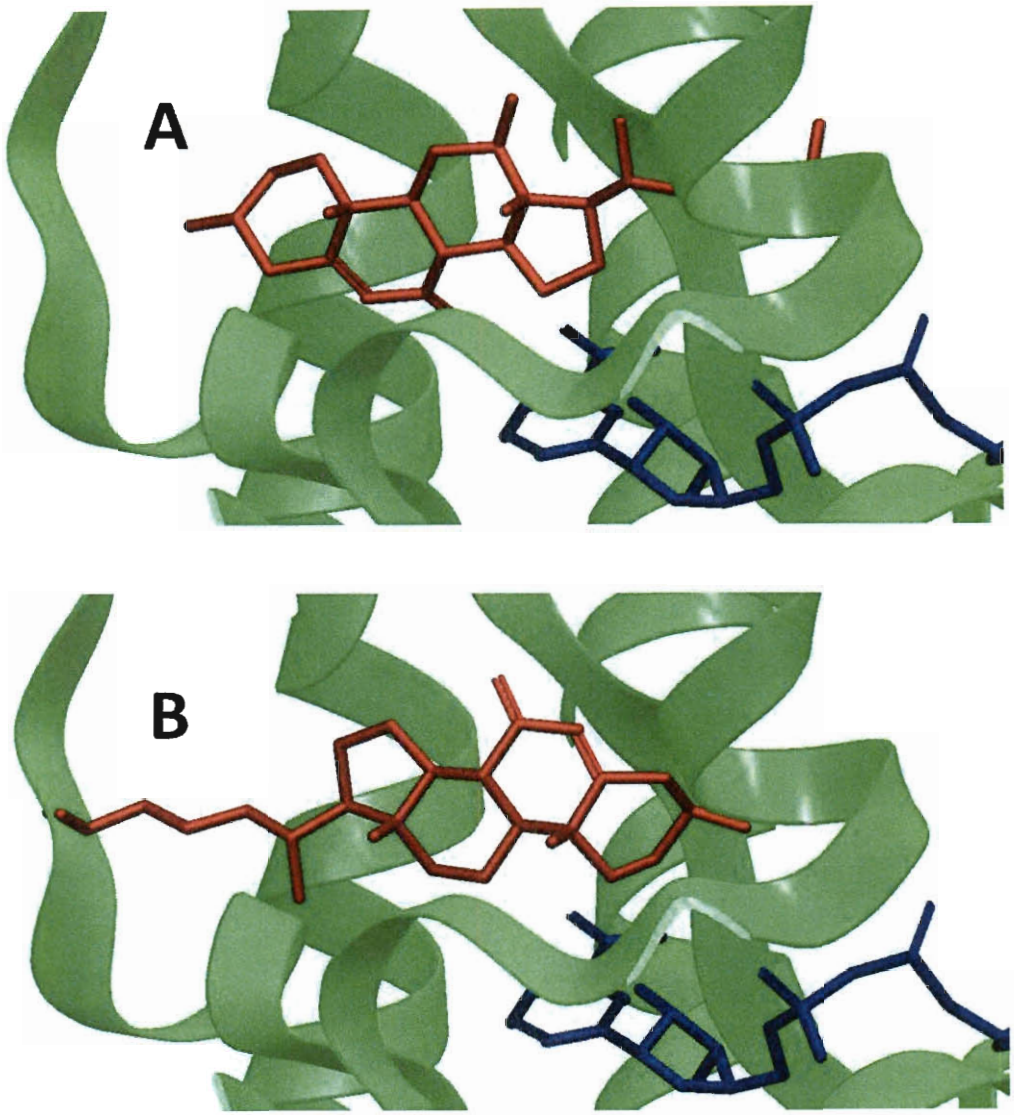

Figure 5-3. Homology model of *B. fragilis* 7α-hydroxysteroid dehydrogenase. A. Docked with 7-ketodeoxycholic acid using the Glide algorithm in Maestro. **B**. Docked with 7-ketocholesterol. 7-ketocholesterol is oriented flipped and turned with respect to 7-ketodeoxycholic acid. Substrates are colored red, NADH is colored blue.

both Cluster 2 and 3 each contain a homolog for *hsaC*, suggesting that the target substrate for the enzymes encoded by these clusters may not be 7KC. It is foreseeable that 7KC may gratuitously induce homologs of cholesterol catabolism genes in Clusters 2 and 3, but some of these homologs may not encode enzymes capable of initiating the catabolism of 7KC or the corresponding metabolites. Given the generally low concentrations of 7KC relative to other sterols in the environment, this is a reasonable, perhaps likely, scenario. Cluster 3 was also highly up-regulated by the presence of cholic acid, a compound similar in structure to 7KC, but more highly oxidized. While both of these compounds harbor functional groups at the C-7 position, bile acids also possess hydroxylated side chains and 3α-OH groups. Recently, evidence was found that C-26 oxidation may be an obligate first step of cholesterol degradation in RHA1 [272]. When we tested our recombinant enzymes on 7KDHEA we failed to detect activity, just as we had with 7KC. The steroid nucleus of this substrate is identical to that of 7KC, except that 7KDHEA lacks a side chain, having a keto group in its place (Fig. 5-4). However, when we first oxidized the 3β-OH groups of 7KDHEA with a cholesterol oxidase, three of our enzymes showed activity against this metabolite, though we have not determined the structure of the resulting product. The same three enzymes that were active against the oxidized 7KDHEA (*ro02480, ro05819,* and *ro05832*) also were active against 7KLC. This compound differs from 7KC in that it possesses both an oxidized side chain and a 3α-OH group instead of a 3β-OH (Fig. 5-4).

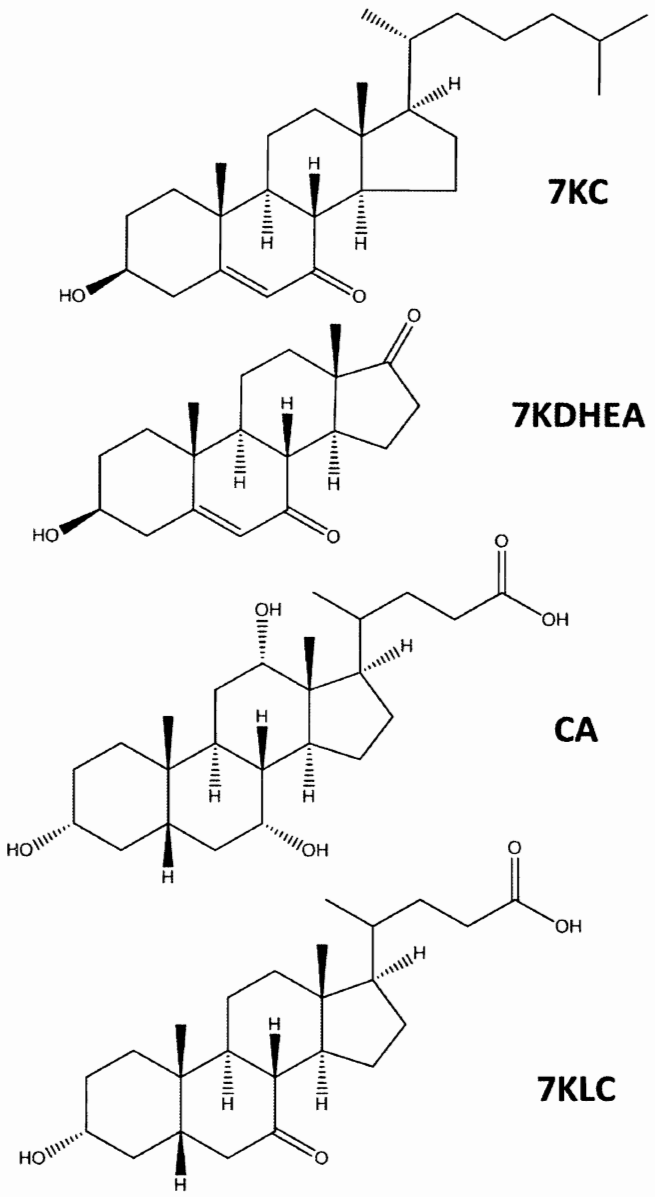

Figure 5-4. Substrates used in enzyme activity assays. 7-ketocholesterol (7KC), 7-ketolithocholic acid (7KLC), and 7-keto dehydroepiandrosterone (7KDHEA) were tested as substrates for several *Rhodococcus jostii* RHA reductases. Cholic acid (CA) was used as a control for reduction reactions and as a growth substrate during transcriptomic analysis.

In many microbial sterol degradation pathways, oxidation of the 3β-OH is the first step, often catalyzed by an extracellular cholesterol oxidase [22, 34, 273]. RHA1 seems to lack extracellular oxidase activity. However, contrary to findings that side chain hydroxylation may be the first step in cholesterol degradation in RHA1 [272], we cloned a putative 3β-hydroxysteroid dehydrogenase (*ro04707*) that was active against cholesterol. Though this enzyme lacked activity against 7KC, it was also inactive against 5-cholestene-26-oic acid-3β-ol. This suggests that oxidation of the 3β-OH group may occur prior to side chain oxidation, though there may be other enzymes that catalyze 3β-OH oxidation with differing substrate specificity. Regardless, it appears that the three reductases we identified have at least one common requirement for activity: isomerization or oxidation of the 3β-OH group. They may also require an oxidized side chain, though further testing needs to be done to validate this hypothesis. This fits wells with our currently proposed cholesterol degradation pathway (Fig. 4-3) as both of these steps precede the reaction catalyzed by HsaC.

In a further effort to understand 7KC degradation, and to evaluate the potential to alter substrate specificity of the cloned enzymes using mutagenesis, we constructed a homology model of the *Bacteroides fragilis* 7α-hydroxysteroid dehydrogenase (7αHSD). We used this enzyme due to its high similarity to another 7αHSD with an available crystal structure complexed with 7-oxo glycochenodeoxycholic acid. In comparison to 7KDC, our docking simulation showed that 7KC binds to the 7αHSD active site in a turned and flipped orientation (Fig. 5-3). This would effectively prevent reduction of the 7-keto group

as it removes it from the proximity of the catalytic residues (Tyr158 and Lys162) as well as NADH. The carboxyl group of 7KDC also forms a polar contact, potentially stabilizing it in the binding site.

In searching for 7KC-transforming enzymes, we did not exhaust all of the potential candidates that could be responsible for 7-keto reduction. One example is *ro05789*, a putative carveol dehydrogenase. We chose to clone *ro02480* over this enzyme as they share high identity and *ro02480* was much more highly expressed during 7KC catabolism. Future work may include investigation of this particular gene, especially considering the failure to identify useful RHA1 enzymes. On the other hand, it is likely that 7KC needs to be transformed sequentially in RHA1, with ring A and side chain oxidation occurring first. Therefore, identifying and expressing active forms of the enzymes responsible for these transformations may be of particular importance.

Chapter 6

Strategies for the mitigation of 7KC-induced cytotoxicity

6.1. Introduction

As presented in previous chapters, 7KC is highly cytotoxic to mammalian cells and may contribute to the initiation or progression of a number of age-related diseases. Therefore, it has been suggested that controlling dietary and endogenous 7KC levels could help reduce the incidence and severity of these diseases [36, 50, 274, 275]. In humans, several enzymes are known to accept 7KC as a substrate, and may help attenuate some of its effects. Sterol 27-hydroxylase (CYP27A1), a mitochondrial enzyme involved in bile acid synthesis and the excretion of excess cholesterol, was previously found capable of 7KC side chain oxidation [223]. Additionally, 27-hydroxylation was shown to render 7KC non-toxic to retinal pigment epithelial cells [210]. Reduction of the 7-keto

moiety, producing 7β-hydroxycholesterol (7β-HC), is catalyzed by 11β-hydroxysteroid dehydrogenase type I (HSD11β1) [259, 276]. Reduction of 7KC can produce either 7α- or 7β-hydroxycholesterol (7α/β-HC). However, human HSD11β1 produces only the β-isomer, as does the HSD11β1 from all mammalian species studied save the golden hamster (*Mesocricetus auratus*) [259, 276]. This is unusual considering 7β-HC is approximately ten-fold more cytotoxic than the α-isomer, and two-fold more than 7KC [150, 260-262]. Esterification of 7KC is catalyzed by plasma lecithin:cholesterol acyltransferase (LCAT) or, intracellularly, by acyl-coenzyme A:cholesterol acyltransferase (ACAT) [277], which has been found to impair the toxicity of oxysterols [278]. Finally, the sterol sulfotransferase SULT2B1b, which participates in cholesterol excretion, also uses 7KC as a substrate [212]. Of these enzymes, only SULT2B1b has been overexpressed in cells to test for its ability to attenuate 7KC-induced cytotoxicity, and though the results suggest some benefit, the effect is relatively small; increasing cell survival approximately 20% [212]. Furthermore, expression of these enzymes does not seem to be sufficient to reduce 7KC levels *in vivo* [279]. One reason for this apparent lack of effectiveness could be the subcellular localization of these enzymes, none of which target to the lysosome.

At micromolar concentrations, 7KC causes lysosomal membrane permeabilization (LMP) which precedes mitochondrial destabilization [146]. The cellular response to LMP depends on the degree of permeabilization, but massive LMP generally leads to necrosis while lesser degrees may induce

apoptosis or apoptosis-like cell death [280]. The initiation of lysosomal cell death signaling is thought to be due to the release of lysosomal cathepsins into the cytosol where they interact with various targets [281]. Lysosomes also receive sterols (including oxysterols) from early endosomes after receptor-mediated endocytosis of LDL, and are a major site of non-enzymatic oxysterol formation. Consequently, 7KC levels are the highest in the endosomal/lysosomal compartments [174], and though enzymes exist which may mitigate 7KC cytotoxicity, those enzymes are primarily present in the ER, mitochondria, and cytoplasm and are not ideally localized to prevent LMP and the subsequent signaling cascade.

In contrast to metabolism in mammalian cells, 7KC is readily mineralized by a diversity of bacteria [37], where its only putatively deleterious effect seems to be mutagenicity [205]. We previously studied the microbial degradation of 7KC in *Rhodococcus jostii* RHA1, and partially elucidated its degradation pathway, which largely, but not completely, overlaps with that of cholesterol [38]. During this investigation we discovered that RHA1 was capable of reducing the 7-keto group and removing it downstream of HsaC, the enzyme that catalyzes cleavage of ring A of the steroid nucleus. We attempted to identify a reductase that would catalyze the reduction of 7KC to 7α-HC, but only isolated reductases from RHA1 that were active against more hydrophilic structural analogs, such as 7-ketolithocholic acid (7KLC). In RHA1, and many other sterol-degrading bacteria, the initial step is either side-chain hydroxylation or oxidation of the 3β-OH group (Fig. 4-3). Reduction of the 7-keto moiety also seems to take place downstream

of these steps in RHA1 at least. We determined that the diketone produced from 3β-oxidation of 7KC displays decreased cytotoxicity in 293T cells [39]. It thus appears that oxidation of 7KC is sufficient to mitigate its toxicity, at least in cell culture, and that the selective oxidation of 7KC could prove useful in reducing its toxicity *in vivo*. However an inability to differentiate between 7KC and cholesterol could be problematic. Most cholesterol oxidases, a bacterial enzyme that catalyzes 3β-oxidation of sterols, also catalyze Δ5-6 to Δ4-5 bond isomerization, producing cholest-4-en-3-one from cholesterol. The addition of cholest-4-en-3-one to membranes in place of cholesterol leads to reduced condensation and increased disorder. So while this form of oxidation may reduce the toxicity of 7KC, it decreases the ability of cholesterol to maintain membrane structure, with consequences for cell integrity [282].

Recently, a cholesterol oxidase from *Chromobacterium sp.* DS1 was isolated that lacks isomerization activity, forming cholest-5-en-3-one [283, 284] (though this compound may undergo further auto-oxidation at C-6 to form 6β-hydroperoxycholest-4-en-3-one) [285]. Unlike cholest-4-en-3-one, cholest-5-en-3-one does not increase membrane permeability [282]. Additionally, the DS1 cholesterol oxidase (DS1 ChOx) is extremely stable; maintaining activity in a variety of solvents, detergents, and at high temperature. Based on these desirable characteristics, we tested the DS1 ChOx for activity against 7KC, assessed the potential to deliver this enzyme to the mammalian lysosome, and assayed its potential efficacy to mitigate 7KC-induced cytotoxicity.

6.2. Materials and methods

6.2.1. Molecular cloning

For protein expression and subsequent purification, DS1 ChOx (obtained from Dr. Noriyuki Doukyu, Toyo University) was subcloned into pET101/D-TOPO (Invitrogen, Carlsbad, CA)(Fig. 5-1) using Gibson assembly [286]. Briefly, the nucleotide sequence for mature DS1 ChOx was PCR amplified using Kapa HiFi polymerase (Kapa Biosystems, Woburn, MA) and primers containing 5' additions homologous to the ends of the linearized vector (Table 6-1). The insert and linearized vector were both gel purified and combined at equimolar concentrations in a reaction mixture containing T5 exonuclease, Phusion polymerase (New England BioLabs, Beverly, MA), and Taq ligase. Isothermal assembly was allowed to proceed for 1 hour at 50°C, and 3 µl of the reaction was used to transform chemically competent *E. cloni* 10G (Lucigen, Middleton, WI) cells. After transformation, cells were plated on LB plates with ampicillin (100 µg/ml) and incubated overnight at 37^0C. The presence of the correct sized insert was verified using colony PCR (T7 primers) in conjunction with gel electrophoresis. The product from positive colonies was sequenced (Seqwright, Houston, TX).

For use in mammalian transient transfections, the genes for DS1 ChOx, HSD11β1 (synthesized by Geneart, Regensburg, Germany) were subcloned into

Table 6-1. Primers used for vector construction in this study.

Amplicon	Purpose	Primers
pET101/D-TOPO	vector linearization	F: 5'-AAGGGCGAGCTCAATTCGAAG-3' R: 5'-GGTGAAGGGCTCCTGAATTCC-3'
pEGFP-N3/LAMP1	vector linearization with LAMP1/GFP deletion	F: 5'-GGATCTGACGGTTCACTAAACC-3' R: 5'-TAAAGCGGCCGCGACTCTA-3'
pEGFP-N3/LAMP1	vector linearization with LAMP1 luminal deletion	F: 5'-CTGCTGGACGAGAACAGCAT-3' R: 5'-CATTGCTGCTGACGCACAATG-3'
DS1 ChOx	pET101/D-TOPO insert	F: 5'-CAGGAGCCCTTCACCATGACTTGCAGC CAACCCAATAATTTCC-3' R: 5'-ATTGAGCTCGCCCTTGAGACCCAGGCT GTCCAGC-3'
DS1 ChOx	pEGFP-N3 insert	F: 5'-GGTTTAGTGAACCGTCAGATCCATGAC TTGCAGCCAACCCAATAATTTCC-3' R: 5'-TAGAGTCGCGGCCGCTTTAGAGACCCA GGCTGTCCAGC-3'
DS1 ChOx	LAMP1 insert	F: 5'-CATTGTGCGTCAGCAGCAATGACTTGC AGCCAACCCAATAATTTCC-3' R: 5'-ATGCTGTTCTCGTCCAGCAGGAGACCC AGGCTGTCCAGC-3'
HSD11β1	pEGFP-N3 insert	F: 5'-CTGGTTTAGTGAACCGTCAGATCCATGG CCTTTATGAAGAAATACTTATTGC-3' R: 5'-TAGAGTCGCGGCCGCTTTACTTATTAA TGAATCGATCCATGTTATAAGA-3'

a variant of pEGFP-N3 (Fig. 6-1) as described above. The variant (obtained from Dr. Esteban Dell'Angelica, UCLA) is a construct containing human LAMP1 cloned in the EcoRI-SalI sites with a mutant GFP that prevents anti-parallel dimerization [287]. The LAMP1 and GFP sequences were deleted during linearization for insertion of the HSD11β1 gene (pMEV-HSD). For the DS1 ChOx sequence, two vectors were created; one in which the LAMP1 and GFP genes were also deleted for cytoplasmic targeting (pMEV-COX), and another in which only the luminal portion of LAMP1 was deleted (pEGFP-COXL1). For this latter construct, the signal peptide and transmembrane domains of LAMP1 were retained for lysosomal targeting of DS1 ChOx. Plasmids were propagated and maintained in *E. cloni* 10G. After transformation, cells were plated on LB plates with kanamycin (50 μg/ml) and incubated overnight at 37^0C. All non-competent bacterial strains were maintained as 20% glycerol stocks at -80^0C. *E. coli* strains were cultivated aerobically in Luria-Bertani (LB) broth or agar plates at 37^0C with the appropriate antibiotic for plasmid maintenance when necessary. Liquid cultures were also shaken at 200 rpm.

6.2.2. Protein expression

The purified pET101/D-TOPO construct was used to transform chemically competent *E. coli* BL21 Star cells (Invitrogen, Carlsbad, CA). Transformed cells were grown overnight in LB broth with ampicillin, and 2 ml of this was used to inoculate 100 ml of additional media. After 2 hours, cultures were induced with 1mM IPTG and allowed to grow for four more hours, at which time they were split

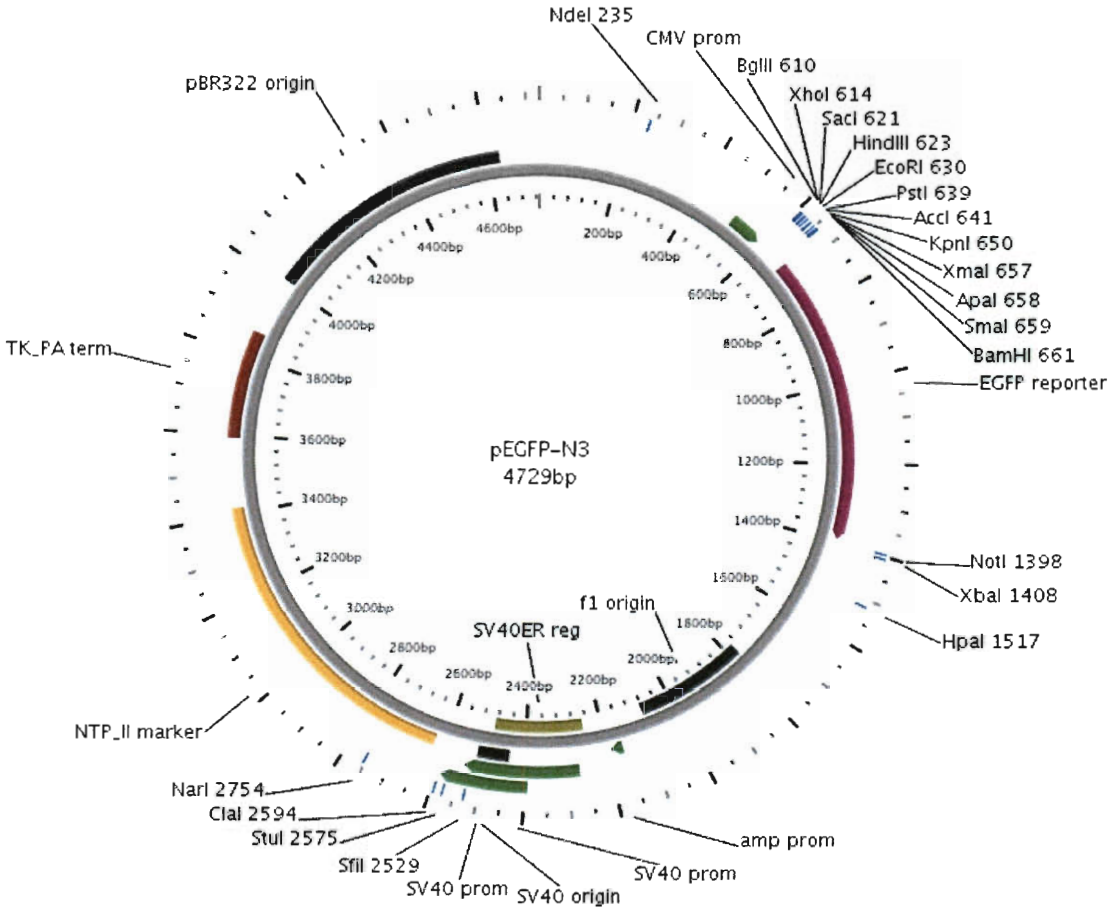

Figure 6-1. pEGFP-N3 plasmid map. Vector used for construction of mammalian expression vectors in this study. For cytoplasmic targeting of enzymes, the polylinker and GFP sequences were deleted during PCR linearization. For lysosomal targeting, the transmembrane domain and signal peptide from LAMP1 were utilized, which was inserted between the *Eco*RI and *Sal*I sites [287].

into 50 ml Falcon tubes and harvested by centrifugation (5000 rpm, 10 min). Cell pellets were aspirated and stored at -80°C.

For protein purification, cells were weighed and subsequently lysed with an appropriate amount of B-PER protein extraction reagent (Thermo Fisher Scientific, Waltham, MA), lysozyme, and DNase I. This was followed by centrifugation (15,000 × *g*, 5 mins) and recovery of the supernatant. Crude extracts were split and half subjected to Ni-NTA column purification (HisPur Ni-NTA resin, Pierce Biotechnologies, Rockford, IL) under native conditions. Columns were loaded with 1.5 ml of resin and rinsed once with sterile water and twice with binding buffer (50 mM NaH_2PO_4, 0.5 M NaCl). 8 ml of lysate was then added and allowed to bind under gentle agitation for 1 hour. The resin was washed four times with wash buffer (binding buffer with 20 mM imidazole), eluted with elution buffer (binding buffer with 250 mM imidazole), and concentrated /desalted using Pierce 9K MWCO protein concentrators and 0.1M potassium phosphate buffer. Proteins were stored at 4°C with the addition of Halt Protease Inhibitor (Pierce Biotechnologies, Rockford, IL).

Protein concentrations were determined using a BCA protein assay (Pierce Biotechnologies, Rockford, IL) according to the manufacturer's instructions. SDS-polyacrylamide gel electrophoresis (SDS-PAGE) was used to determine the presence of the correct size protein band as well as protein purity. Aliquots of protein from different stages in the purification process were mixed with equal volumes Laemmli sample buffer (containing 0.5% 2-mercaptoethanol)

and boiled for 5 minutes in a water bath. 20 µl was loaded into each well of a 4-20% ReadyGel Tris-HCl precast gel in a Mini-PROTEAN Tetra Cell (Bio-Rad, Richmond, CA). Spectra™ Multicolor Broad Range Protein Ladder (Fermentas, Hanover, MD) was used to monitor the progress of electrophoresis and determine protein size. Gels were stained with Coomassie brilliant blue G-250 and allowed to destain overnight.

6.2.3. Cholesterol oxidase activity assays

DS1 ChOx was indirectly assayed for activity against cholesterol and 7KC by monitoring oxidation of o-Dianisidine at 500 nm [288]. The reaction buffer consisted of 100 mM potassium phosphate buffer containing 0.01% o-Dianisidine (w/v). 10 U of horseradish peroxidase solution and 10 µg of DS1 ChOx were then added to 1.8 ml of reaction buffer and allowed to equilibrate. Reactions were initiated by the addition 200 µl of different concentrations of substrate dissolved in 1% Triton X-100, bringing the final volume to 2 ml. Reaction progress was monitored by the change in A_{500} over three minutes.

HPLC-based assays for DS1 ChOx were also performed with 7KC (absorption maxima = 235.8 nm) using 100 mM potassium phosphate as reaction buffer and 0.1% Triton X-100 for detergent micelle formation, and incubating the reactions overnight at room temperature with gentle shaking. Lipids were then extracted using the method of Bligh and Dyer [268]. Briefly, 7.5 ml chloroform:methanol (1:2 v/v) was added to each 2 ml reaction and vortexed. This was followed by the addition of 2.5 ml of chloroform with vortexing. 2.5 ml of

water was added and, following vortexing, each sample was centrifuged (1000 rpm, 5 mins) to give a two phase separation. 1 ml of the bottom organic layer was removed by Pasteur pipette, filtered through a 0.22 µm ReZist filter (Whatman, Piscataway, NJ), and allowed to evaporate to dryness under a nitrogen stream inside an analytical vial. Each sample was analyzed by reverse phase HPLC (1.0 ml min^{-1}, 100% methanol) using a Waters 2695 Separation Module with a Waters 996 photodiode array (235 nm) and a Waters NovaPak C_{18} column (3.9 by 150 mm). Fractions were collected at 30 second intervals for GC-MS, and chromatographic data was analyzed with the Empower 2 software suite (Waters, Milford, MA).

6.2.4. GC-MS and NMR analysis of DS1 ChOx metabolites

GC-MS analysis was performed on an Agilent 5973 MSD connected to an Agilent 6890 GC system (Agilent, Palo Alto, CA). Samples were injected in pulsed splitless mode with an injector temperature of 280°C. The Restek Rtx-35ms GC column (30 m x 0.25 mm i.d. x 0.1 µm film thickness) was temperature programmed as follows: 110 °C (1 min), then 30 °C/min to 240 °C, then 1.3 °C/min to 280 °C. MS data were acquired with electron impact (EI) ionization at 70 eV in full-scan mode (50 to 650 amu) after a 5-min solvent delay. Trimethylsilyl (TMS) ether derivatives of sterols were prepared by dissolving each sample in 1:1 pyridine/BSTFA, heating the mixture at 60 °C for 1 h, and injecting 2 µL of the mixture.

Proton 1D NMR spectra were obtained on a 600 MHz Varian (Agilent, Palo Alto, CA) Inova NMR spectrometer with an HCN cold probe. Samples were dissolved in 99.9% $CDCl_3$ with 0.05% TMS as a proton chemical shift standard. The spectrum of the crude reaction mixture was acquired at 25°C with 128 scans over a sweep width of 5300 Hz (8.8 ppm). The acquisition time was 6 sec. with a relaxation delay of 4 sec.; a 45 degree proton excitation pulse was used. The sample was spun at 20 Hz during the acquisition of the spectrum. Since resonances from 7KC and the products from its reaction with DS1 ChOx were obscured by proton signals from membrane components, the reaction products were purified by HPLC. An NMR spectrum of this sample were collected over a 12-ppm sweep width by taking 640 scans with a 3 sec. acquisition time, a 1 sec. relaxation delay, and a 90 degree pulse. Since the HPCL-purified sample was less concentrated than the crude reaction mixture, an instrumental artifact from the residual protonated chloroform obscured vinyl signals of interest at 5.71 ppm; to remedy this, a presaturation pulse of 1 sec was applied at the chemical shift of the protonated chloroform (7.26 ppm) to remove this artifact. The spectra obtained of the HPLC-purified sample did not allow sufficient time for full relaxation; therefore intensity patterns may be skewed due to different relaxation rates of different protons.

6.2.5. Cytotoxicity assays

WT primary fibroblasts (GM00498) were obtained from Coriell Cell Repositories (Camden, NJ). Fibroblasts were grown in minimal essential medium

with Earle's salts supplemented with 10% heat-inactivated fetal bovine serum and 1% glutamine-penicillin-strepomycin solution at 37°C in 5% CO_2. Cell medium was replaced every 3 or 4 days. Monolayers were passaged upon reaching confluency with TrypLE Express (Invitrogen, Carlsbad, CA).

For cytotoxicity assays, fibroblasts were seeded at approximately 2 x 10^5 cells per well in 6-well plates or 5 x 10^3 cells in 96-well plates containing Eagle's minimum essential media (EMEM) with 10% fetal bovine serum and 1% glutamine-penicillin-strepomycin solution, and allowed to recover overnight. Cells were exposed to varying concentrations of cholesterol, 7KC, 7KDHEA, or 7KLC (ethanol stocks; each well contained a final concentration of 1% ethanol) for 24 hours and evaluated for cytotoxicity using an XTT Cell Viability Assay Kit (Biotium, Hayward, CA) and monitoring absorbance at 450 nm. Some cells were also treated with hydroxypropyl β-cyclodextrin and 7KC simultaneously. Additionally, fibroblasts treated with cholesterol or 7KC were collected and cell toxicity tested with the CytoGLO Annexin V-FITC Apoptosis Detection Kit (IMGENEX, San Diego, CA) according to the manufacturer's instruction, and analyzed by flow cytometry using a FACSCanto II with a 488-nm argon laser (Becton Dickinson, Franklin Lakes, NJ). Normal, apoptotic, and dead cell percentages were determined for each treatment using 10,000 gated events (approximately 10,000 cells).

To study the effects of heterologous gene expression, fibroblasts were seeded in 96-well plates as indicated above, and subsequently transfected with

Table 6-2. Plasmids used in this study.

Plasmid	Product	Type	Product Target	Source
pcDNA3.1-MC	mCherry	mammalian	cytoplasm	Segatori
pMEV-HSD	11β-hydroxysteroid dehydrogenase	mammalian	ER	This study
pEGFP-LAMP1	LAMP1-GFP fusion	mammalian	lysosome	Dell'Angelica [287]
pBScox	*Chromobacterium sp.* DS1 cholesterol oxidase	*E. coli*	cytoplasm	Doukyu [283]
pET101-COX	DS1 cholesterol oxidase with 6xHis tag	*E. coli*	cytoplasm	This study
pMEV-COX	DS1 cholesterol oxidase	mammalian	cytoplasm	This study
pEGFP-COXL1	Engineered cholesterol oxidase-GFP fusion	mammalian	lysosome	This study
pCMV6-XL4-CYP27	CYP27A1	mammalian	mitochondria	Origene

plasmid DNA (Table 6-2) using jetPRIME transfection reagent (Polyplus, New York, NY) according to the manufacturer's instructions. Fibroblasts were co-transfected with a small amount of plasmid encoding the fluorescent reporter mCherry to evaluate transfection efficiency. After 4 hours, the media was exchanged and the cells were allowed to recover for an additional 18 hours before the addition of varying concentrations of 7KC. Some non-transfected cell populations were amended with either 0.9% or 4.5% hydroxypropyl β-cyclodextrin as well. Cell viability was measured after 24 hours using the XTT assay as described above. Prior to exposure to 7KC, transfection efficiency was gauged by fluorescent plate reader (Excitation 587/Emission 610) as well as visualization by fluorescence microscopy. The intracellular expression and localization of GFP was observed using an inverted fluorescence microscope (IX-71, Olympus America, Melville, NY) with a FITC filter set and attached digital camera. Images were processed using cellSENS Dimension software.

6.3. Results

6.3.1. DS1 cholesterol oxidase is active against 7KC

The mature form of the DS1 cholesterol oxidase [283] was successfully cloned into pET101/D-TOPO using Gibson assembly, expressed in batch, and purified to homogeneity using affinity purification. The enzyme was active against both cholesterol and 7KC in detergent and mixed micelles. This was supported

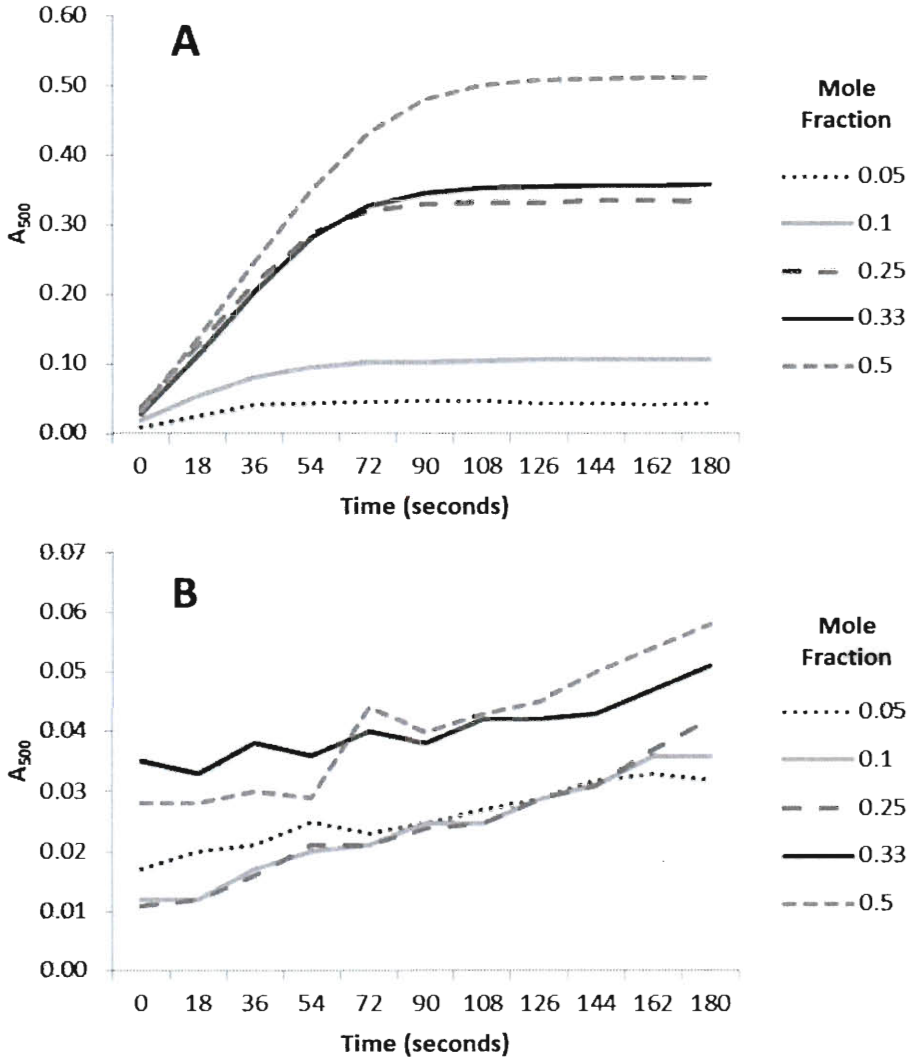

Figure 6-2. DS1 cholesterol oxidase reaction progress curves. Enzyme activity against either **A**. cholesterol or **B**. 7KC was measured indirectly by monitoring oxidation of o-Dianisidine at 500 nm in 100 mM potassium phosphate buffer (pH 7). Substrate mole fraction in detergent micelles (0.1% Triton X-100) varied between 0.05 and 0.50.

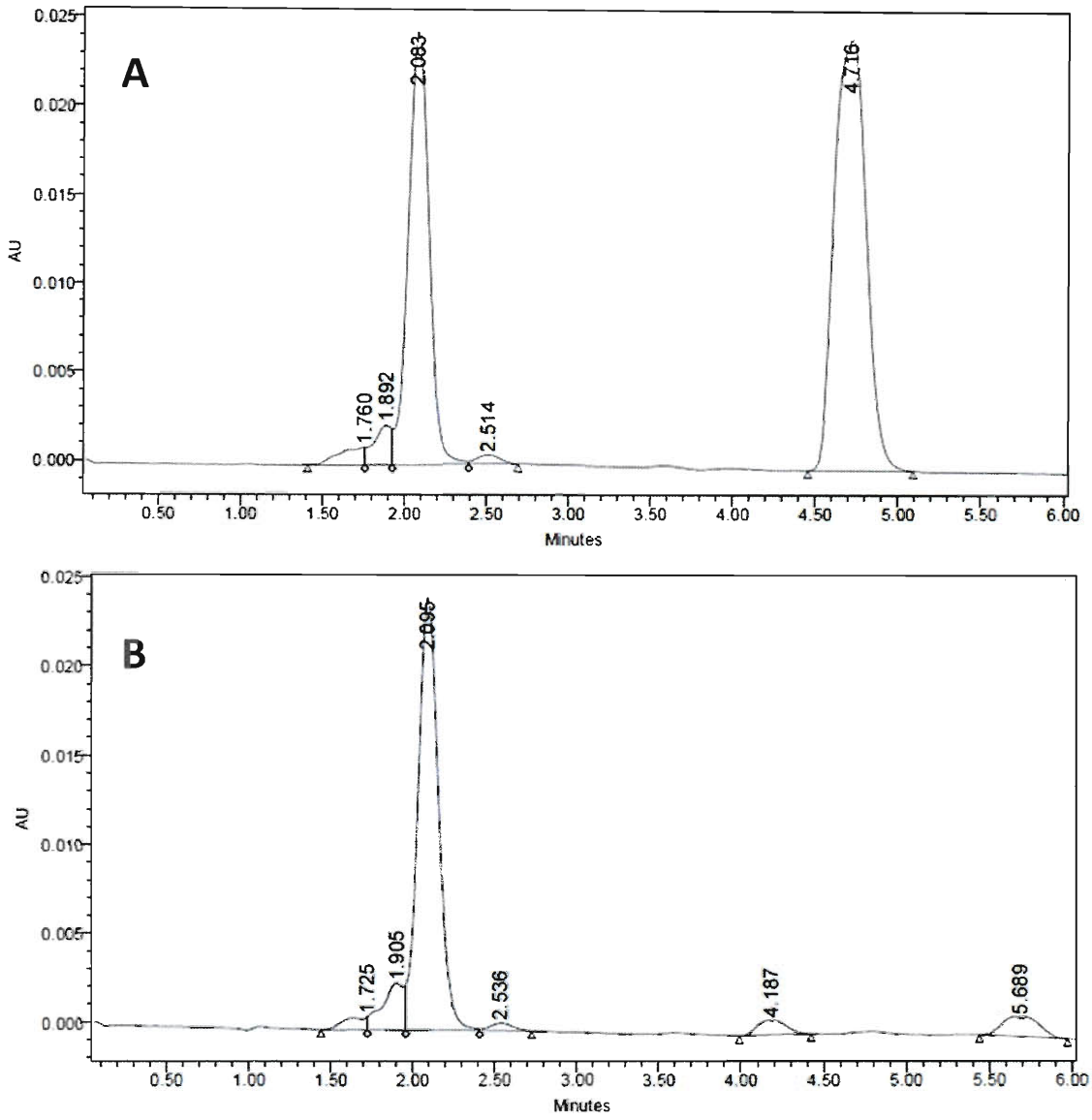

Figure 6-3. HPLC-based oxidase assays. Purified DS1 cholesterol oxidase was incubated for 12 hours with 200 µM 7KC in 100 mM potassium phosphate buffer containing 0.1% Triton X-100 (pH 7). Sterols were extracted by the method of Bligh and Dyer [268] and separated by reverse phase HPLC. Absorbance was monitored at 235 nm. **A.** Control reaction (no enzyme) showing the 7KC peak at 4.5 mins. **B.** Enzymatic reaction with the peak at 4.5 mins completely degraded, and showing two additional peaks at 4.184 and 5.689 mins. The major product possessed an absorption maximum of 319 nm (peak at 5.689 mins).

by both indirect and HPLC-based assays (Figs. 6-2 and 6-3). Enzyme activity against both cholesterol and 7KC increased at higher substrate mole fractions. The reaction rate was approximately 8-fold higher for cholesterol than for 7KC at a mole fraction of 0.05, and increased to 26-fold higher at a mole fraction of 0.50.

GC-MS of the HPLC fractions from the 7KC reaction revealed the presence of two large peaks, one corresponding to the molecular weight of 7KC and the other with a molecular weight two less than that of 7KC (Fig. 6-4). This is supportive of 3β-oxidation, which would result in the loss of two hydrogen atoms. NMR spectra revealed the presence of two additional shifted peaks at approximately 0.7 and 5.7 ppm, which are likely the products of the enzyme reaction (Fig. 6-5). Since there is only one additional peak observed during GC-MS, the two products may be isomers, though we cannot conclusively determine this using 1D NMR.

6.3.2. 7KC causes necrosis of human fibroblasts

7KC caused decreased viability of human fibroblasts as determined by the XTT assay (Fig. 6-6). 7KC solubilized in ethanol (7KC:EtOH) was more toxic than 7KC in cyclodextrin (7KC:cyclo) at the same molarity. After 24 hours there was a slight decrease in the average viable cell fraction for both treatments at 10 μM (0.96±0.11 for 7KC:EtOH and 0.96±0.02 for 7KC:cyclo). A noticeable divergence between treatments occurred at 25 μM with 7KC:EtOH-treated cells experiencing a reduction to 0.15±0.12 viable cell fraction compared to 0.83±0.10 for the

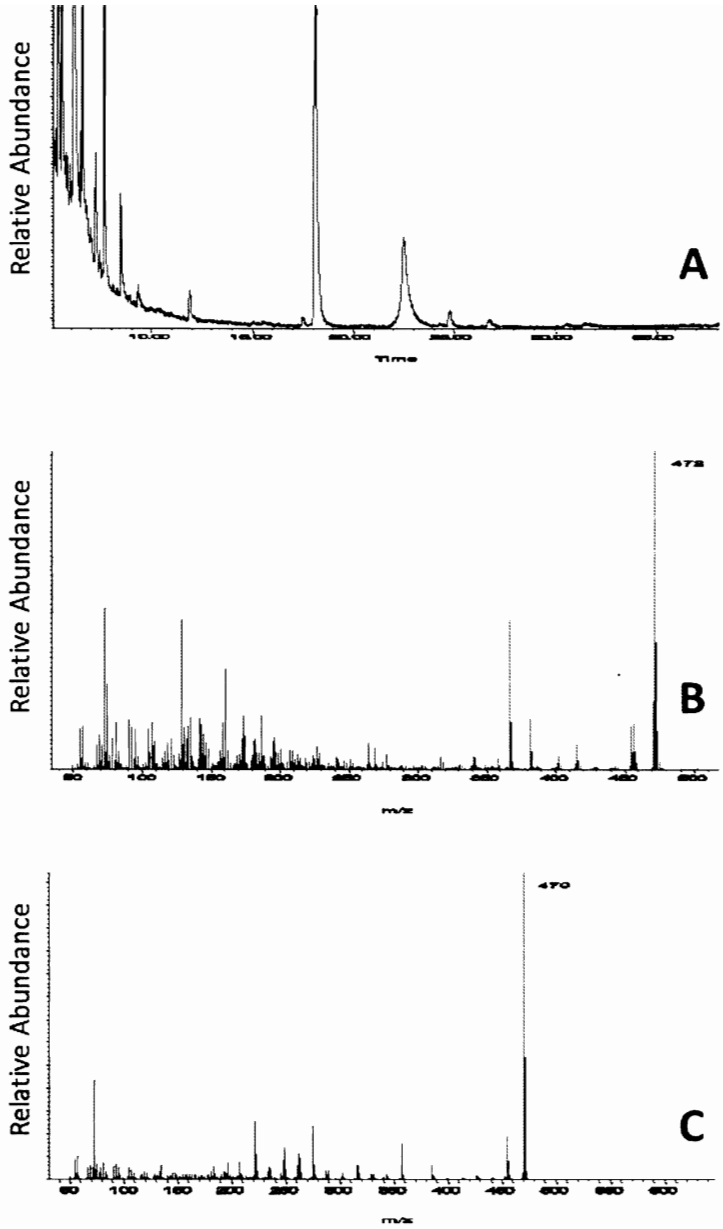

Figure 6-4. GC-MS spectra of 7KC metabolite. Fractions from the HPLC-based assay of DS1 cholesterol oxidase were screen using GC-MS. **A**. Two major peaks were observed with derivitized masses of **B**. 472 and **C**. 470. These correspond to molecular weights of 400 and 398. The molecular weight of 7KC is 400 and that of its 3β-oxidized diketone would be 398, providing strong evidence for the activity of the DS1 oxidase on 7KC.

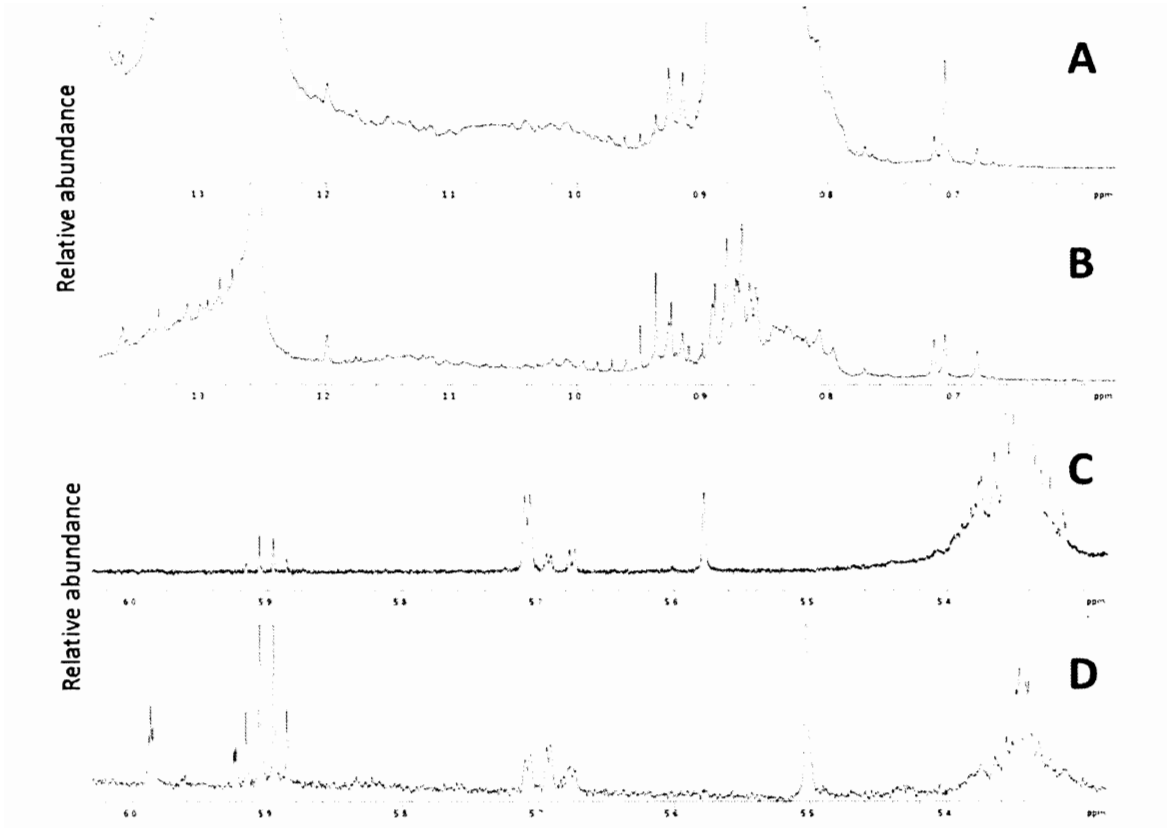

Figure 6-5. Proton 1D spectra of the 7KC methyl/methylene (0.65-1.4 ppm) and vinyl regions (5.15-5.8 ppm). **A.** and **C.** Crude enzymatic reaction, **B.** and **D.** HPLC-purified reaction mixture. H18 and H19 methyl groups are indicated at 0.683 and 1.199 ppm of 7-ketocholesterol (7KC). H6 vinyl proton is indicated at 5.692 ppm of 7KC.

7KC:cyclo-treated cells. At 50 μM none of the 7KC:EtOH cells remained, while a few of the 7KC:cyclo cells were still viable (0.09±0.04).

In order to better understand the potential benefits of enzymatically transforming 7KC, we also assayed the structurally similar compounds 7KLC and 7KDHEA (Fig. 5-4) for the ability to reduce fibroblast viability. 7KLC is a more highly oxidized molecule that we tested to determine the effect that further oxidation of 7KC might have. 7KDHEA possesses the same steroid nucleus as 7KC, but differs in that the side chain is replaced by a keto group. As expected, neither of these compounds showed any toxicity up to 200 μM, suggesting that oxidation of either the steroid nucleus or side chain is sufficient to reduce 7KC toxicity and that further oxidation would not be detrimental. Increasing concentrations of both 7KLC and 7KDHEA were actually associated with increases in cell viability. While not statistically significant for 7KLC, the effect was significant at 50 and 100 μM for 7KDHEA, with increases in viable cell fraction of 44% and 26% respectively (1.44±0.20 and 1.26±0.10, $p < 0.05$).

Flow cytometry to assess membrane permeabilization revealed an increase in propidium iodide (PI) staining that was positively correlated with 7KC concentration (Fig. 6-7). A noticeable PI signal was present at 25 μM 7KC, indicating a loss of membrane integrity and the presence of dead or necrotic cells. No change was apparent in Annexin V-FITC at any concentration, suggesting an absence of apoptotic cells. Treatment with the same concentrations of cholesterol did not result in increased staining of either PI

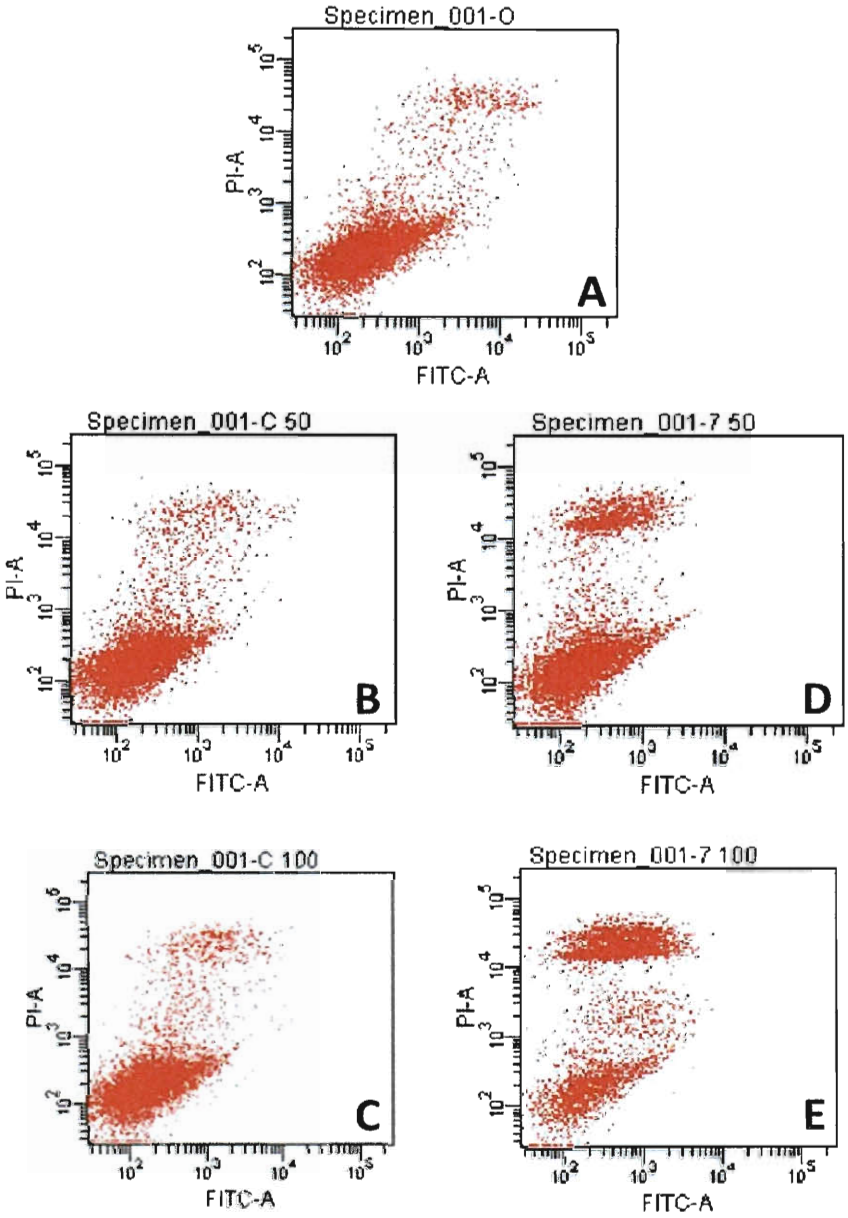

Figure 6-6. Flow cytometry of cholesterol- and 7KC-treated fibroblasts. Cells were treated with either cholesterol or 7KC for 24 hours and then stained with Annexin V-FITC and propidium iodide (PI) and analyzed by flow cytometry. **A.** Untreated control; **B**. 50 µM cholesterol; **C**. 100 µM cholesterol; **D**. 50 µM 7KC; and **E**. 100 µM 7KC. A clear increase in PI signal occurs in 7KC treatments with no corresponding increase in FITC. This is indicative of PI uptake due to membrane permeabilization, likely due to cell necrosis. No change occurred in cholesterol-treated cells.

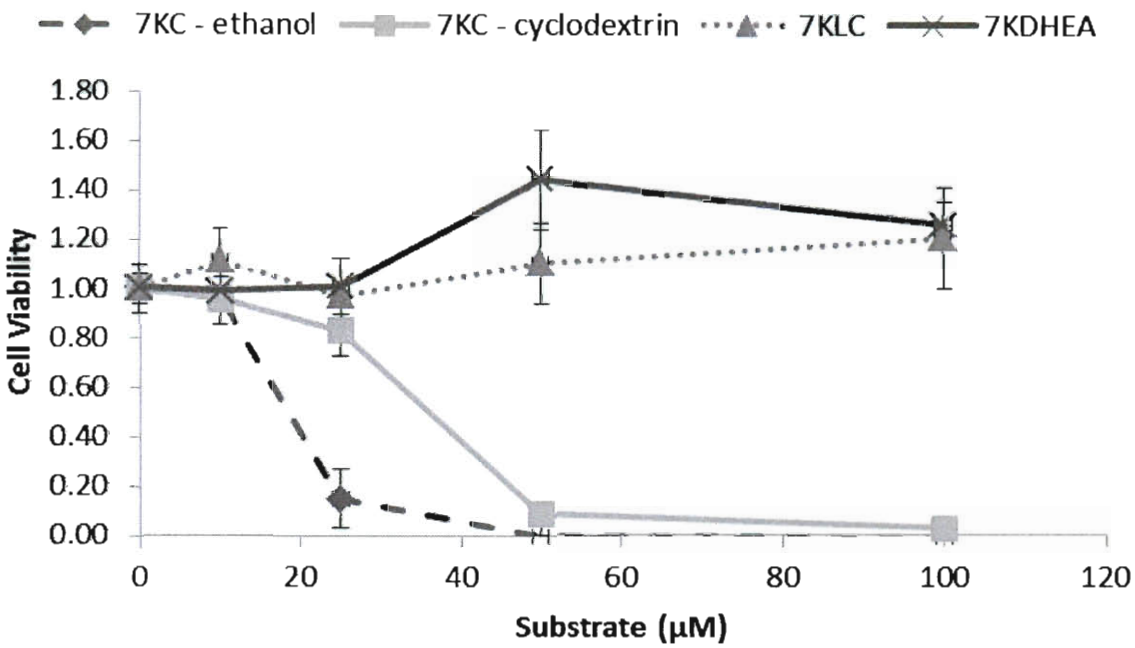

Figure 6-7. XTT cell viability assay. Human fibroblasts were treated with 7KC (in ethanol), 7KC (in cyclodextrin), 7KLC (in ethanol), or 7KDHEA (in ethanol) at concentrations from 0 to 100 μM. 7KC (in ethanol) displayed the highest toxicity while there were slight improvements in cell viability (fraction viable compared to untreated) in 7KLC- and 7KDHEA-treated cells. Cells treated with ethanol alone showed no change in cell viability (data not shown).

or FITC up to 100 μM.

6.3.1. 7KC-induced cytotoxicity is attenuated by cyclodextrin or transient transfection of lysosomally-targeted cholesterol oxidase

Transient transfection of fibroblasts with pEGFP-COXL1, which encodes a lysosomally-targeted DS1 ChOx, resulted in significant reduction of the cytotoxicity exerted by up to 50 μM 7KC in comparison to cells transfected with pcDNA3.1-MC (control) or pEGFP-LAMP1 ($p \leq 0.05$)(Fig. 6-8). pEGFP-COXL1 transfected populations displayed 120% and 160% increased cell viability over those transfected with pcDNA3.1-MC at both 25 and 37.5 μM 7KC, respectively. Interestingly, there was also an increase of 44% in cell viability in pEGFP-COXL1 transfected, but untreated (no 7KC) cell populations when compared to controls. pMEV-COX was also protective to a lesser extent at both 37.5 and 50 μM. However, there was no statistically significant difference compared to pcDNA3.1-MC at 25 μM. Additionally, transfection with pEGFP-LAMP1 resulted in an average increased cell viability to 50 μM, although this increase was only statistically significant at 37.5 μM 7KC. GFP expression was verified for both pEGFP-COXL1 and pEGFP-LAMP1 (Fig. 6-9). There was no discernible difference between transfection with pCMV6-XL4-CYP27 and the control plasmid. However, there was a decrease in cell viability in populations transfected with pMEV-HSD. The changes were significant at 0, 37.5, and 50 μM 7KC, with 41%, 38%, and 58% decreases respectively.

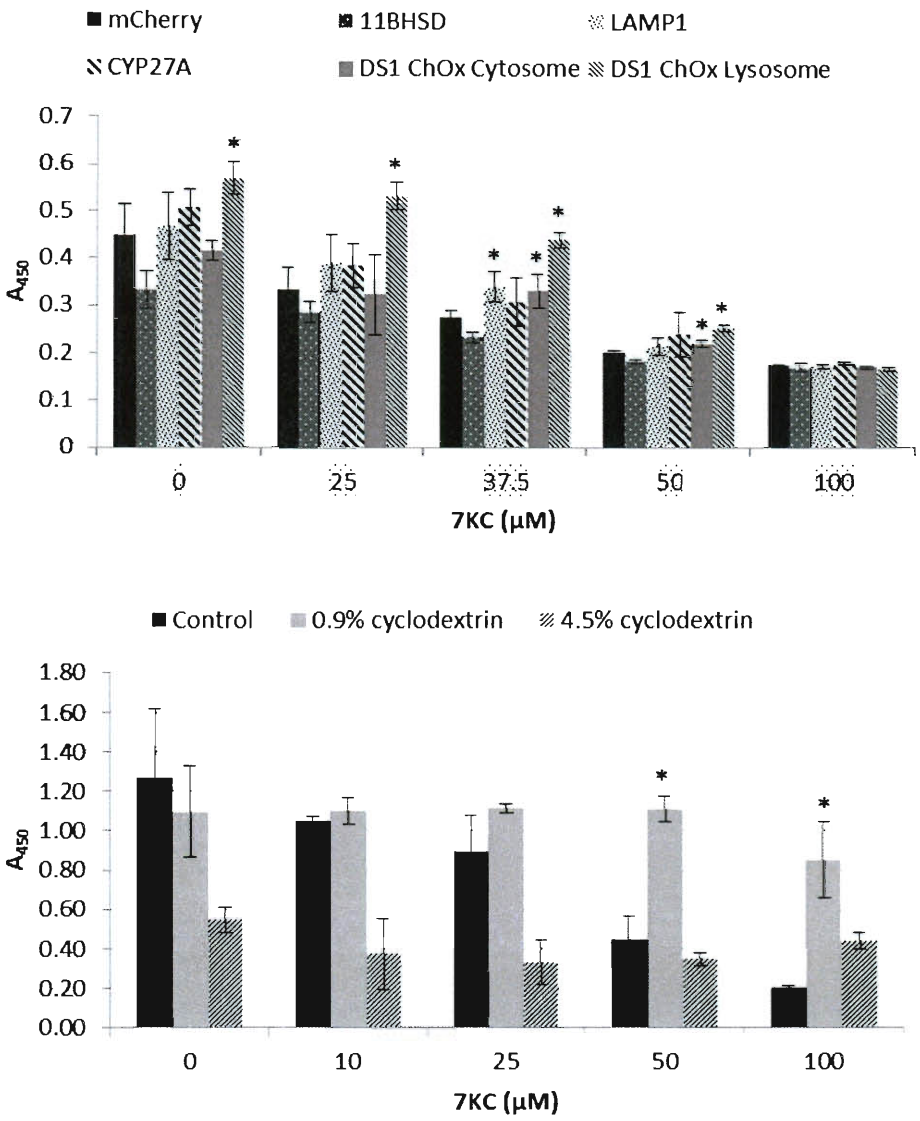

Figure 6-8. Cytotoxicity analysis of treated human fibroblasts. Both graphs show changes in absorbance (450 nm) of XTT due to reduction coupled to mitochondrial dehydrogenase that corresponds to differences in cell viability (XTT assay). The top panel shows the effect of transfected genes on cell viability. Significant differences existed amongst treatments up to 50 μM 7KC, with transfection by lysosomally-targeted DS1 ChOx being the most cytoprotective. The bottom panel shows the effect of either 0.9% or 4.5% HPβCD on cell viability. The lower concentration of HPβCD proved to be significantly protective from 50 to 100 μM 7KC, while the higher dose was toxic by itself. Asterisks (*) denote statistical significance ($p \leq 0.05$).

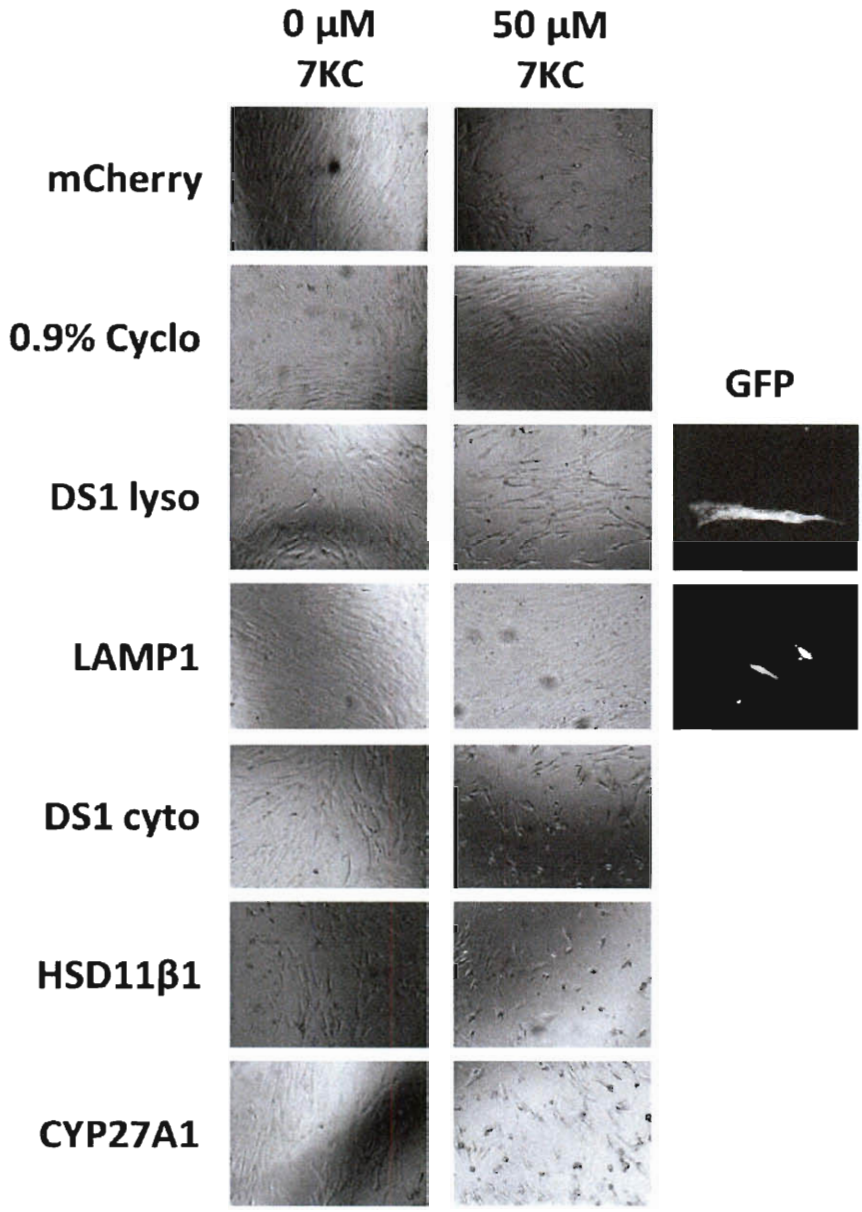

Figure 6-9. Micrographs of transiently transfected fibroblasts. Brightfield micrographs taken at 10X of human fibroblasts transfected with 7KC-active enzymes (or mCherry control) and incubated for 24 hours in either 0 or 50 µM 7KC. Also, a micrograph of non-transfected cells treated with 0.9% cyclodextrin. The two images to the right were taken using fluorescence microscopy to show GFP expression in the DS1 ChOx-LAMP1-GFP and LAMP1-GFP constructs (25 µM 7KC).

Concurrent amendment of non-transfected cells with 7KC (ethanol stock) and 0.9% hydroxypropyl β-cyclodextrin provided a high degree of cytoprotection against 7KC-induced toxicity up to 100 μM, though this was only significant at 50 μM and 100 μM (Fig. 6-8). Changes in cell morphology were not apparent by microscopy at 50 μM (Fig. 6-9), though they were at 100 μM. The addition of 4.5% was toxic to the fibroblasts without 7KC and at all concentrations.

6.4. Discussion

Although oxysterols are potent initiators of apoptosis and necrosis [146, 156, 209, 260, 279], very few studies have considered methods to control their levels *in vivo*. Overexpression of cholesterol sulfotransferase impairs LXR signaling by reducing oxysterol levels [289], and the same enzyme was found to reduce 7KC toxicity in 293T cells [212]. To our knowledge, this is the only case besides this study of an enzyme being overexpressed *in vivo* for the purpose of reducing oxysterol toxicity. Oxysterols are subject to esterification by ACAT, which has been shown to attenuate their toxicity [290]. This is supported by reports that ACAT deficiency, though facilitating a reduction in atherosclerotic plaque size, also results in increased cell death [291-293]. Similar to ACAT deficiency, overexpression of cholesteryl ester hydrolase (CEH) in macrophages was found to reduce atherosclerotic plaque size [292], although without a concomitant increase in cell death. CEH is known to hydrolyze oxysterol esters [294], which should have an adverse effect given the resultant increase in the

active oxysterol pool, but in this particular case it appears that the combination of enhanced efflux and re-esterification is sufficiently rapid to prevent detrimental effects. When re-esterification is inhibited, as in ACAT deficiency, toxicity ensues. Hydrolysis of steryl esters also takes place in the lysosome. This is catalyzed by lysosomal acid lipase (LAL), which has been shown to reduce coronary and aortic atheromatous lesions when introduced intravenously in LDL receptor deficient mice [227]. However, this results in an increased oxysterol pool which may be cytotoxic and could inhibit sterol efflux [136, 277, 295].

All of these pathways serve to either promote the efflux of sterols or their esterification outside of the endosomal/lysosomal compartments. No enzymes exist in the lysosome that are capable of detoxifying oxysterols, though reactive oxygen species generated oxysterols are primarily formed and stored there. In oxLDL-loaded macrophage foam cells, approximately 54% of the 7KC is stored in the endosomal/lysosomal system, with another 40% being stored in the plasma membrane [174]. It was for this reason that we investigated the effect of targeting a 7KC-transforming enzyme to the lysosome. Most other enzymes that are capable of transforming oxysterols are localized to the ER, cytoplasm, or mitochondria, making it unlikely they would be capable of preventing lysosomal membrane permeabilization. Our results suggest that this is true; transient transfection of fibroblasts with plasmid expressing CYP27A1, a mitochondrially-localized hydroxylase, did not display increased viability.

The lysosome-associated membrane proteins (LAMP) are transmembrane proteins that possess short cytoplasmic tails and highly glycosylated intraluminal domains thought to protect the lysosomal membrane from hydrolytic attack. Though their function is still not entirely understood, they seem to have roles in both lysosome dynamics [287, 296] and stability. Knockdown of either LAMP1 or LAMP2 sensitized cells to siramesine-induced cell death and photooxidation–induced lysosomal destabilization, while overexpression was found to be protective [297]. Our results extend the protective effect of LAMP1 to oxysterol-induced cytotoxicity. The largest increases in cell viability were observed in transfections with pEGFP-COXL1 and pEGFP-LAMP1, and for treatment with hydroxypropyl β-cyclodextrin (HPβCD). Both of the former appeared to be successfully expressed and lysosomally targeted as indicated by fluorescence microscopy. Additionally, it has recently been discovered that the ability of HPβCD to facilitate cholesterol efflux from Niemann-Pick type C fibroblasts occurs within late endosomes or lysosomes, and is not due to extraction from the cytoplasmic membrane [298, 299].

The efficacy of our DS1 ChOx/LAMP1 construct to protect fibroblasts from 7KC-mediated cell death (which performed better than other treatments) is supportive of our main hypothesis that lysosomally-targeted enzymes are necessary for the greatest protection against oxysterol-induced toxicity. Furthermore, cytoplasmically-targeted DS1 ChOx, though showing some cytoprotective benefit, was inferior to lysosomal DS1 ChOx or LAMP1. Overexpression of HSD11β1 actually resulted in increased cell death (due to

formation of 7β-HC), though the effect was of a lower magnitude and statistical significance than our lysosomal treatments, which we feel further supports our conclusion. Moreover, HPβCD treatment, which showed the greatest overall benefit (but which is not directly comparable to transfected cells), is believed to increase 7KC efflux from the lysosome to the ER [298-300], where it is capable of being esterified by ACAT.

In summary, we identified a 7KC-active bacterial cholesterol oxidase and targeted it to the mammalian lysosome by fusion to the LAMP1 signal sequence and transmembrane domain. When transfected in human fibroblasts, this construct was superior to other treatments in protecting against 7KC-induced cell death. Taken together, these results indicate that the lysosome should be the target for treatment of oxysterol-mediated toxicity, and support the utility of using microbial enzymes for therapeutic benefit.

Chapter 7

Conclusions and Recommendations

7.1. Conclusions

This thesis investigated the microbial degradation of 7-ketocholesterol, its toxicity in cell culture, and potential strategies for mitigating its effects. The following points highlight our findings relative to specific objectives:

1. Determine whether bacteria capable of metabolizing 7KC exist in the environment and assess their diversity.
    a. Seven species of bacteria from the Proteobacteria and Actinobacteria phyla were isolated from three soil samples and one activated sludge sample from a wastewater treatment plant based on their ability to exploit the biodegradation of 7KC as a metabolic niche. Carbon dioxide evolution in incubations with 7KC (but not in unamended controls) indicated extensive mineralization. Growth on

7KC as sole carbon source was also demonstrated by monitoring substrate degradation over time using HPLC. This suggests that oxysterol degradation is a commonly occurring microbial trait.

2. Determine the genetic basis of 7-ketocholesterol degradation in a microorganism.
    a. 7KC degradation was studied in *Rhodococcus jostii* RHA1 using a whole genome microarray as well as RT-qPCR. Growth on 7KC up-regulated two large gene clusters of homologs of sterol-catabolizing enzymes, in addition to a previously identified cluster required for cholesterol degradation.
    b. Growth on 7KC was completely abolished by the replacement of *hsaC* and deletion of *cyp125*, individually. This strongly implicates the ring-cleavage dioxygenase, HsaC, and the cytochrome P450, Cyp125, in the pathway for degradation of 7KC. Deletion of *hsaA*, encoding the oxygenase of a two-component hydroxylase, partially impaired, but did not prevent growth on 7KC, suggesting that HsaA contributes to 7KC catabolism but is not essential.
    c. Metabolic screening using GC-MS and NMR analysis of culture media identified four accumulating metabolites in a *ΔhsaC* mutant, providing evidence that reduction and removal of the 7-keto substituent occurs prior to the step catalyzed by HsaC.

3. Characterize candidate enzymes for their ability to transform 7KC, and assess their feasibility for use in controlling oxysterol levels.
    a. While we identified several enzymes in *Rhodococcus jostii* RHA1 involved in 7KC degradation, we were not successful in determining which enzymes initiated transformation, though this is likely CYP125 and an unidentified 3β-hydroxysteroid dehydrogenase. CYP125 was determined to be critical for 7KC catabolism, and was capable of initiating transformation of cholesterol [272]. Additionally, we were able to clone and express three reductases active against analogs structurally similar to 7KC, and likely involved in catalysis against a downstream metabolite.
    b. We determined that oxidation of either the 3β-hydroxyl group or side chain of 7KC is sufficient to reduce its toxicity in cell based culture. We expressed *Chromobacterium sp.* DS1 cholesterol oxidase and found it capable of oxidizing the 3β-hydroxyl group of 7KC based on indirect assays, NMR, and GC-MS.
    c. Lysosomally-targeted DS1 cholesterol oxidase was successful in partially attenuating 7KC cytotoxicity and provided a higher degree of protection than either LAMP1, cytoplasmically-targeted DS1 oxidase, or CYP27A1 overexpression.

7.2. Recommendations

During the course of this thesis we investigated methods of oxysterol transformation, with a particular interest in enzymatic transformations that attenuate 7KC toxicity. We discovered several microbial species that may become sources of enzymes for future work, and we identified catabolic pathways in *Rhodococcus jostii* RHA1 that helped us elucidate how bacteria catabolize oxysterols. However, the ultimate objective of our work is to develop a method of reducing cytotoxic oxysterol levels *in vivo*, either for therapeutic use, or to use as a tool to further study oxysterol formation and effects. In an advance toward this, we assayed a 7KC-active cholesterol oxidase from *Chromobacterium sp*. DS1 for its ability to protect human fibroblasts against 7KC cytotoxicity. Our preliminary results are promising and indicate that overexpression of our construct may be useful in accomplishing this, however much work also remains.

Our cytotoxicity assays were done using human fibroblasts transiently transfected with constitutively expressed plasmids. While this proved useful as an initial screening method, the process of transfection is itself toxic and may interfere with results. More definitive conclusions could be made utilizing stably transfected cell lines with inducible expression. And while we were able to determine protein expression by the presence of GFP (in the case of pEGFP-COXL1), we cannot assume that enzyme activity was present inside the lysosome. LAMP1, the protein we used to target the DS1 oxidase, is itself

protective against 7KC, so the possibility cannot be excluded that the effect comes from other properties of the construct than its catalytic activity. Nevertheless, our results are strongly suggestive that intralysosomal transformation of 7KC is cytoprotective, and that targeting treatments to the lysosome is the best way to attenuate the detrimental effects of oxysterols *in vivo*.

Appendix A

Functional groups of differentially expressed genes in *Rhodococcus jostii*

Gene ID	Product	Expression ratio		
		CHO/ PYR	7KC/ PYR	7KC/ CHO
	Signaling and transcriptional regulation			
ro01881	possible tyrosine protein phosphatase	1.2	15.7	4.1
ro02115	anti-sigma factor antagonist	1.6	10.1	1.3
ro02116	conserved hypothetical protein	0.9	1.6	0.7
ro02117	possible anti-sigma factor	ND	11.0	0.9
ro02118	sigma factor, sigma 70 type, group 3	ND	9.1	0.8
ro02829	possible transcriptional regulator	1.4	4.5	0.8
ro03251	possible transcriptional regulator, WhiB family	ND	3.7	0.7
ro04316	possible transcriptional regulator, WhiB family	1.9	6.4	1.0
ro04454	transcriptional regulator, GntR family	1.6	3.9	0.6
ro05371	probable transcriptional regulator, ArsR family	1.5	7.8	0.8
ro05735	possible protein-tyrosine kinase, C-terminal	0.7	35.7	0.9
ro06593	hypothetical protein	ND	141.9	0.7
ro06594	possible transcriptional regulator, AraC family	1.2	24.1	0.6
ro10163	transcriptional regulator	0.4	5.8	0.5
ro10389	protein kinase/ transcriptional regulator, LuxR family	0.9	5.0	0.6
	Catabolism			
ro01882	short chain dehydrogenase	1.1	9.1	4.8
ro01883	short chain dehydrogenase	1.1	22.7	5.0
ro03609	steroid delta-isomerase	2.6	6.8	2.2
ro03841	probable 3-oxoacyl-[acyl-carrier-protein] reductase	0.6	2.8	2.4
ro04283	possible acyl-CoA dehydrogenase	1.3	10.2	4.7

ro04427	conserved hypothetical protein	1.8	2.6	0.9
ro04428	probable thiocyanate hydrolase gamma subunit	2.8	16.3	0.6
ro04429	probable thiocyanate hydrolase alpha subunit	1.5	8.1	0.5
ro04430	probable thiocyanate hydrolase beta subunit	1.1	2.2	0.6
ro04431	conserved hypothetical protein	1.4	9.1	0.6
ro04432	possible dithiol-disulfide isomerase	0.8	1.2	1.2
ro04433	hypothetical protein	0.6	0.8	1.6
ro04434	conserved hypothetical protein	1.3	2.7	1.3
ro04601	hydrogenase nickel incorporation protein HypA	1.5	2.0	0.6
ro04602	hydrogenase nickel incorporation protein HypB	1.0	1.7	0.4
ro04603	Ni-Fe hydrogenase small subunit	1.2	4.1	0.6
ro04604	Ni-dependent hydrogenase large subunit	7.5	24.8	0.6
ro04605	possible nitrogen fixation protein	0.9	0.9	1.0
ro04606	conserved hypothetical protein	1.1	1.8	0.8
ro04607	conserved hypothetical protein	ND	4.6	0.9
ro04608	conserved hypothetical protein	0.9	2.4	0.9
ro04609	hydrogenase maturation protease	1.7	14.5	0.6
ro06637	3-oxoacyl-[acyl-carrier-protein] reductase	1.2	4.0	1.9
ro06638	conserved hypothetical protein	ND	9.6	5.7
	Possible gas vesicle synthesis			
ro00203	conserved hypothetical protein	0.9	12.5	0.2
ro00204	conserved hypothetical protein	1.4	3.2	0.4
ro00205	gas vesicle synthesis protein	1.1	1.8	0.3
ro00206	probable gas vesicle synthesis protein	3.1	6.8	0.5
ro00207	possible gas vesicle synthesis protein	1.5	2.1	0.7
ro00208	probable gas vesicle synthesis protein	ND	3.0	0.6
ro00209	gas vesicle synthesis protein	0.6	0.6	1.0
ro00210	probable gas vesicle synthesis protein	1.5	2.2	0.6
ro00211	probable gas vesicle protein	0.9	2.0	1.1
ro00705	conserved hypothetical protein	1.3	3.0	2.4
ro00706	conserved hypothetical protein	ND	5.6	0.5
ro00707	gas vesicle structural protein	ND	1.1	0.4
ro00708	possible gas vesicle synthesis protein	ND	1.7	1.0
ro00709	possible gas vesicle synthesis protein	ND	1.1	0.8
ro00710	possible gas vesicle synthesis protein	ND	4.6	0.7
ro00711	gas vesicle protein	ND	2.3	0.8
ro00712	probable gas vesicle protein	ND	1.4	1.1
ro00713	possible gas vesicle synthesis protein	1.2	1.2	1.0
	Transport			
ro00071	multidrug resistance transporter, MFS superfamily	0.7	14.2	5.2
ro00301	metabolite transporter, MFS superfamily	0.4	0.2	1.0
ro01597	possible transcriptional activator TenA	0.3	0.3	1.0
ro01598	probable ABC transporter, permease component	0.3	0.3	1.1
ro01599	ABC transporter, permease component	0.4	0.3	1.0
ro01600	ABC transporter, ATP-binding component	1.1	0.4	1.4
ro05372	conserved hypothetical protein	1.9	10.0	1.0
ro06547	metabolite transporter, MFS superfamily	0.5	0.2	1.0
	Cell wall synthesis			
ro01087	UDP-N-acetylmuramate--L-alanine ligase	0.7	0.8	1.5
ro01088	beta-N-acetylglucosaminyltransferase	0.7	0.7	1.0
ro01089	cell division protein, FtsW	0.8	0.7	0.9

ro01090	UDP-N-acetylmuramoylalanine--D-glutamate ligase	1.6	1.0	0.8
ro01091	phospho-N-acetylmuramoyl-pentapeptide-transferase	0.6	0.7	1.5
ro01092	UDP-N-acetylmuramoyl-tripeptide--D-alanyl-D-alanine ligase	0.6	0.4	1.6
ro01093	UDP-N-acetylmuramoylalanyl-D-glutamate--2,6-diaminopimelate ligase	1.1	0.4	1.7
ro01094	peptidoglycan glycosyltransferase	9.0	0.6	1.0
ro01095	possible conserved membrane protein	0.9	0.5	1.3
ro01096	S-adenosyl-methyltransferase	0.5	0.4	0.8
ro01097	possible protein MraZ	0.6	0.4	0.5
ro01921	elongation factor EF1A	0.3	0.3	1.4
ro01922	elongation factor G	0.4	0.4	1.5
ro04058	probable mycolyltransferase	0.6	0.5	1.8
ro04059	probable antigen 85 complex protein	0.3	0.2	0.9
ro04060	probable antigen 85 complex protein	0.4	0.4	1.3
ro05733	conserved hypothetical protein	1.2	3.1	0.9
ro05734	possible mannuronan epimerase	1.1	15.5	1.0
ro05736	hypothetical protein	5.3	47.0	0.4
ro05737	conserved hypothetical protein	1.3	8.8	0.6
ro05738	probable O-antigen transporter, MOP superfamily	1.1	2.9	0.8
ro05739	possible glycosyltransferase	1.3	6.4	1.1
ro05740	probable glycosyltransferase	1.0	8.1	0.8
ro05741	possible glycosyl transferase	1.2	3.6	0.7
ro05742	sugar transferase	2.2	11.2	0.7
ro05743	possible transferase	ND	26.9	1.1
ro05744	dTDP-4-dehydrorhamnose 3,5-epimerase	1.3	1.5	1.2
ro05745	probable UDP-glucose 4-epimerase	1.4	3.3	0.7
ro05746	conserved hypothetical protein	2.2	19.4	0.8
ro05747	probable glucose-1-phosphate cytidylyltransferase	0.7	1.3	0.7
ro05748	probable methyltransferase	1.5	2.3	0.9
	Electron transport			
ro01133	ubiquinol-cytochrome c reductase cytochrome b subunit	0.7	1.2	0.8
ro01134	possible transport protein	0.7	1.3	0.9
ro01135	probable transcriptional regulator, TetR family	1.2	1.8	0.8
ro01136	conserved hypothetical protein	0.9	0.7	1.0
ro01137	probable cytochrome c oxidase subunit II	0.4	0.2	1.3
ro02032	cytochrome c assembly membrane protein	0.3	0.3	0.9
ro02033	possible cytochrome c biogenesis membrane protein	0.7	1.0	1.0
ro02034	cytochrome c biogenesis membrane protein	0.7	0.6	1.6
ro02035	possible thioredoxin	0.8	0.7	1.5
ro02036	conserved hypothetical protein	0.6	0.4	1.3
ro04847	cytochrome bd ubiquinol oxidase subunit I	0.6	0.3	1.0
ro04848	cytochrome bd ubiquinol oxidase subunit II		0.4	1.0
ro04849	transport ATP-binding protein CydD	0.9	0.6	1.4
ro04850	transport ATP-binding protein CydC	1.2	0.7	1.2
ro06461	probable 3-demethylubiquinone-9 3-O-methyltransferase	0.4	0.3	0.9
ro06462	electron transfer flavoprotein beta-subunit	0.5	0.2	1.7
ro06463	electron transfer flavoprotein alpha-subunit	0.6	0.3	1.1
	H^+-driven ATPase			
ro01471	H(+)-transporting two-sector ATPase epsilon subunit	1.0	0.6	1.3
ro01472	H(+)-transporting two-sector ATPase beta subunit	0.3	0.1	1.3
ro01473	H(+)-transporting two-sector ATPase gamma subunit	0.3	0.2	1.2

ro01474	H(+)-transporting two-sector ATPase alpha subunit	0.2	0.1	1.2
ro01475	ATP synthase delta subunit	0.3	0.2	1.1
ro01476	H(+)-transporting two-sector ATPase subunit B	0.7	0.4	0.8
ro01477	H(+)-transporting two-sector ATPase subunit C	0.3	0.2	1.1
ro01478	probable H(+)-transporting two-sector ATPase subunit A	0.4	0.2	1.7
	Tricarboxylic-acid cycle and glycolysis			
ro02070	phosphoglycerate mutase	0.4	0.2	0.9
ro02122	isocitrate lyase	0.3	0.2	0.9
ro02123	conserved hypothetical protein		1.1	0.8
ro06238	isocitrate dehydrogenase (NADP+)	0.4	0.2	1.5
ro06244	malate dehydrogenase	0.4	0.7	1.4
ro06245	succinate dehydrogenase Fe-S protein	0.3	0.3	1.1
ro06246	succinate dehydrogenase	0.3	0.3	1.5
ro06247	probable succinate dehydrogenase hydrophobic membrane anchor protein	0.6	0.3	1.1
ro06248	probable succinate dehydrogenase hydrophobic membrane anchor protein	0.3	0.2	1.2
ro07177	glyceraldehyde 3-phosphate dehydrogenase	0.3	0.2	0.9
ro07178	phosphoglycerate kinase	0.4	0.5	1.2
ro07179	triose-phosphate isomerase	1.0	0.4	1.0
ro07180	possible protein-export membrane protein	0.4	0.4	1.0
ro07181	phosphoenolpyruvate carboxylase	0.8	0.9	0.8
ro07182	6-phosphogluconolactonase	0.9	0.8	1.2
ro07183	conserved hypothetical protein	0.4	0.5	0.9
ro07184	glucose-6-phosphate 1-dehydrogenase	0.4	0.6	0.9
ro07185	transaldolase	0.4	0.5	1.2
ro07186	transketolase	0.5	0.7	1.1
ro07207	aconitate hydratase	0.3	0.2	0.9
	Translation			
ro01923	30S ribosomal protein S7	0.5	0.3	1.2
ro01924	30S ribosomal protein S12	0.6	0.4	1.1
ro01975	50S ribosomal protein L7/L12	0.3	0.2	1.1
ro01976	50S ribosomal protein L10	0.2	0.2	1.8
ro01977	possible antibiotic efflux protein	1.4	1.5	0.6
ro01978	50S ribosomal protein L1	0.4	0.2	0.6
ro01979	50S ribosomal protein L11	0.9	1.3	0.5
ro01980	transcription antitermination protein	0.3	0.4	1.0
ro01981	probable protein translocation complex preprotein translocase subunit	0.6	0.9	1.0
ro01982	tRNA-Trp (CCA)		0.6	0.9
ro01983	possible fatty acid synthase beta subunit	0.6	0.7	0.8
ro01984	conserved hypothetical protein	0.4	0.4	1.1
ro01985	50S ribosomal protein L33 type 2	0.4	0.4	2.1
ro05085	possible translation initiation factor	0.8	0.3	0.8
ro06132	30S ribosomal protein S10	0.5	0.6	2.1
ro06133	50S ribosomal protein L3	0.4	0.3	2.4
ro06134	50S ribosomal protein L4	0.6	0.6	1.9
ro06135	50S ribosomal protein L23	0.5	0.4	1.7
ro06136	50S ribosomal protein L2	0.4	0.4	1.8
ro06137	30S ribosomal protein S19	0.5	0.3	1.6
ro06138	50S ribosomal protein L22	0.4	0.2	2.1

ro06139	30S ribosomal protein S3	0.4	0.3	1.4
ro06140	50S ribosomal protein L16	0.4	0.2	1.4
ro06141	50S ribosomal protein L29	0.4	0.3	2.1
ro06142	30S ribosomal protein S17	0.4	0.4	1.4
ro06143	50S ribosomal protein L14	0.4	0.3	1.2
ro06144	50S ribosomal protein L24	0.3	0.3	1.6
ro06145	50S ribosomal protein L5	0.4	0.3	1.5
ro06146	30S ribosomal protein S14	0.3	0.3	1.8
ro06147	30S ribosomal protein S8		0.3	2.0
ro06148	50S ribosomal protein L6	0.3	0.3	1.5
ro06149	50S ribosomal protein L18	0.3	0.2	1.3
ro06150	30S ribosomal protein S5		0.3	1.4
ro06151	50S ribosomal protein L30	0.3	0.3	2.4
ro06152	50S ribosomal protein L15	0.5	0.3	1.6
ro06153	preprotein translocase	0.6	0.4	1.6
ro06154	adenylate kinase	0.4	0.4	1.1
ro06155	methionyl aminopeptidase	0.4	0.4	1.2
ro06156	D-tyrosyl-tRNA(Tyr) deacylase	1.0	1.0	0.7
ro06157	translation initiation factor IF1		0.4	1.7
ro06158	50S ribosomal protein L36		0.4	2.1
ro06159	30S ribosomal protein S13		0.3	1.0
ro06160	30S ribosomal protein S11	0.4	0.6	2.0
ro06161	30S ribosomal protein S4	0.4	0.2	1.3
ro06162	DNA-directed RNA polymerase alpha subunit	0.3	0.3	1.6
ro06163	50S ribosomal protein L17	0.3	0.3	2.1
ro06164	pseudouridylate synthase	1.2	0.5	1.3
ro06165	conserved hypothetical protein	2.3	3.1	0.5
ro06166	conserved hypothetical protein		0.1	1.4
ro06167	probable transcriptional regulator, AsnC family		1.2	1.3
ro06168	conserved hypothetical protein	2.0	1.7	1.0
ro06169	ornithine--oxo-acid transaminase	1.1	0.9	1.3
ro06170	50S ribosomal protein L13	0.7	0.4	0.9
ro06171	30S ribosomal protein S9	0.5	0.3	1.3
	Chaperones			
ro02146	60 kDa chaperonin GroEL	0.3	0.1	0.6
ro05497	heat shock protein Hsp70	0.8	0.2	0.5
ro05498	heat shock protein GrpE	1.2	0.3	1.0
ro05892	chaperone protein HtpG (heat shock protein HtpG)	0.4	0.3	0.8
ro06190	chaperone protein	0.4	0.1	1.2

Appendix B

Expression ratios of *Rhodococcus jostii* RHA1 steroid degradation clusters

Gene ID	Product	Expression ratio[1]		
		CHO versus PYR	7KC versus PYR	7KC versus CHO
	Cluster 1			
ro04531	possible MaoC family protein	**3.2**	**3.7**	0.9
ro04532	probable succinate dehydrogenase flavoprotein	**3.3**	2.4	0.8
ro04533	hydratase	2.0	1.5	1.3
ro04534	acetaldehyde dehydrogenase	**3.2**	**4.3**	1.2
ro04535	4-hydroxy-2-oxovalerate aldolase	**5.1**	1.8	1.0
ro04536	conserved hypothetical protein	1.5	1.7	0.8
ro04537	conserved hypothetical protein	2.6	2.3	1.4
ro04538	probable terminal oxygenase fot steroid degradation	**4.6**	**4.0**	0.4
ro04539	possible hydroxylase	**20.3**	**12.0**	0.6
ro04540	alpha/beta-fold C-C bond hydrolase	**9.2**	**4.9**	0.8
ro04541	extradiol dioxygenase, type I	**2.1**	2.2	1.3
ro04542	oxidoreductase	9.3	2.0	1.0
ro04679	cytochrome P450 CYP125	**11.0**	**5.7**	0.9
ro04680	possible erythromycin esterase	**3.2**	1.8	0.8
ro04681	conserved hypothetical protein	2.4	**5.7**	1.2
ro04682	conserved hypothetical protein	1.0	1.4	0.8
ro04683	probable nonspecific lipid carrier protein	**3.7**	**2.6**	0.9
ro04684	probable thiolase	1.3	1.2	1.5

ro04685	conserved hypothetical protein	**3.4**	**4.1**	1.1
ro04686	reductase	1.8	2.3	0.9
ro04687	conserved hypothetical protein	1.5	1.5	1.7
ro04688	probable enoyl-CoA hydratase	1.8	**2.5**	0.5
ro04689	AMP-binding CoA ligase	**12.5**	**11.1**	0.5
ro04690	probable 2-nitropropane dioxygenase	**5.5**	**4.0**	0.6
ro04691	probable long-chain fatty-acid--CoA ligase	**3.6**	2.2	1.2
ro04692	CoA dehydrogenase	1.7	0.7	1.1
ro04693	probable acyl-CoA dehydrogenase	**9.5**	**8.5**	0.8
ro04694	possible ferredoxin		**7.1**	0.5
ro04695	probable 3-oxoacyl-[acyl-carrier-protein] reductase	**7.2**	3.2	0.9
ro04696	conserved hypothetical protein	3.6	**2.7**	0.9
ro04697	conserved hypothetical protein	**2.7**	1.1	1.3
ro04698	possible Mce family protein	2.3	1.6	0.6
ro04699	possible Mce family protein	2.2	**2.7**	0.8
ro04700	possible Mce family protein	2.5	1.7	0.5
ro04701	possible Mce family protein	1.7	1.4	1.0
ro04702	possible Mce family protein	**3.0**	1.7	0.9
ro04703	possible Mce family protein	0.8	1.0	1.2
ro04704	conserved hypothetical protein	1.7	1.6	0.8
ro04705	conserved hypothetical protein	0.8	0.7	1.3
ro04706	conserved hypothetical protein	0.8	1.0	1.5
ro04707	reductase	**5.0**	2.1	0.7
	Cluster 2			
ro02478	short-chain dehydrogenase	**2.0**	3.4	1.0
ro02479	conserved hypothetical protein	**1.5**	1.8	1.1
ro02480	carveol dehydrogenase	0.9	**69.6**	**7.9**
ro02481	carveol dehydrogenase	1.3	**6.5**	**5.6**
ro02482	conserved hypothetical protein	0.9	29.4	**8.0**
ro02483	3-ketosteroid-delta-1-dehydrogenase	0.9	12.8	2.9
ro02484	probable nitrilotriacetate monooxygenase component B	0.6	1.3	2.4
ro02485	transcriptional regulator, PadR family	0.3	0.8	1.1
ro02486	probable sterase / lipase	**2.1**	**38.0**	**6.4**
ro02487	transcriptional regulator, IclR family	0.8	**2.6**	**2.7**
ro02488	extradiol dioxygenase, type I	1.1	**42.9**	**10.4**
ro02489	pigment production hydroxylase	0.8	**10.6**	**11.5**
ro02490	probable dioxygenase Rieske iron-sulfur component	**2.2**	**148.4**	**7.3**
ro02491	hypothetical protein	1.0	2.8	**3.1**
ro02492	cyclohexanone monooxygenase	0.8	**59.3**	**11.8**
	Cluster 3			
ro05787	probable transcriptional regulator, AraC family	1.1	1.7	**2.4**
ro05788	probable transcriptional regulator, MarR family	1.0	2.1	1.3
ro05789	(+)-trans-carveol dehydrogenase	1.6	**9.1**	2.9
ro05790	probable 3-oxoacyl-[acyl-carrier-protein] reductase	6.0	**19.5**	**6.5**
ro05791	dehydrogenase	0.9	8.4	4.1
ro05792	multidrug transporter, MFS superfamily	0.9	**18.4**	**7.4**
ro05793	conserved hypothetical protein	1.2	**5.2**	**2.2**
ro05794	conserved hypothetical protein	1.1	**5.6**	**2.9**
ro05795	probable transcriptional regulator, IclR family	0.7	**20.0**	**3.5**

ro05796	probable oxidoreductase	0.5	0.9	1.3
ro05797	alpha/beta-fold C-C bond hydrolase	1.4	**5.1**	**3.7**
ro05798	possible dehydrogenase	**1.8**	**5.7**	**5.9**
ro05799	2-keto-4-pentenoate hydratase, bphE homolog	1.4	**15.7**	**4.8**
ro05800	acetaldehyde dehydrogenase (acetylating)	0.8	**3.1**	2.9
ro05801	4-hydroxy-2-oxovalerate aldolase, bphF homolog		**2.2**	1.6
ro05802	hydroxylase	1.0	5.8	3.3
ro05803	extradiol dioxygenase, type I	1.6	**2.2**	1.2
ro05804	conserved hypothetical protein	0.6	**29.7**	**5.9**
ro05805	conserved hypothetical protein	1.3	1.1	1.4
ro05806	conserved hypothetical protein	1.0	1.7	1.3
ro05807	possible transmembrane protein	0.5	0.9	2.0
ro05808	conserved hypothetical protein	0.5	2.7	1.3
ro05809	probable 3-oxoacyl-[acyl-carrier-protein] reductase	0.7	1.7	0.9
ro05810	probable dehydrogenase	1.1	**6.2**	**3.6**
ro05811	probable dioxygenase Rieske iron-sulfur component	**1.7**	**53.2**	**9.8**
ro05812	probable hydroxylase	1.8	**5.4**	**2.1**
ro05813	probable 3-oxosteroid 1-dehydrogenase	1.2	**22.0**	3.4
ro05814	probable transcriptional regulator, TetR family	1.3	**4.2**	**2.9**
ro05815	probable thiolase	0.9	31.6	**4.8**
ro05816	possible acyl-CoA dehydrogenase	1.0	**27.9**	**6.6**
ro05817	possible MaoC family dehydratase	0.8	**5.9**	**7.1**
ro05818	conserved hypothetical protein	0.6	4.4	6.1
ro05819	probable (+)-trans-carveol dehydrogenase	1.6	**13.2**	**7.2**
ro05820	CoA ligase	**1.6**	**3.9**	1.3
ro05821	probable NADH-dependent flavin oxidoreductase		**18.4**	**5.8**
ro05822	acyl-CoA synthetase	1.0	**2.8**	1.9
ro05823	conserved hypothetical protein	1.1	1.9	**2.0**
ro05824	conserved hypothetical protein	**2.1**	**2.9**	**2.1**
ro05825	acyl-CoA dehydrogenase	**1.8**	**4.6**	1.8
ro05826	conserved hypothetical protein	0.5	3.5	**4.9**
ro05827	acyl-CoA dehydrogenase	0.8	**3.2**	2.4
ro05828	conserved hypothetical protein		4.2	**1.7**
ro05829	conserved hypothetical protein	1.0	**4.0**	2.9
ro05830	conserved hypothetical protein	0.6	1.1	1.7
ro05831		0.7		
ro05832	reductase	1.4	**2.2**	**2.1**
ro05833	probable oxidoreductase	1.5	1.0	0.9
	Cluster 4			
ro09002	oxygenase reductase KshB	1.5	1.6	1.1
ro09003	terminal oxygenase KshA	**6.2**	45.1	**8.2**
ro09004	probable hydroxylase	1.3	0.9	1.0
ro09005	extradiol ring-cleavage dioxygenase, BphC homolog	1.1	2.5	**2.4**
ro09006	conserved hypothetical protein	1.8	0.8	0.8
ro09007	probable short-chained dehydrogenase	1.0	1.2	0.8
ro09008	conserved hypothetical protein	1.2	1.0	0.8
ro09009	probable transposase	1.0	0.9	1.0
ro09010	probable lipase/esterase	1.3	0.9	0.7
ro09011	hypothetical protein		1.2	1.1

ro09012	possible flavoprotein oxidoreductase	1.5	1.0	1.0
ro09013	conserved hypothetical protein	1.6	1.2	0.8
ro09014	alpha/beta-fold C-C bond hydrolase	0.8	1.0	1.1
ro09015	conserved hypothetical protein		0.9	1.0
ro09016	conserved hypothetical protein	**1.6**	1.1	0.8
ro09017	transcriptional regulator, PadR family		1.0	1.3
ro09018	acetaldehyde dehydrogenase	1.8	0.2	0.8
ro09019	4-hydroxy-2-oxovalerate aldolase	0.7	0.9	1.2
ro09020	hypothetical protein		1.0	1.0
ro09021		0.9		
ro09022	transcriptional regulator, IclR family	**1.9**	**2.4**	1.3
ro09023	probable fumarate reductase	1.1	1.5	0.9
ro09024	fragment of 3-ketosteroid-1-dehydrogenase	**2.5**	1.4	0.8
ro09025	fragment of 3-ketosteroid-1-dehydrogenase	1.0	1.1	1.1
ro09026	probable lipase/esterase	0.8	0.7	0.4
ro09027	transcriptional regulator, GntR family	0.9	0.8	1.0
ro09028	possible CoA-transferase	0.7	1.0	1.0
ro09029	acyl-CoA dehydrogenase	1.3	0.9	0.9
ro09030	probable acyl-CoA dehydrogenase		1.4	1.7
ro09031	possible enoyl-CoA hydratase		0.9	1.2
ro09032	short-chained dehydrogenase	0.6	1.6	0.9
ro09033	hypothetical protein		0.6	1.0
ro09034	transcriptional regulator, IclR family	1.4	1.1	0.9
ro09035	monooxygenase	1.3	1.1	1.1
ro09036	lipase/esterase	1.5	0.9	0.8
ro09037	possible short-chained dehydrogenase	1.0	0.7	1.0
ro09038	probable short-chained dehydrogenase	**1.6**	1.0	1.0
ro09039	probable monooxygenase	0.7	0.9	0.7
ro09040	3-ketosteroid delta(1)-dehydrogenase	1.5	1.0	1.0

[1] Expression ratios that are statistically significant ($p \leq 0.05$) are bolded.

[2] Data adapted from Van der Geize et al. (37)

Chapter 8

References

1. Van der Geize, R., et al., *A gene cluster encoding cholesterol catabolism in a soil actinomycete provides insight into Mycobacterium tuberculosis survival in macrophages.* Proc Natl Acad Sci U S A, 2007. **104**(6): p. 1947-52.

2. Rosłoniec, K., et al., *Cytochrome P450 125 (CYP125) catalyzes C26-hydroxylation to initiate sterol side chain degradation.* 2009.

3. Yam, K.C., et al., *Studies of a ring-cleaving dioxygenase illuminate the role of cholesterol metabolism in the pathogenesis of Mycobacterium tuberculosis.* PLoS Pathog, 2009. **5**(3): p. e1000344.

4. Cox, R.H. and E.Y. Spencer, *The Effect of 7-Ketocholesterol on the Rabbit.* Science, 1949. **110**(2844): p. 11.

5. Hughes, H., et al., *Cytotoxicity of oxidized LDL to porcine aortic smooth muscle cells is associated with the oxysterols 7-ketocholesterol and 7-hydroxycholesterol.* Arterioscler Thromb, 1994. **14**(7): p. 1177-85.

6. Bjorkhem, I., et al., *Oxysterols and neurodegenerative diseases.* Mol Aspects Med, 2009. **30**(3): p. 171-9.

7. Casserly, I. and E. Topol, *Convergence of atherosclerosis and Alzheimer's disease: inflammation, cholesterol, and misfolded proteins.* Lancet, 2004. **363**(9415): p. 1139-46.

8. Seet, R.C.S., et al., *Oxidative damage in Parkinson disease: Measurement using accurate biomarkers.* Free Radical Biology and Medicine, 2010. **48**(4): p. 560-566.

9. Mol, M.J., et al., *Plasma levels of lipid and cholesterol oxidation products and cytokines in diabetes mellitus and cigarette smoking: effects of vitamin E treatment.* Atherosclerosis, 1997. **129**(2): p. 169-76.

10. Kahn, E., et al., *Iron nanoparticles increase 7-ketocholesterol-induced cell death, inflammation, and oxidation on murine cardiac HL1-NB cells.* Int J Nanomedicine, 2010. **5**: p. 185-95.

11. Miyajima, H., et al., *Increased oxysterols associated with iron accumulation in the brains and visceral organs of acaeruloplasminaemia patients.* QJM, 2001. **94**(8): p. 417-422.

12. Hung, Y.H., et al., *Paradoxical condensation of copper with elevated beta-amyloid in lipid rafts under cellular copper deficiency conditions: implications for Alzheimer disease.* J Biol Chem, 2009. **284**(33): p. 21899-907.

13. Ding, X., M. Patel, and C.C. Chan, *Molecular pathology of age-related macular degeneration.* Prog Retin Eye Res, 2009. **28**(1): p. 1-18.

14. Javitt, N.B. and J.C. Javitt, *The retinal oxysterol pathway: a unifying hypothesis for the cause of age-related macular degeneration.* Curr Opin Ophthalmol, 2009. **20**(3): p. 151-7.

15. Malvitte, L., et al., *[Analogies between atherosclerosis and age-related maculopathy: expected roles of oxysterols].* J Fr Ophtalmol, 2006. **29**(5): p. 570-8.

16. Liu, H., et al., *Cholestane-3β,5α,6β-triol inhibits osteoblastic differentiation and promotes apoptosis of rat bone marrow stromal cells.* Journal of Cellular Biochemistry, 2005. **96**(1): p. 198-208.

17. Porter, F.D., et al., *Cholesterol oxidation products are sensitive and specific blood-based biomarkers for Niemann-Pick C1 disease.* Sci Transl Med, 2010. **2**(56): p. 56ra81.

18. Soehngen, N.L., *Einfluss von Kolloiden auf mikrobiologische Prozesse.* Zentr. Bakteriol. Parasitenk. Orig., 1913. **38**: p. 621-647.

19. Turfitt, G.E., *The microbiological degradation of steroids: 2. Oxidation of cholesterol by Proactinomyces spp.* Biochem J, 1944. **38**(5): p. 492-6.

20. Turfitt, G.E., *The microbiological degradation of steroids: 4. Fission of the steroid molecule.* Biochem J, 1948. **42**(3): p. 376-83.

21. Hogg, J.A., *Steroids, the steroid community, and Upjohn in perspective: a profile of innovation.* Steroids, 1992. **57**(12): p. 593-616.

22. Voets, J.P. and E. Lamot, *Microbial degradation of cholesterol.* Zeitschrift für allgemeine Mikrobiologie, 1974. **14**(1): p. 77-79.

23. Tak, J., *On bacteria decomposing cholesterol.* Antonie van Leeuwenhoek, 1942. **8**(1): p. 32-40.

24. Van der Geize, R., et al., *A gene cluster encoding cholesterol catabolism in a soil actinomycete provides insight into Mycobacterium tuberculosis survival in macrophages.* Proceedings of the National Academy of Sciences, 2007. **104**(6): p. 1947-1952.

25. Horinouchi, M., et al., *Identification of 9,17-dioxo-1,2,3,4,10,19-hexanorandrostan-5-oic acid, 4-hydroxy-2-oxohexanoic acid, and 2-hydroxyhexa-2,4-dienoic acid and related enzymes involved in testosterone degradation in Comamonas testosteroni TA441.* Appl Environ Microbiol, 2005. **71**(9): p. 5275-81.

26. Wovcha, M.G., et al., *Bioconversion of sitosterol to useful steroidal intermediates by mutants of Mycobacterium fortuitum.* Biochim Biophys Acta, 1978. **531**(3): p. 308-21.

27. Mallonee, D.H., M.A. Lijewski, and P.B. Hylemon, *Expression in Escherichia coli and characterization of a bile acid-inducible 3 alpha-hydroxysteroid dehydrogenase from Eubacterium sp. strain VPI 12708.* Curr Microbiol, 1995. **30**(5): p. 259-63.

28. Datcheva, V.K., et al., *Synthesis of 9 alpha-hydroxysteroids by a Rhodococcus sp.* Steroids, 1989. **54**(3): p. 271-86.

29. Angelova, B., et al., *9 alpha-hydroxylation of 4-androstene-3,17-dione by resting Rhodococcus sp cells.* Process Biochemistry, 1996. **31**(2): p. 179-184.

30. Fernandes, P., et al., *Microbial conversion of steroid compounds: recent developments.* Enzyme and Microbial Technology, 2003. **32**(6): p. 688-705.

31. Nobile, A., et al., *Microbiological Transformation of Steroids .1. Delta-1,4-Diene-3-Ketosteroids.* Journal of the American Chemical Society, 1955. **77**(15): p. 4184-4184.

32. van Der Geize, R., et al., *Targeted disruption of the kstD gene encoding a 3-ketosteroid delta(1)-dehydrogenase isoenzyme of Rhodococcus erythropolis strain SQ1.* Appl Environ Microbiol, 2000. **66**(5): p. 2029-36.

33. Osipowicz, B., Z. Krezel, and A. Siewinski, *Biotransformations .32. Oxidation of 3-Beta-Hydroxysteroids and 17-Beta-Hydroxysteroids by Nocardia-Rubra Cells in Heptane-Water System.* Journal of Basic Microbiology, 1992. **32**(3): p. 215-216.

34. Mahato, S.B. and A. Mukherjee, *Steroid Transformations by Microorganisms.* Phytochemistry, 1984. **23**(10): p. 2131-2154.

35. Miyamoto, M., et al., *Bacterial Steroid Monooxygenase Catalyzing the Baeyer-Villiger Oxidation of C-21-Ketosteroids from Rhodococcus-Rhodochrous - the Isolation and Characterization.* Biochimica Et Biophysica Acta-Protein Structure and Molecular Enzymology, 1995. **1251**(2): p. 115-124.

36. Mathieu, J.M., et al., *Medical bioremediation of age-related diseases.* Microb Cell Fact, 2009. **8**: p. 21.

37. Mathieu, J., et al., *Microbial degradation of 7-ketocholesterol.* Biodegradation, 2008. **19**(6): p. 807-13.

38. Mathieu, J.M., et al., *7-ketocholesterol catabolism by Rhodococcus jostii RHA1.* Appl Environ Microbiol, 2010. **76**(1): p. 352-5.

39. Schloendorn, J., et al., *Medical bioremediation: a concept moving toward reality.* Rejuvenation Res, 2009. **12**(6): p. 411-9.

40. Brown, A.J. and W. Jessup, *Oxysterols and atherosclerosis.* Atherosclerosis, 1999. **142**(1): p. 1-28.

41. Wielkoszynski, T., et al., *Cellular toxicity of oxycholesterols.* Bioessays, 2006. **28**(4): p. 387-98.

42. Zhou, Q., et al., *An excess concentration of oxysterols in the plasma is cytotoxic to cultured endothelial cells.* Atherosclerosis, 2000. **149**(1): p. 191-7.

43. Vaya, J. and H.M. Schipper, *Oxysterols, cholesterol homeostasis, and Alzheimer disease.* J Neurochem, 2007. **102**(6): p. 1727-37.

44. Nelson, T.J. and D.L. Alkon, *Oxidation of cholesterol by amyloid precursor protein and beta-amyloid peptide.* J Biol Chem, 2005. **280**(8): p. 7377-87.

45. Ong, J.M., et al., *Oxysterol-induced toxicity in R28 and ARPE-19 cells.* Neurochem Res, 2003. **28**(6): p. 883-91.

46. Bosco, D.A., et al., *Elevated levels of oxidized cholesterol metabolites in Lewy body disease brains accelerate alpha-synuclein fibrilization.* Nat Chem Biol, 2006. **2**(5): p. 249-53.

47. Sato, H., et al., *Oxysterol regulation of estrogen receptor alpha-mediated gene expression in a transcriptional activation assay system using HeLa cells.* Biosci Biotechnol Biochem, 2004. **68**(8): p. 1790-3.

48. Christianson-Heiska, I., et al., *Endocrine modulating actions of a phytosterol mixture and its oxidation products in zebrafish (Danio rerio).* Comp Biochem Physiol C Toxicol Pharmacol, 2007. **145**(4): p. 518-27.

49. Schroepfer, G.J., *Oxysterols: Modulators of Cholesterol Metabolism and Other Processes.* Physiological Reviews, 2000. **80**(1): p. 361-554.

50. de Grey, A.D., et al., *Medical bioremediation: prospects for the application of microbial catabolic diversity to aging and several major age-related diseases.* Ageing Res Rev, 2005. **4**(3): p. 315-38.

51. Linseisen, J. and G. Wolfram, *Absorption of cholesterol oxidation products from ordinary foodstuff in humans.* Ann Nutr Metab, 1998. **42**(4): p. 221-30.

52. Crosignani, A., et al., *Plasma oxysterols in normal and cholestatic children as indicators of the two pathways of bile acid synthesis.* Clin Chim Acta, 2008. **395**(1-2): p. 84-8.

53. Joffre, C., et al., *Oxysterols Induced Inflammation and Oxidation in Primary Porcine Retinal Pigment Epithelial Cells.* Current Eye Research, 2007. **32**(3): p. 271 - 280.

54. Teunissen, C.E., et al., *Serum cholesterol, precursors and metabolites and cognitive performance in an aging population.* Neurobiol Aging, 2003. **24**(1): p. 147-55.

55. Gardner, H.W., *Oxygen radical chemistry of polyunsaturated fatty acids.* Free Radic Biol Med, 1989. **7**(1): p. 65-86.

56. Brown, A.J., et al., *7-Hydroperoxycholesterol and its products in oxidized low density lipoprotein and human atherosclerotic plaque.* J. Lipid Res., 1997. **38**(9): p. 1730-1745.

57. Murphy, R.C. and K.M. Johnson, *Cholesterol, reactive oxygen species, and the formation of biologically active mediators.* J Biol Chem, 2008. **283**(23): p. 15521-5.

58. Smith, L.L., *Review of progress in sterol oxidations: 1987-1995.* Lipids, 1996. **31**(5): p. 453-87.

59. Watabe, T., et al., *A mechanism for epoxidation of cholesterol by hepatic microsomal lipid hydroperoxides.* Biochim Biophys Acta, 1984. **795**(1): p. 60-6.

60. Russell, D.W., *Oxysterol biosynthetic enzymes.* Biochim Biophys Acta, 2000. **1529**(1-3): p. 126-35.

61. Lund, E.G., et al., *cDNA cloning of mouse and human cholesterol 25-hydroxylases, polytopic membrane proteins that synthesize a potent oxysterol regulator of lipid metabolism.* J Biol Chem, 1998. **273**(51): p. 34316-27.

62. Lund, E.G., J.M. Guileyardo, and D.W. Russell, *cDNA cloning of cholesterol 24-hydroxylase, a mediator of cholesterol homeostasis in the brain.* Proc Natl Acad Sci U S A, 1999. **96**(13): p. 7238-43.

63. Andersson, S., et al., *Cloning, structure, and expression of the mitochondrial cytochrome P-450 sterol 26-hydroxylase, a bile acid biosynthetic enzyme.* J Biol Chem, 1989. **264**(14): p. 8222-9.

64. Johnsson, L. and P. Dutta, *Characterization of side-chain oxidation products of sitosterol and campesterol by chromatographic and spectroscopic methods.* Journal of the American Oil Chemists' Society, 2003. **80**(8): p. 767-776.

65. Popova, E.V., et al., *Oxidation of the side chains of ergosterol derivatives.* Chemistry of Natural Compounds, 1978. **14**(1): p. 70-72.

66. Ponce, M.A., et al., *A new look into the reaction between ergosterol and singlet oxygen in vitro.* Photochem Photobiol Sci, 2002. **1**(10): p. 749-56.

67. Jakob, L. and W. Günther, *Origin, metabolism, and adverse health effects of cholesterol oxidation products.* Lipid - Fett, 1998. **100**(6): p. 211-218.

68. Shan, H., et al., *Chromatographic behavior of oxygenated derivatives of cholesterol.* Steroids, 2003. **68**(3): p. 221-33.

69. Breuer, O. and I. Bjorkhem, *Simultaneous quantification of several cholesterol autoxidation and monohydroxylation products by isotope-dilution mass spectrometry.* Steroids, 1990. **55**(4): p. 185-92.

70. Dzeletovic, S., et al., *Determination of cholesterol oxidation products in human plasma by isotope dilution-mass spectrometry.* Anal Biochem, 1995. **225**(1): p. 73-80.

71. Javitt, N.B., et al., *26-Hydroxycholesterol. Identification and quantitation in human serum.* J Biol Chem, 1981. **256**(24): p. 12644-6.

72. Griffiths, W.J., et al., *Discovering oxysterols in plasma: a window on the metabolome.* J Proteome Res, 2008. **7**(8): p. 3602-12.

73. McDonald, J.G., et al., *Extraction and analysis of sterols in biological matrices by high performance liquid chromatography electrospray ionization mass spectrometry.* Methods Enzymol, 2007. **432**: p. 145-70.

74. Gutierrez, A., J.C. del Rio, and A.T. Martinez, *Microbial and enzymatic control of pitch in the pulp and paper industry.* Appl Microbiol Biotechnol, 2009. **82**(6): p. 1005-18.

75. Cook, D.L., et al., *Characterization of plant sterols form 22 us pulp and paper mills.* Water Science and Technology, 1997. **35**(2-3): p. 297-303.

76. Freire, C.S.R., A.J.D. Silvestre, and C.P. Neto, *Lipophilic Extractives in Eucalyptus globulus Kraft Pulps. Behavior during ECF Bleaching.* Journal of Wood Chemistry & Technology, 2005. **25**(1/2): p. 67-80.

77. Stumpf, M., et al., *Determination of natural and synthetic estrogens in sewage plants and river water.* Vom Wasser, 1996. **87**: p. 251-261.

78. Quintana, J.B., et al., *Determination of natural and synthetic estrogens in water by gas chromatography with mass spectrometric detection.* Journal of Chromatography A, 2004. **1024**(1-2): p. 177-185.

79. Tremblay, L. and G. Van Der Kraak, *Comparison between the effects of the phytosterol β-sitosterol.* Environmental Toxicology and Chemistry, 1999. **18**(2): p. 329-336.

80. Davis, W.P. and S.A. Bortone, *Effects of Kraft Mill effluent on the sexuality of fishes: An environmental early warning*, in *Other Information: Pub. in Chemically Induced Alterations in Sexuality of Fishes, p113-127 1992. See also PB--91-199893.* 1992. p. Medium: X; Size: Pages: (17 p).

81. Nakari, T. and K. Erkomaa, *Effects of phytosterols on zebrafish reproduction in multigeneration test.* Environmental Pollution, 2003. **123**(2): p. 267-273.

82. Hewitt, L.M., et al., *Altered reproduction in fish exposed to pulp and paper mill effluents: roles of individual compounds and mill operating conditions.* Environ Toxicol Chem, 2008. **27**(3): p. 682-97.

83. Jenkins, R.L., et al., *Androstenedione and Progesterone in the Sediment of a River Receiving Paper Mill Effluent.* Toxicol. Sci., 2003. **73**(1): p. 53-59.

84. Denton, T.E., et al., *Masculinization of female mosquitofish by exposure to plant sterols andMycobacterium smegmatis.* Bulletin of Environmental Contamination and Toxicology, 1985. **35**(1): p. 627-632.

85. Puglisi, E., et al., *Cholesterol, {beta}-Sitosterol, Ergosterol, and Coprostanol in Agricultural Soils.* J Environ Qual, 2003. **32**(2): p. 466-471.

86. Turfitt, G.E., *The microbiological degradation of steroids: 1. The sterol content of soils.* Biochem J, 1943. **37**(1): p. 115-7.

87. Lake, R. and P. Scholes, *Consumption of cholesterol oxides from fast foods fried in beef fat in New Zealand.* Journal of the American Oil Chemists' Society, 1997. **74**(9): p. 1069-1075.

88. Nourooz-Zadeh, J. and L.-Å. Appelqvist, *Isolation and quantitative determination of sterol oxides in plant-based foods: Soybean oil and wheat flour.* Journal of the American Oil Chemists' Society, 1992. **69**(3): p. 288-293.

89. van de Bovenkamp, P., T. Kosmeijer-Schuil, and M. Katan, *Quantification of oxysterols in dutch foods: Egg products and mixed diets.* Lipids, 1988. **23**(11): p. 1079-1085.

90. Ryan, E., et al., *Phytosterol Oxidation Products: Their Formation, Occurrence, and Biological Effects.* Food Reviews International, 2009. **25**: p. 157-174.

91. Paniangvait, P., et al., *Cholesterol Oxides in Foods of Animal Origin.* Journal of Food Science, 1995. **60**(6): p. 1159-1174.

92. Yan, P.S., *Cholesterol oxidation products. Their occurrence and detection in our foodstuffs.* Adv Exp Med Biol, 1999. **459**: p. 79-98.

93. Soupas, L., et al., *Effects of sterol structure, temperature, and lipid medium on phytosterol oxidation.* J Agric Food Chem, 2004. **52**(21): p. 6485-91.

94. Pie, J.E., K. Spahis, and C. Seillan, *Cholesterol oxidation in meat products during cooking and frozen storage.* Journal of Agricultural and Food Chemistry, 1991. **39**(2): p. 250-254.

95. Jacobson, M., *Cholesterol Oxides in Indian Ghee: Possible Cause of Unexplained High Risk of Atherosclerosis in Indian Immigrant Populations.* The Lancet, 1987. **330**(8560): p. 656-658.

96. Abramsson-Zetterberg, L., M. Svensson, and L. Johnsson, *No evidence of genotoxic effect in vivo of the phytosterol oxidation products triols and epoxides.* Toxicol Lett, 2007. **173**(2): p. 132-9.

97. Kuhlmann, K., et al., *Simulation of prospective phytosterol intake in Germany by novel functional foods.* British Journal of Nutrition, 2005. **93**(03): p. 377-385.

98. Osada, K., E. Sasaki, and M. Sugano, *Lymphatic absorption of oxidized cholesterol in rats.* Lipids, 1994. **29**(8): p. 555-9.

99. Tomoyori, H., et al., *Phytosterol oxidation products are absorbed in the intestinal lymphatics in rats but do not accelerate atherosclerosis in apolipoprotein E-deficient mice.* J Nutr, 2004. **134**(7): p. 1690-6.

100. Szedlacsek, S.E., et al., *Esterification of oxysterols by human plasma lecithin-cholesterol acyltransferase.* J Biol Chem, 1995. **270**(20): p. 11812-9.

101. Lin, C.Y. and D.W. Morel, *Esterification of oxysterols in human serum: effects on distribution and cellular uptake.* J Lipid Res, 1996. **37**(1): p. 168-78.

102. Staprans, I., et al., *Oxidized lipids in the diet are incorporated by the liver into very low density lipoprotein in rats.* J Lipid Res, 1996. **37**(2): p. 420-30.

103. Vine, D.F., et al., *Absorption of dietary cholesterol oxidation products and incorporation into rat lymph chylomicrons.* Lipids, 1997. **32**(8): p. 887-93.

104. Vine, D.F., et al., *Effect of dietary cholesterol oxidation products on the plasma clearance of chylomicrons in the rat.* Lipids, 2002. **37**(5): p. 455-62.

105. Moore, E.H., et al., *Protection of chylomicron remnants from oxidation by incorporation of probucol into the particles enhances their uptake by human macrophages and increases lipid accumulation in the cells.* Eur J Biochem, 2004. **271**(12): p. 2417-27.

106. Moore, E.H., et al., *Incorporation of lycopene into chylomicron remnant-like particles enhances their induction of lipid accumulation in macrophages.* Biochem Biophys Res Commun, 2003. **312**(4): p. 1216-9.

107. Russell, D.W., *Cholesterol biosynthesis and metabolism.* Cardiovasc Drugs Ther, 1992. **6**(2): p. 103-10.

108. Grundy, S.M., *Absorption and metabolism of dietary cholesterol.* Annu Rev Nutr, 1983. **3**: p. 71-96.

109. Dietschy, J.M., *Regulation of cholesterol metabolism in man and in other species.* Klin Wochenschr, 1984. **62**(8): p. 338-45.

110. Steinbrecher, U.P., et al., *Modification of low density lipoprotein by endothelial cells involves lipid peroxidation and degradation of low density lipoprotein phospholipids.* Proc Natl Acad Sci U S A, 1984. **81**(12): p. 3883-7.

111. Goldstein, J.L., et al., *Binding site on macrophages that mediates uptake and degradation of acetylated low density lipoprotein, producing massive cholesterol deposition.* Proc Natl Acad Sci U S A, 1979. **76**(1): p. 333-7.

112. Nozaki, S., et al., *Reduced uptake of oxidized low density lipoproteins in monocyte-derived macrophages from CD36-deficient subjects.* J Clin Invest, 1995. **96**(4): p. 1859-65.

113. Moriwaki, H., et al., *Ligand specificity of LOX-1, a novel endothelial receptor for oxidized low density lipoprotein.* Arterioscler Thromb Vasc Biol, 1998. **18**(10): p. 1541-7.

114. Sparrow, C.P., S. Parthasarathy, and D. Steinberg, *A macrophage receptor that recognizes oxidized low density lipoprotein but not acetylated low density lipoprotein.* J Biol Chem, 1989. **264**(5): p. 2599-604.

115. Jialal, I., D.A. Freeman, and S.M. Grundy, *Varying susceptibility of different low density lipoproteins to oxidative modification.* Arterioscler Thromb, 1991. **11**(3): p. 482-8.

116. Wen, Y. and D.S. Leake, *Low density lipoprotein undergoes oxidation within lysosomes in cells.* Circ Res, 2007. **100**(9): p. 1337-43.

117. Pulfer, M.K. and R.C. Murphy, *Formation of biologically active oxysterols during ozonolysis of cholesterol present in lung surfactant.* J Biol Chem, 2004. **279**(25): p. 26331-8.

118. Pulfer, M.K., et al., *Ozone exposure in vivo and formation of biologically active oxysterols in the lung.* J Pharmacol Exp Ther, 2005. **312**(1): p. 256-64.

119. Takeuchi, C., et al., *Proatherogenic effects of the cholesterol ozonolysis products, atheronal-A and atheronal-B.* Biochemistry, 2006. **45**(23): p. 7162-70.

120. Mesmin, B. and F.R. Maxfield, *Intracellular sterol dynamics.* Biochim Biophys Acta, 2009. **1791**(7): p. 636-45.

121. Maxfield, F.R. and M. Mondal, *Sterol and lipid trafficking in mammalian cells.* Biochem. Soc. Trans., 2006. **34**(Pt 3): p. 335-339.

122. Huang, J. and G.W. Feigenson, *A microscopic interaction model of maximum solubility of cholesterol in lipid bilayers.* Biophys J, 1999. **76**(4): p. 2142-57.

123. Ali, M.R., K.H. Cheng, and J. Huang, *Assess the nature of cholesterol-lipid interactions through the chemical potential of cholesterol in phosphatidylcholine bilayers.* Proceedings of the National Academy of Sciences, 2007. **104**(13): p. 5372-5377.

124. Bacia, K., P. Schwille, and T. Kurzchalia, *Sterol structure determines the separation of phases and the curvature of the liquid-ordered phase in model membranes.* Proc Natl Acad Sci U S A, 2005. **102**(9): p. 3272-7.

125. Li, X.M., et al., *Sterol structure and sphingomyelin acyl chain length modulate lateral packing elasticity and detergent solubility in model membranes.* Biophys J, 2003. **85**(6): p. 3788-801.

126. Wenz, J.J. and F.J. Barrantes, *Steroid structural requirements for stabilizing or disrupting lipid domains.* Biochemistry, 2003. **42**(48): p. 14267-76.

127. Xu, X. and E. London, *The effect of sterol structure on membrane lipid domains reveals how cholesterol can induce lipid domain formation.* Biochemistry, 2000. **39**(5): p. 843-9.

128. Massey, J.B. and H.J. Pownall, *Structures of biologically active oxysterols determine their differential effects on phospholipid membranes.* Biochemistry, 2006. **45**(35): p. 10747-58.

129. Anderson, R.G. and K. Jacobson, *A role for lipid shells in targeting proteins to caveolae, rafts, and other lipid domains.* Science, 2002. **296**(5574): p. 1821-5.

130. Lee, A.G., *Lipid-protein interactions in biological membranes: a structural perspective.* Biochim Biophys Acta, 2003. **1612**(1): p. 1-40.

131. Anderson, R.G., *The caveolae membrane system.* Annu Rev Biochem, 1998. **67**: p. 199-225.

132. Bach, D., et al., *Interaction of 7-ketocholesterol with two major components of the inner leaflet of the plasma membrane: phosphatidylethanolamine and phosphatidylserine.* Biochemistry, 2008. **47**(9): p. 3004-12.

133. Meaney, S., et al., *On the rate of translocation in vitro and kinetics in vivo of the major oxysterols in human circulation: critical importance of the position of the oxygen function.* J Lipid Res, 2002. **43**(12): p. 2130-5.

134. Kauffman, J.M., P.W. Westerman, and M.C. Carey, *Fluorocholesterols, in contrast to hydroxycholesterols, exhibit interfacial properties similar to cholesterol.* J Lipid Res, 2000. **41**(6): p. 991-1003.

135. Theunissen, J.J., et al., *Membrane properties of oxysterols. Interfacial orientation, influence on membrane permeability and redistribution between membranes.* Biochim Biophys Acta, 1986. **860**(1): p. 66-74.

136. Gaus, K., et al., *Apolipoprotein A-1 interaction with plasma membrane lipid rafts controls cholesterol export from macrophages.* FASEB J., 2004. **18**(3): p. 574-576.

137. Berthier, A., et al., *Involvement of a calcium-dependent dephosphorylation of BAD associated with the localization of Trpc-1 within lipid rafts in 7-ketocholesterol-induced THP-1 cell apoptosis.* Cell Death Differ, 2004. **11**(8): p. 897-905.

138. Sleer, L.S., A.J. Brown, and K.K. Stanley, *Interaction of caveolin with 7-ketocholesterol.* Atherosclerosis, 2001. **159**(1): p. 49-55.

139. Girao, H., S. Catarino, and P. Pereira, *7-Ketocholesterol modulates intercellular communication through gap-junction in bovine lens epithelial cells.* Cell Commun Signal, 2004. **2**(1): p. 2.

140. Ayuyan, A.G. and F.S. Cohen, *Raft Composition at Physiological Temperature and pH in the Absence of Detergents.* Biophysical Journal, 2008. **94**(7): p. 2654-2666.

141. Chiang, Y.W., et al., *New method for determining tie-lines in coexisting membrane phases using spin-label ESR.* Biochim Biophys Acta, 2005. **1668**(1): p. 99-105.

142. Peng, S.K., et al., *Influence of cholesterol oxidation derivatives on membrane bound enzymes in cultured aortic smooth muscle cells.* Proc Soc Exp Biol Med, 1985. **180**(1): p. 126-32.

143. Krull, U.J., et al., *Langmuir Blodgett Film Characteristics and Phospholipid Membrane Ion Conduction .1. Modification by Cholesterol and Oxidized Derivatives.* Analytica Chimica Acta, 1985. **174**(Aug): p. 83-94.

144. Anderson, N. and J. Borlak, *Drug-induced phospholipidosis.* FEBS Lett, 2006. **580**(23): p. 5533-40.

145. Vejux, A., L. Malvitte, and G. Lizard, *Side effects of oxysterols: cytotoxicity, oxidation, inflammation, and phospholipidosis.* Braz J Med Biol Res, 2008. **41**(7): p. 545-56.

146. Larsson, D.A., et al., *Oxysterol mixtures, in atheroma-relevant proportions, display synergistic and proapoptotic effects.* Free Radic Biol Med, 2006. **41**(6): p. 902-10.

147. Vindis, C., et al., *Two distinct calcium-dependent mitochondrial pathways are involved in oxidized LDL-induced apoptosis.* Arterioscler Thromb Vasc Biol, 2005. **25**(3): p. 639-45.

148. Yamashima, T., et al., *Transient brain ischaemia provokes Ca2+, PIP2 and calpain responses prior to delayed neuronal death in monkeys.* Eur J Neurosci, 1996. **8**(9): p. 1932-44.

149. Yamashima, T., et al., *Inhibition of ischaemic hippocampal neuronal death in primates with cathepsin B inhibitor CA-074: a novel strategy for neuroprotection based on 'calpain-cathepsin hypothesis'.* Eur J Neurosci, 1998. **10**(5): p. 1723-33.

150. Rimner, A., et al., *Relevance and mechanism of oxysterol stereospecifity in coronary artery disease.* Free Radic Biol Med, 2005. **38**(4): p. 535-44.

151. Spyridopoulos, I., et al., *Alcohol enhances oxysterol-induced apoptosis in human endothelial cells by a calcium-dependent mechanism.* Arterioscler Thromb Vasc Biol, 2001. **21**(3): p. 439-44.

152. Han, J.H., et al., *Prevention of 7-ketocholesterol-induced mitochondrial damage and cell death by calmodulin inhibition.* Brain Res, 2007. **1137**(1): p. 11-9.

153. Lizard, G., et al., *Induction of apoptosis in endothelial cells treated with cholesterol oxides.* Am J Pathol, 1996. **148**(5): p. 1625-38.

154. Sevanian, A., et al., *Characterization of endothelial cell injury by cholesterol oxidation products found in oxidized LDL.* J Lipid Res, 1995. **36**(9): p. 1971-86.

155. Girao, H., F. Shang, and P. Pereira, *7-ketocholesterol stimulates differentiation of lens epithelial cells.* Mol Vis, 2003. **9**: p. 497-501.

156. Ryan, E., et al., *Qualitative and quantitative comparison of the cytotoxic and apoptotic potential of phytosterol oxidation products with their corresponding cholesterol oxidation products.* Br J Nutr, 2005. **94**(3): p. 443-51.

157. Ross, R., *The pathogenesis of atherosclerosis: a perspective for the 1990s.* Nature, 1993. **362**(6423): p. 801-9.

158. Ross, R., *The pathogenesis of atherosclerosis--an update.* N Engl J Med, 1986. **314**(8): p. 488-500.

159. McGill, H.C., Jr., *George Lyman Duff memorial lecture. Persistent problems in the pathogenesis of atherosclerosis.* Arteriosclerosis, 1984. **4**(5): p. 443-51.

160. Suzuki, H., et al., *A role for macrophage scavenger receptors in atherosclerosis and susceptibility to infection.* Nature, 1997. **386**(6622): p. 292-6.

161. Leonarduzzi, G., et al., *Oxidation as a crucial reaction for cholesterol to induce tissue degeneration: CD36 overexpression in human promonocytic cells treated with a biologically relevant oxysterol mixture.* Aging Cell, 2008. **7**(3): p. 375-82.

162. Cox, B.E., et al., *Effects of cellular cholesterol loading on macrophage foam cell lysosome acidification.* J. Lipid Res., 2007. **48**(5): p. 1012-1021.

163. Steinberg, D., et al., *Beyond cholesterol. Modifications of low-density lipoprotein that increase its atherogenicity.* N Engl J Med, 1989. **320**(14): p. 915-24.

164. Jessup, W., L. Kritharides, and R. Stocker, *Lipid oxidation in atherogenesis: an overview.* Biochem. Soc. Trans., 2004. **32**(Pt 1): p. 134-138.

165. Cheruku, S.R., et al., *Mechanism of cholesterol transfer from the Niemann-Pick type C2 protein to model membranes supports a role in lysosomal cholesterol transport.* J Biol Chem, 2006. **281**(42): p. 31594-604.

166. Neufeld, E.B., et al., *Intracellular trafficking of cholesterol monitored with a cyclodextrin.* J Biol Chem, 1996. **271**(35): p. 21604-13.

167. Yancey, P.G. and W.G. Jerome, *Lysosomal sequestration of free and esterified cholesterol from oxidized low density lipoprotein in macrophages of different species.* J Lipid Res, 1998. **39**(7): p. 1349-61.

168. Griffin, E.E., et al., *Aggregated LDL and lipid dispersions induce lysosomal cholesteryl ester accumulation in macrophage foam cells.* J Lipid Res, 2005. **46**(10): p. 2052-60.

169. Jerome, W.G., et al., *Lysosomal lipid accumulation from oxidized low density lipoprotein is correlated with hypertrophy of the Golgi apparatus and trans-Golgi network.* J Lipid Res, 1998. **39**(7): p. 1362-71.

170. Nishio, E., S. Arimura, and Y. Watanabe, *Oxidized LDL Induces Apoptosis in Cultured Smooth Muscle Cells: A Possible Role for 7-Ketocholesterol.* Biochemical and Biophysical Research Communications, 1996. **223**(2): p. 413-418.

171. Lougheed, M., H.F. Zhang, and U.P. Steinbrecher, *Oxidized low density lipoprotein is resistant to cathepsins and accumulates within macrophages.* J Biol Chem, 1991. **266**(22): p. 14519-25.

172. Jessup, W., E.L. Mander, and R.T. Dean, *The intracellular storage and turnover of apolipoprotein B of oxidized LDL in macrophages.* Biochim Biophys Acta, 1992. **1126**(2): p. 167-77.

173. Jessup, W. and L. Kritharides, *Metabolism of oxidized LDL by macrophages.* Curr Opin Lipidol, 2000. **11**(5): p. 473-81.

174. Brown, A.J., et al., *Cholesterol and oxysterol metabolism and subcellular distribution in macrophage foam cells. Accumulation of oxidized esters in lysosomes.* J Lipid Res, 2000. **41**(2): p. 226-37.

175. Yuan, X.M., et al., *Lysosomal destabilization during macrophage damage induced by cholesterol oxidation products.* Free Radic Biol Med, 2000. **28**(2): p. 208-18.

176. Pedruzzi, E., et al., *NAD(P)H oxidase Nox-4 mediates 7-ketocholesterol-induced endoplasmic reticulum stress and apoptosis in human aortic smooth muscle cells.* Mol Cell Biol, 2004. **24**(24): p. 10703-17.

177. Lemaire, S., et al., *Different patterns of IL-1beta secretion, adhesion molecule expression and apoptosis induction in human endothelial cells treated with 7alpha-, 7beta-hydroxycholesterol, or 7-ketocholesterol.* FEBS Lett, 1998. **440**(3): p. 434-9.

178. Sung, S.C., et al., *7-Ketocholesterol Upregulates Interleukin-6 via Mechanisms That Are Distinct from Those of Tumor Necrosis Factor-alpha, in Vascular Smooth Muscle Cells.* J Vasc Res, 2008. **46**(1): p. 36-44.

179. Liu, Y., L.M. Hulten, and O. Wiklund, *Macrophages isolated from human atherosclerotic plaques produce IL-8, and oxysterols may have a regulatory function for IL-8 production.* Arterioscler Thromb Vasc Biol, 1997. **17**(2): p. 317-23.

180. Garcia-Cruset, S., et al., *Oxysterol profiles of normal human arteries, fatty streaks and advanced lesions.* Free Radic Res, 2001. **35**(1): p. 31-41.

181. Dreizen, S., M.H. Stern, and B.M. Levy, *Diet-induced arteriopathies in the rabbit aorta and oral vasculature.* J Dent Res, 1978. **57**(2): p. 412-7.

182. Brooks, C.J., W.A. Harland, and G. Steel, *Squalene, 26-hydroxycholesterol and 7-ketocholesterol in human atheromatous plaques.* Biochim Biophys Acta, 1966. **125**(3): p. 620-2.

183. Carter, C.J., *Convergence of genes implicated in Alzheimer's disease on the cerebral cholesterol shuttle: APP, cholesterol, lipoproteins, and atherosclerosis.* Neurochem Int, 2007. **50**(1): p. 12-38.

184. Hebert, L.E., et al., *Annual incidence of Alzheimer disease in the United States projected to the years 2000 through 2050.* Alzheimer Dis Assoc Disord, 2001. **15**(4): p. 169-73.

185. Brookmeyer, R., S. Gray, and C. Kawas, *Projections of Alzheimer's disease in the United States and the public health impact of delaying disease onset.* Am J Public Health, 1998. **88**(9): p. 1337-42.

186. Glenner, G.G., et al., *The amyloid deposits in Alzheimer's disease: their nature and pathogenesis.* Appl Pathol, 1984. **2**(6): p. 357-69.

187. Glenner, G.G. and C.W. Wong, *Alzheimer's disease: initial report of the purification and characterization of a novel cerebrovascular amyloid protein.* Biochem Biophys Res Commun, 1984. **120**(3): p. 885-90.

188. Yang, A.J., et al., *Intracellular accumulation of insoluble, newly synthesized abetan-42 in amyloid precursor protein-transfected cells that have been treated with Abeta1-42.* J Biol Chem, 1999. **274**(29): p. 20650-6.

189. Alonso, A., et al., *Hyperphosphorylation induces self-assembly of tau into tangles of paired helical filaments/straight filaments.* Proc Natl Acad Sci U S A, 2001. **98**(12): p. 6923-8.

190. Nixon, R.A., *Niemann-Pick Type C disease and Alzheimer's disease: the APP-endosome connection fattens up.* Am J Pathol, 2004. **164**(3): p. 757-61.

191. Nixon, R.A., *Endosome function and dysfunction in Alzheimer's disease and other neurodegenerative diseases.* Neurobiol Aging, 2005. **26**(3): p. 373-82.

192. Trojanowski, J.Q. and V.M. Lee, *"Fatal attractions" of proteins. A comprehensive hypothetical mechanism underlying Alzheimer's disease and other neurodegenerative disorders.* Ann N Y Acad Sci, 2000. **924**: p. 62-7.

193. Wang, D.S., D.W. Dickson, and J.S. Malter, *Tissue Transglutaminase, Protein Cross-linking and Alzheimer's Disease: Review and Views.* Int J Clin Exp Pathol, 2008. **1**(1): p. 5-18.

194. He, X., et al., *Apolipoprotein D modulates F2-isoprostane and 7-ketocholesterol formation and has a neuroprotective effect on organotypic hippocampal cultures after kainate-induced excitotoxic injury.* Neuroscience Letters, 2009. **455**(3): p. 183-186.

195. Dietschy, J.M. and S.D. Turley, *Cholesterol metabolism in the central nervous system during early development and in the mature animal.* J Lipid Res, 2004. **45**(8): p. 1375-97.

196. Congdon, N., et al., *Causes and prevalence of visual impairment among adults in the United States.* Arch Ophthalmol, 2004. **122**(4): p. 477-85.

197. Friedman, D.S., et al., *Prevalence of age-related macular degeneration in the United States.* Arch Ophthalmol, 2004. **122**(4): p. 564-72.

198. Jager, R.D., W.F. Mieler, and J.W. Miller, *Age-related macular degeneration.* N Engl J Med, 2008. **358**(24): p. 2606-17.

199. Moreira, E.F., et al., *7-Ketocholesterol is present in lipid deposits in the primate retina: potential implication in the induction of VEGF and CNV formation.* Invest Ophthalmol Vis Sci, 2009. **50**(2): p. 523-32.

200. Rodriguez, I.R. and S.J. Fliesler, *Photodamage generates 7-keto- and 7-hydroxycholesterol in the rat retina via a free radical-mediated mechanism.* Photochem Photobiol, 2009. **85**(5): p. 1116-25.

201. Rodriguez, I.R. and I.M. Larrayoz, *Cholesterol oxidation in the retina: implications of 7KCh formation in chronic inflammation and age-related macular degeneration.* J Lipid Res, 2010. **51**(10): p. 2847-62.

202. Ohishi, K., et al., *Iron release analyses from ferritin by visible light irradiation.* Free Radic Res, 2005. **39**(8): p. 875-82.

203. Yurkova, I., D. Huster, and J. Arnhold, *Free radical fragmentation of cardiolipin by cytochrome c.* Chem Phys Lipids, 2009. **158**(1): p. 16-21.

204. Gramajo, A.L., et al., *Mitochondrial DNA damage induced by 7-ketocholesterol in human retinal pigment epithelial cells in vitro.* Invest Ophthalmol Vis Sci, 2010. **51**(2): p. 1164-70.

205. Smith, L.L., V.B. Smart, and G.A.S. Ansari, *Mutagenic cholesterol preparations.* Mutation Research/Genetic Toxicology, 1979. **68**(1): p. 23-30.

206. Jusakul, A., et al., *Mechanisms of oxysterol-induced carcinogenesis.* Lipids Health Dis, 2011. **10**: p. 44.

207. Liu, J., et al., *Stimulation of Akt poly-ubiquitination and proteasomal degradation in P388D1 cells by 7-ketocholesterol and 25-hydroxycholesterol.* Arch Biochem Biophys, 2009. **487**(1): p. 54-8.

208. Zhang, Y., et al., *Cholesterol Is Superior to 7-Ketocholesterol or 7alpha - Hydroxycholesterol as an Allosteric Activator for Acyl-coenzyme A:Cholesterol Acyltransferase 1.* J. Biol. Chem., 2003. **278**(13): p. 11642-11647.

209. van Reyk, D.M., et al., *Oxysterols in biological systems: sources, metabolism and pathophysiological relevance.* Redox Rep, 2006. **11**(6): p. 255-62.

210. Lee, J.W., et al., *Expression and localization of sterol 27-hydroxylase (CYP27A1) in monkey retina.* Exp Eye Res, 2006. **83**(2): p. 465-9.

211. Ma, Y., et al., *25-Hydroxycholesterol-3-sulfate regulates macrophage lipid metabolism via the LXR/SREBP-1 signaling pathway.* Am J Physiol Endocrinol Metab, 2008. **295**(6): p. E1369-79.

212. Fuda, H., et al., *Oxysterols are substrates for cholesterol sulfotransferase.* J Lipid Res, 2007. **48**(6): p. 1343-52.

213. Fukuda, M., et al., *Spontaneous reconstitution of discoidal HDL from sphingomyelin-containing model membranes by apolipoprotein A-I.* J Lipid Res, 2007. **48**(4): p. 882-9.

214. Terasaka, N., et al., *High-density lipoprotein protects macrophages from oxidized low-density lipoprotein-induced apoptosis by promoting efflux of 7-ketocholesterol via ABCG1.* Proc Natl Acad Sci U S A, 2007. **104**(38): p. 15093-8.

215. Engel, T., et al., *Expression of ATP binding cassette-transporter ABCG1 prevents cell death by transporting cytotoxic 7beta-hydroxycholesterol.* FEBS Lett, 2007. **581**(8): p. 1673-80.

216. Jessup, W., et al., *Roles of ATP binding cassette transporters A1 and G1, scavenger receptor BI and membrane lipid domains in cholesterol export from macrophages.* Curr Opin Lipidol, 2006. **17**(3): p. 247-57.

217. Jessup, W., et al., *Oxidized lipoproteins and macrophages.* Vascul Pharmacol, 2002. **38**(4): p. 239-48.

218. Bjorkhem, I., et al., *Cholesterol homeostasis in human brain: turnover of 24S-hydroxycholesterol and evidence for a cerebral origin of most of this oxysterol in the circulation.* J Lipid Res, 1998. **39**(8): p. 1594-600.

219. Lutjohann, D., et al., *Cholesterol homeostasis in human brain: evidence for an age-dependent flux of 24S-hydroxycholesterol from the brain into the circulation.* Proc Natl Acad Sci U S A, 1996. **93**(18): p. 9799-804.

220. Bjorkhem, I., *Mechanism of degradation of the steroid side chain in the formation of bile acids.* J Lipid Res, 1992. **33**(4): p. 455-71.

221. Javitt, N.B., *26-Hydroxycholesterol: synthesis, metabolism, and biologic activities.* J Lipid Res, 1990. **31**(9): p. 1527-33.

222. Bjorkhem, I., et al., *Atherosclerosis and sterol 27-hydroxylase: evidence for a role of this enzyme in elimination of cholesterol from human macrophages.* Proc Natl Acad Sci U S A, 1994. **91**(18): p. 8592-6.

223. Brown, A.J., et al., *Sterol 27-hydroxylase acts on 7-ketocholesterol in human atherosclerotic lesions and macrophages in culture.* J Biol Chem, 2000. **275**(36): p. 27627-33.

224. Jessup, W., N. B. and M. Brown, K. A. J., *Novel routes for metabolism ofCholesterol 7-ketocholesterol alpha-hydroxylase.* RejuvenationJ Lipid Res, 20051977. **818**(12): p. 9-12135-53.

225. Myant, N.B. and K.A. Mitropoulos, *Cholesterol 7 alpha-hydroxylase.* J Lipid Res, 1977. **18**(2): p. 135-53.

226. van der Geize, R. and L. Dijkhuizen, *Harnessing the catabolic diversity of rhodococci for environmental and biotechnological applications.* Current Opinion in Microbiology, 2004. **7**(3): p. 255-261.

227. Du, H., et al., *Reduction of atherosclerotic plaques by lysosomal acid lipase supplementation.* Arterioscler Thromb Vasc Biol, 2004. **24**(1): p. 147-54.

228. Bjorkhem, I., *Do oxysterols control cholesterol homeostasis?* J Clin Invest, 2002. **110**(6): p. 725-30.

229. Larsson, D.A., et al., *Oxysterol mixtures, in atheroma-relevant proportions, display synergistic and proapoptotic effects.* Free Radical Biology and Medicine, 2006. **41**(6): p. 902-910.

230. Neyses, L., et al., *Stereospecific modulation of the calcium channel in human erythrocytes by cholesterol and its oxidized derivatives.* Biochem J, 1985. **227**(1): p. 105-12.

231. Hayden, J.M., et al., *Induction of monocyte differentiation and foam cell formation in vitro by 7-ketocholesterol.* J Lipid Res, 2002. **43**(1): p. 26-35.

232. Dushkin, M., et al., *Effects of oxysterols upon macrophage and lymphocyte functions in vitro.* Prostaglandins Other Lipid Mediat, 1998. **55**(4): p. 219-36.

233. Kandutsch, A.A. and H.W. Chen, *Inhibition of Sterol Synthesis in Cultured Mouse Cells by 7agr-Hydroxycholesterol, 7{beta}-Hydroxycholesterol, and 7-Ketocholesterol.* J. Biol. Chem., 1973. **248**(24): p. 8408-8417.

234. Conner, A.H., et al., *Microbial conversion of tall oil sterols to C19 steroids.* Appl Environ Microbiol, 1976. **32**(2): p. 310-1.

235. Margaritis, A., et al., *Biosurfactant production by Nocardia erythropolis.* Developments in Industrial Microbiology, 1979. **20**: p. 623-630.

236. West, C.C. and J.H. Harwell, *Surfactants and Subsurface Remediation.* Environmental Science & Technology, 1992. **26**(12): p. 2324-2330.

237. Oberbremer, A., R. Muller-Hurtig, and F. Wagner, *Effect of the addition of microbial surfactants on hydrocarbon degradation in a soil population in a stirred reactor.* Appl Microbiol Biotechnol, 1990. **32**(4): p. 485-9.

238. Nouroozzadeh, J., *Determination of the Autoxidation Products from Free or Total Cholesterol - a New Multistep Enrichment Methodology Including the Enzymatic Release of Esterified Cholesterol.* Journal of Agricultural and Food Chemistry, 1990. **38**(8): p. 1667-1673.

239. Roussi, S., et al., *Mitochondrial perturbation, oxidative stress and lysosomal destabilization are involved in 7beta-hydroxysitosterol and 7beta-hydroxycholesterol triggered apoptosis in human colon cancer cells.* Apoptosis, 2007. **12**(1): p. 87-96.

240. Koschutnig, K., et al., *Cytotoxic and apoptotic effects of single and mixed oxides of [beta]-sitosterol on HepG2-cells.* Toxicology in Vitro. **In Press, Corrected Proof**.

241. Mathieu, J., et al., *Microbial degradation of 7-ketocholesterol.* Biodegradation, 2008.

242. McLeod, M.P., et al., *The complete genome of Rhodococcus sp. RHA1 provides insights into a catabolic powerhouse.* Proc Natl Acad Sci U S A, 2006. **103**(42): p. 15582-7.

243. Mohn, W.W., et al., *The actinobacterial mce4 locus encodes a steroid transporter.* J Biol Chem, 2008. **283**(51): p. 35368-74.

244. Horinouchi, M., et al., *A new bacterial steroid degradation gene cluster in Comamonas testosteroni TA441 which consists of aromatic-compound degradation genes for seco-steroids and 3-ketosteroid dehydrogenase genes.* Applied and Environmental Microbiology, 2003. **69**(8): p. 4421-4430.

245. Horinouchi, M., T. Hayashi, and T. Kudo, *The genes encoding the hydroxylase of 3-hydroxy-9,10-secoandrosta-1,3,5(10)-triene-9,17-dione in steroid degradation in Comamonas testosteroni TA441.* J Steroid Biochem Mol Biol, 2004. **92**(3): p. 143-54.

246. van der Geize, R., et al., *Unmarked gene deletion mutagenesis of kstD, encoding 3-ketosteroid Delta(1)-dehydrogenase, in Rhodococcus erythropolis SQ1 using*

sacB as counter-selectable marker. Fems Microbiology Letters, 2001. **205**(2): p. 197-202.

247. van der Geize, R., et al., *Molecular and functional characterization of kshA and kshB, encoding two components of 3-ketosteroid 9 alpha-hydroxylase, a class IA monooxygenase, in Rhodococcus erythropolis strain SQ1.* Molecular Microbiology, 2002. **45**(4): p. 1007-1018.

248. Atlas, R.M. and L.C. Parks, *Handbook of microbiological media*. 1993, Boca Raton: CRC Press. v, 1079 p.

249. Goncalves, E.R., et al., *Transcriptomic assessment of isozymes in the biphenyl pathway of Rhodococcus sp. strain RHA1.* Appl Environ Microbiol, 2006. **72**(9): p. 6183-93.

250. LeBlanc, J.C., E.R. Goncalves, and W.W. Mohn, *Global response to desiccation stress in the soil actinomycete Rhodococcus jostii RHA1.* Appl Environ Microbiol, 2008. **74**(9): p. 2627-36.

251. Overbeek, R., et al., *The subsystems approach to genome annotation and its use in the project to annotate 1000 genomes.* Nucleic Acids Res, 2005. **33**(17): p. 5691-702.

252. Hua, S. and Z. Sun, *Support vector machine approach for protein subcellular localization prediction.* Bioinformatics, 2001. **17**(8): p. 721-8.

253. Bendtsen, J.D., et al., *Improved prediction of signal peptides: SignalP 3.0.* J Mol Biol, 2004. **340**(4): p. 783-95.

254. Gardy, J.L., et al., *PSORTb v.2.0: expanded prediction of bacterial protein subcellular localization and insights gained from comparative proteome analysis.* Bioinformatics, 2005. **21**(5): p. 617-23.

255. Simon, R., U. Priefer, and A. Puhler, *A Broad Host Range Mobilization System for In Vivo Genetic Engineering: Transposon Mutagenesis in Gram Negative Bacteria.* Nat Biotech, 1983. **1**(9): p. 784-791.

256. Linder, R. and A.W. Bernheimer, *Enzymatic oxidation of membrane cholesterol in relation to lysis of sheep erythrocytes by corynebacterial enzymes.* Arch Biochem Biophys, 1982. **213**(2): p. 395-404.

257. Pei, Y., et al., *Cholesterol oxidase (ChoE) is not important in the virulence of Rhodococcus equi.* Vet Microbiol, 2006. **118**(3-4): p. 240-6.

258. Yang, X., et al., *Rv1106c from Mycobacterium tuberculosis is a 3beta-hydroxysteroid dehydrogenase.* Biochemistry, 2007. **46**(31): p. 9058-67.

259. Arampatzis, S., et al., *Comparative enzymology of 11beta-hydroxysteroid dehydrogenase type 1 from six species.* J Mol Endocrinol, 2005. **35**(1): p. 89-101.

260. Lemaire-Ewing, S., et al., *Comparison of the cytotoxic, pro-oxidant and pro-inflammatory characteristics of different oxysterols.* Cell Biol Toxicol, 2005. **21**(2): p. 97-114.

261. Miguet, C., et al., *Ceramide generation occurring during 7beta-hydroxycholesterol- and 7-ketocholesterol-induced apoptosis is caspase independent and is not required to trigger cell death.* Cell Death Differ, 2001. **8**(1): p. 83-99.

262. Miguet-Alfonsi, C., et al., *Analysis of oxidative processes and of myelin figures formation before and after the loss of mitochondrial transmembrane potential during 7beta-hydroxycholesterol and 7-ketocholesterol-induced apoptosis: comparison with various pro-apoptotic chemicals.* Biochem Pharmacol, 2002. **64**(3): p. 527-41.

263. Ralser, M., et al., *An efficient and economic enhancer mix for PCR.* Biochem Biophys Res Commun, 2006. **347**(3): p. 747-51.

264. Quan, J. and J. Tian, *Circular polymerase extension cloning of complex gene libraries and pathways.* PLoS One, 2009. **4**(7): p. e6441.

265. Baron, S.F., C.V. Franklund, and P.B. Hylemon, *Cloning, sequencing, and expression of the gene coding for bile acid 7 alpha-hydroxysteroid dehydrogenase from Eubacterium sp. strain VPI 12708.* J Bacteriol, 1991. **173**(15): p. 4558-69.

266. Bennett, M.J., S.L. McKnight, and J.P. Coleman, *Cloning and characterization of the NAD-dependent 7alpha-Hydroxysteroid dehydrogenase from Bacteroides fragilis.* Curr Microbiol, 2003. **47**(6): p. 475-84.

267. Coleman, J.P., L.L. Hudson, and M.J. Adams, *Characterization and regulation of the NADP-linked 7 alpha-hydroxysteroid dehydrogenase gene from Clostridium sordellii.* J Bacteriol, 1994. **176**(16): p. 4865-74.

268. Bligh, E.G. and W.J. Dyer, *A rapid method of total lipid extraction and purification.* Can J Biochem Physiol, 1959. **37**(8): p. 911-7.

269. Jacobson, M.P., et al., *On the Role of the Crystal Environment in Determining Protein Side-chain Conformations.* Journal of Molecular Biology, 2002. **320**(3): p. 597-608.

270. Jacobson, M.P., et al., *A hierarchical approach to all-atom protein loop prediction.* Proteins: Structure, Function, and Bioinformatics, 2004. **55**(2): p. 351-367.

271. Friesner, R.A., et al., *Glide: A New Approach for Rapid, Accurate Docking and Scoring. 1. Method and Assessment of Docking Accuracy.* Journal of Medicinal Chemistry, 2004. **47**(7): p. 1739-1749.

272. Rosloniec, K.Z., et al., *Cytochrome P450 125 (CYP125) catalyses C26-hydroxylation to initiate sterol side-chain degradation in Rhodococcus jostii RHA1.* Molecular Microbiology, 2009. **9999**(9999).

273. Stevenson, E. and E. Staple, *Oxidation of various simple steroids by the cholesterol oxidase system.* Arch Biochem Biophys, 1962. **97**: p. 485-90.

274. de Grey, A.D.N.J., *Bioremediation meets biomedicine: therapeutic translation of microbial catabolism to the lysosome.* Trends in Biotechnology, 2002. **20**(11): p. 452-455.

275. de Grey, A.D.N.J. and J.A.C. Archer, *Why don't graveyards fluoresce?Anti-aging applications of the bacterial degradation of lysosomal aggregates.* J Am Aging Assoc, 2001. **24**(118).

276. Jessup, W. and A.J. Brown, *Novel routes for metabolism of 7-ketocholesterol.* Rejuvenation Res, 2005. **8**(1): p. 9-12.

277. Gelissen, I.C., et al., *Sterol efflux is impaired from macrophage foam cells selectively enriched with 7-ketocholesterol.* J Biol Chem, 1996. **271**(30): p. 17852-60.

278. Monier, S., et al., *Impairment of the cytotoxic and oxidative activities of 7[beta]-hydroxycholesterol and 7-ketocholesterol by esterification with oleate.* Biochemical and Biophysical Research Communications, 2003. **303**(3): p. 814-824.

279. Brown, A.J. and W. Jessup, *Oxysterols: Sources, cellular storage and metabolism, and new insights into their roles in cholesterol homeostasis.* Mol Aspects Med, 2009.

280. Groth-Pedersen, L. and M. Jaattela, *Combating apoptosis and multidrug resistant cancers by targeting lysosomes.* Cancer Lett, 2010.

281. Johansson, A.C., et al., *Regulation of apoptosis-associated lysosomal membrane permeabilization.* Apoptosis, 2010. **15**(5): p. 527-40.

282. Ghoshroy, K.B., W. Zhu, and N.S. Sampson, *Investigation of membrane disruption in the reaction catalyzed by cholesterol oxidase.* Biochemistry, 1997. **36**(20): p. 6133-40.

283. Doukyu, N., et al., *Cloning, sequence analysis, and expression of a gene encoding Chromobacterium sp. DS-1 cholesterol oxidase.* Appl Microbiol Biotechnol, 2009. **82**(3): p. 479-90.

284. Sagermann, M., et al., *Structural characterization of the organic solvent-stable cholesterol oxidase from Chromobacterium sp. DS-1.* J Struct Biol, 2010. **170**(1): p. 32-40.

285. de la Mare, P.B.D. and R.D. Wilson, *Autoxidation of cholest-5-en-3-one, and its accompanying isomerization, in acetic acid.* Journal of the Chemical Society, Perkin Transactions 2, 1977(2): p. 157-162.

286. Gibson, D.G., et al., *Enzymatic assembly of DNA molecules up to several hundred kilobases.* Nat Methods, 2009. **6**(5): p. 343-5.

287. Falcon-Perez, J.M., et al., *Distribution and dynamics of Lamp1-containing endocytic organelles in fibroblasts deficient in BLOC-3.* J Cell Sci, 2005. **118**(Pt 22): p. 5243-55.

288. Tarbutton, P.N. and C.R. Gunter, *Enzymatic Determination of Total Cholesterol in Serum.* Clin Chem, 1974. **20**(6): p. 724-725.

289. Chen, W., et al., *Enzymatic Reduction of Oxysterols Impairs LXR Signaling in Cultured Cells and the Livers of Mice.* Cell Metabolism, 2007. **5**(1): p. 73-79.

290. Monier, S., et al., *Impairment of the cytotoxic and oxidative activities of 7 beta-hydroxycholesterol and 7-ketocholesterol by esterification with oleate.* Biochem Biophys Res Commun, 2003. **303**(3): p. 814-24.

291. Dove, D.E., et al., *ACAT1 Deficiency Disrupts Cholesterol Efflux and Alters Cellular Morphology in Macrophages.* Arterioscler Thromb Vasc Biol, 2005. **25**(1): p. 128-134.

292. Zhao, B., et al., *Macrophage-specific transgenic expression of cholesteryl ester hydrolase significantly reduces atherosclerosis and lesion necrosis in Ldlr mice.* J Clin Invest, 2007. **117**(10): p. 2983-92.

293. Yagyu, H., et al., *Absence of ACAT-1 attenuates atherosclerosis but causes dry eye and cutaneous xanthomatosis in mice with congenital hyperlipidemia.* J Biol Chem, 2000. **275**(28): p. 21324-30.

294. Kamido, H., et al., *Identification of core aldehydes among in vitro peroxidation products of cholesteryl esters.* Lipids, 1993. **28**(4): p. 331-336.

295. Gaus, K., et al., *Inhibition of cholesterol efflux by 7-ketocholesterol: comparison between cells, plasma membrane vesicles, and liposomes as cholesterol donors.* Biochemistry, 2001. **40**(43): p. 13002-14.

296. Huynh, K.K., et al., *LAMP proteins are required for fusion of lysosomes with phagosomes.* EMBO J, 2007. **26**(2): p. 313-24.

297. Fehrenbacher, N., et al., *Sensitization to the Lysosomal Cell Death Pathway by Oncogene-Induced Down-regulation of Lysosome-Associated Membrane Proteins 1 and 2.* Cancer Research, 2008. **68**(16): p. 6623-6633.

298. Rosenbaum, A.I., et al., *Endocytosis of beta-cyclodextrins is responsible for cholesterol reduction in Niemann-Pick type C mutant cells.* Proceedings of the National Academy of Sciences, 2010. **107**(12): p. 5477-5482.

299. Ramirez, C., et al., *Quantitative role of LAL, NPC2, and NPC1 in lysosomal cholesterol processing defined by genetic and pharmacological manipulations.* J Lipid Res, 2011.

300. Kritharides, L., et al., *Hydroxypropyl-β-cyclodextrin-mediated Efflux of 7-Ketocholesterol from Macrophage Foam Cells.* Journal of Biological Chemistry, 1996. **271**(44): p. 27450-27455.